AD_____

Award Number: DAMD17-03-1-0480

TITLE: Theoretical Modeling of Molecular Mechanisms, Time Scales, and Strains in Prion Diseases

PRINCIPAL INVESTIGATOR: Daniel L. Cox, Ph.D.
Rajiv R. P. Singh

CONTRACTING ORGANIZATION: University of California, Davis
Davis, California 95616-8671

REPORT DATE: July 2004

TYPE OF REPORT: Annual

PREPARED FOR: U.S. Army Medical Research and Materiel Command
Fort Detrick, Maryland 21702-5012

REPORT DOCUMENTATION PAGE

Form Approved
OMB No. 074-0188

1. AGENCY USE ONLY (Leave blank)	2. REPORT DATE	3. REPORT TYPE AND DATES COVERED
	July 2004	Annual (15 Jun 03-14 Jun 04)

4. TITLE AND SUBTITLE
Theoretical Modeling of Molecular Mechanisms, Time Scales, and Strains in Prion Diseases

5. FUNDING NUMBERS
DAMD17-03-1-0480

6. AUTHOR(S)
Daniel L. Cox, Ph.D.
Rajiv R. P. Singh

7. PERFORMING ORGANIZATION NAME(S) AND ADDRESS(ES)
University of California, Davis
Davis, California 95616-8671

E-Mail: cox@physics.ucdavis.edu

8. PERFORMING ORGANIZATION REPORT NUMBER

9. SPONSORING / MONITORING AGENCY NAME(S) AND ADDRESS(ES)
U.S. Army Medical Research and Materiel Command
Fort Detrick, Maryland 21702-5012

10. SPONSORING / MONITORING AGENCY REPORT NUMBER

11. SUPPLEMENTARY NOTES

12a. DISTRIBUTION / AVAILABILITY STATEMENT
Approved for Public Release; Distribution Unlimited

12b. DISTRIBUTION CODE

13. ABSTRACT (Maximum 200 Words)

We have obtained significant research results on: 1) modeling the role of oligomeric intermediates in prion disease incubation dynamics and aggregation, 2) using an amino acid specific monte carlo code for modeling membrane insertion of a related peptide, 3) electronic structure studies of the binding of divalent transition metal ions in the octarepeat regions of the prion protein, and (4) developing stochastic algorithm models for aggregation processes in prion disease. In the coming year we will (1) attempt to extend our monte carlo code to allow for beta-sheet interactions between peptides, (2) develop more realistic electronic structure models for metal ions in prion diseases, (3) extend our stochastic kinetics algorithm to the study of strains, first in prion-like proteins for yeast, and (4) explore the possibility of a novel, non-invasive detection scheme based upon observations of metal ions content fluctuations both in vivo and in vitro.

14. SUBJECT TERMS	15. NUMBER OF PAGES
Theory/Simulations; Autocatalytic Aggregation; Oligomeric Aggregation; Theories of Strains; Theories of Clearance	131
	16. PRICE CODE

17. SECURITY CLASSIFICATION OF REPORT	18. SECURITY CLASSIFICATION OF THIS PAGE	19. SECURITY CLASSIFICATION OF ABSTRACT	20. LIMITATION OF ABSTRACT
Unclassified	Unclassified	Unclassified	Unlimited

Table of Contents

Introduction

In this first year of our award, we have made significant progress on several areas of theoretical research on the prion problem as outlined in our original proposal and the subsequent amendments aimed at developing experimental collaboration with Prof. Glen Millhauser's group at UC Santa Cruz, and a consultative relationship with Dr. Holger Wille of UC San Francisco. Notably, we have published two long papers on modeling prion oligomer aggregation and molecular specific peptide/membrane interactions, and graduated one student in this area (Dr. David Mobley) who has moved to a high profile postdoctoral position in the molecular simulation group of Prof. Ken Dill at UC San Francisco. Two more papers will be shortly forthcoming to report our accomplishments on simulations of prion-transition metal ion interactions relevant to the work of Prof. Millhauser, and on development of stochastic kinetic algorithm based codes for modeling one dimensional aggregation models most clearly relevant to prion-like proteins in yeast, but pointing towards studies of the strain phenomenon. We also foresee a number of fruitful extensions to these studies in the coming year.

The PI has been honored with a J.S. Guggenheim Memorial Fellowship for ``Studies in Theoretical Biological Physics,'' which he is using to carry out a sabbatical year leave at the Center for Theoretical Biological Physics at UC San Diego from July 2004-June 2005. About 35% of his research time on this sabbatical will be covering research associated with this award. Prof. Cox will maintain close collaboration with associates at Davis via monthly visits paid for by the Guggenheim fellowship, and will also bring junior associates down for sequential 3 month periods during this time frame.

Key Research Accomplishments

1. ***Demonstration of the feasibility of an oligomeric based aggregation model for prion diseases.*** In this work, the Biophysical Journal article presented in App. B, we carried out stochastic cellular automata simulations and kinetics calculations to study a model in which *oligomers* of prions attach and aggregate to infectious seeds. We demonstrated that with little effort, this oligomer model retains the previous attractive incubation time statistics of our oversimplified monomer model (see Figs. 4,5,10 of paper in App. B), and this model also points to experimental directions to search for ``nonhardened'' or noninfectious oligomers in the native organism (see discussion in the three complete paragraphs of p. 2222 [the 10^{th} page] of the paper in App. B) . This work was important in strengthening our consultative relationship with Dr. Holger Wille of UC San Francisco (in the Prusiner lab), and represents the culmination of our preliminary results in this direction discussed in our proposal to the Army.
2. ***Demonstration of novel insertion characteristics for mutated Aβ peptides in model membranes as precursor to study of prion insertion.*** In this paper, contained as App. C, we have employed a Monte Carlo code to study insertion of Alzheimer's peptides into model membranes. The model in the code is amino acid specific but biased towards intra-membrane alpha helix formation. The membrane and water regions are characterized by three profile functions, i) a

water profile which decays sharply within the lipid head region, (ii) a polarity profile which is large in the water and head region and decays sharply within the lipid tail region, and (iii) a hydrophobicity profile which has a two stage decay from large values within the lipid tail region. Residues are characterized as hard spheres with three parameters, a) a polar energy associated with interaction with water, b) a hydrophobicity energy associated with energy change upon membrane insertion, and c) a hydrogen bonding index associated with intra-membrane alpha helix formation. Our main findings were: (A) wild type Aβ42 peptide, which is the predominant peptide implicated in post mortem plaque content, ``hangs up'' within the membrane far more than wild type Aβ40 (see Fig. 5-7 of the paper in App. C, which display observed probability of location of selected residues at given positions with respect to the membrane center). The reason is that the additional residues are relatively hydrophobic. The potential consequence is that the outer-leaflet ``hang up'' of Aβ42, seen in the shoulder of the distribution of configurations in Fig. 5-7(b) of the paper in App. C, is more favorable to formation of oligomeric pores which allow excess calcium into neurons. (B) Of all known mutations of the APP protein (parent to these peptides) implicated in early onset Alzheimer's disease, all but one induce a high probability of insertion into a configuration compatible with models for oligomeric pores of both Aβ40 and Aβ42 peptides (again, see Figs. 5-7 of the paper in App. C). These pores have been implicated in excess calcium transport in *vitro* on supported bilayers and cultured neurons, and potentially are related in *vivo* to reduced synaptic plasticity. The relevance of this work to our ongoing investigation of prion diseases is two fold: (i) we are interested in exploring with molecular specificity the insertion properties of the prion protein in model membranes an issue of considerable importance in the transport of PrP from the cell nucleus to neuronal surface—abnormal membrane insertion, in particular, is correlated with disease, and (ii) we intend to extend this molecularly specific code to allow for beta sheet interactions, which is obviously of great importance in the prion aggregates and which we touch on in the research directions section below.

3. ***Electronic structure studies of metal binding in prion octarepeat regions*** We commenced this work to initiate our collaborative relationship with Prof. Glen Millhauser of UC Santa Cruz[1,2,], whose specialty is examining the transition metal binding sites of the prion protein using electron spin resonance and crystallography methods. In this approach, we employed SIESTA 1.3 local basis density functional program[3] to examine the reduced 5-amino acid HGGGW sequence identified by Millhauser and collaborators as the binding unit for Cu^{2+} in the octarepeat region. (Within SIESTA, we used the generalized gradient approximation in the PBE form, a double zeta polarization basis with approximate Slater orbitals confined to hard spheres via the FIREBALL approach of Sankey and collaborators, and the TM pseudopotential.) We have several results which will form the basis of a paper for submission in the very near future: *a) Bound equilibrium configurations for* Cu^{2+}, Zn^{2+}, Ni^{2+}, *and* Mn^{2+}. By commencing with the experimental geometry determined from crystallography and ESR data for the HGGGW fragment + six waters + divalent transition metal ion and optimizing, we obtained stable equilibrium configurations for all four of the transition metal

ions considered relevant in the experimental literature for prion binding. In the case of Cu^{2+}, the difference between the optimized theoretical geometry and the experimental geometry is well within the structural error bars. *b) Asymmetry of Cu^{2+} electron density in the bound complex.* An observation from the crystallography data (unpublished, G. Millhauser, 2003) is that the electron charge density around the Cu site appears quite asymmetric in the basal plane of the approximate square pyramidal coordination environment. We find an asymmetry in our calculations and will compare with the experimental data. *c) Binding energy trends for transition metal ions.* A significant controversy in the experimental literature is how strongly the different transition metal ions bind[4,5]. We sought to explore this question theoretically by considering the following oversimplified model: we calculate the total energy of three constructs—i) the prion octarepeat fragment with six waters and the transition metal ion denoted as E(HGGGW-M^{2+}-$6H_2O$), (ii) the divalent metal ion coordinated to six waters denoted as E(M^{2+}-$6H_2O$), and (iii) the remaining prion fragment alone denoted as E(HGGGW). The binding energy for the metal ion is then estimated as

$$E(M^{2+}) = E(M^{2+}\text{-}6H_2O) + E(HGGGW) - E(HGGGW\text{-}M^{2+}\text{-}6H_2O)$$

with stability indicated by a positive value for E(M^{2+}). Within this approach we find all four of the relevant metal ions bind with energies of order ~20 eV within the simple model, with stability ranking E(Cu^{2+})>> E(Ni^{2+})> E(Zn^{2+})>> E(Mn^{2+}), with the Zn and Ni binding energies quite close (probably within overall systematic error of the method). It is interesting that this is precisely the binding affinity for the octarepeat region identified in the most comprehensive study in the literature[4]. We obtain magnitudes for our relative binding energies comparable to those inferred from the affinity data, and trends in reasonable agreement (apart from the reversal of Zn and Ni for the non-octarepeat site). The table below gives results for both the octarepeat sites in comparison with experiment of the Collinge group[4], and preliminary results for the non-octarepeat site in comparison with experiment. To infer the relative binding energies (to Cu(II)) for each site, we have taken the logarithm of the measured affinities in Ref. [4]; strictly speaking, we are comparing a low temperature enthalpy contribution to a room temperature free energy contribution by this method, but the comparison should be strong since the presumed metal ion configurations in all cases are expected to be very similar and thus have similar entropy differences. We report all energies in electron volts. Note that our preliminary results also show the non-octarepeat site to have higher binding energy than the octarepeat site, in agreement with findings by Millhauser and collaborators [1,2].

Metal ion	*EB Calc (Octa.) (eV)*	*EB Calc (nonocta) (eV)*	*EB Expt ('Octa') (eV)*	*EB Expt (Nonocta) (eV)*
Cu	0.0	0.0	0.0	0.0
Ni	0.36	0.48	0.37	0.33
Zn	0.60	0.36	0.48	0.38
Mn	1.38	1.75	0.67	0.58

Table: Relative binding energies (measured with respect to Cu) of divalent metal ions to PrP^C protein—comparison of theory (columns 2,3) with experiment (Ref. [4], columns 4,5).

4. ***Development of Gillespie algorithm for studying one dimensional aggregation models for strain modeling.*** We have developed a Gillespie algorithm[6] based code for modeling one dimensional aggregation of coarse-grained prion proteins as a first step towards modeling strains. This model is fundamentally relevant to aggregation of yeast prion-like proteins[7]. The Gillespie algorithm is an increasingly popular continuous time stochastic approach to kinetics, which lacks spatial explicitness but is capable of simulating rare temporal events unlike strict kinetics models. The essence of the Gillespie algorithm is: (i) to generate rates or propensities for all fundamental kinetic process rates for a given (time dependent) configuration of molecular species, corresponding, e.g., to nucleation, aggregate growth by monomer addition, or aggregate fissioning, to propensities, and in one Monte Carlo step to determine via the cumulative rate what the waiting time is to the next reaction (assuming a simple exponential in time distribution), and (ii) use a second Monte Carlo step to determine by importance sampling which kind of event should occur given that a reaction is determined to take place. The one dimensional problem with fundamental processes of (a) slow nucleation from, eg, two monomers to a dimer, (b) growth by monomer addition, and (c) fission of aggregated polymers has been studied before both by analytic and numerical means using standard kinetics models and the Gillespie approach[8]. What has not been carried out is: (i) an extensive search for what behaviors can arise for all model parameters, (ii) an investigation of the nature of the length distribution (which we find to fit the Weibull distribution very well). We have been able to demonstrate a dependence of the mean length upon the square root of the fission rate. We are writing up these initial results into a short paper for submission to .Physical Review E.

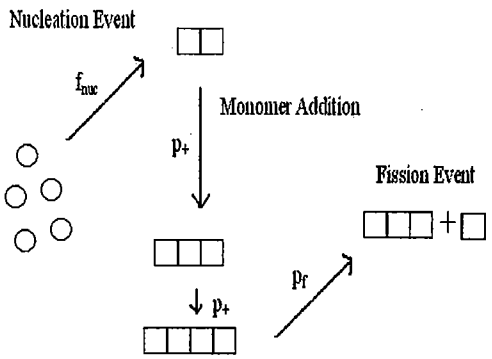

Fig. 1: Schematics of 1D prion aggregation model. Monomers can nucleate into aggregate slowly at the dimer level (f_{nuc} the second order kinetic rate coefficient, with g_{nuc} being the propensity in the stochastic Gillespie model); aggregates grow by monomer addition with second order rate coefficient p_+ (propensity g_+ in the Gillespie approach); aggregates fission at a first order rate p_f (propensity g_f in the Gillespie approach).

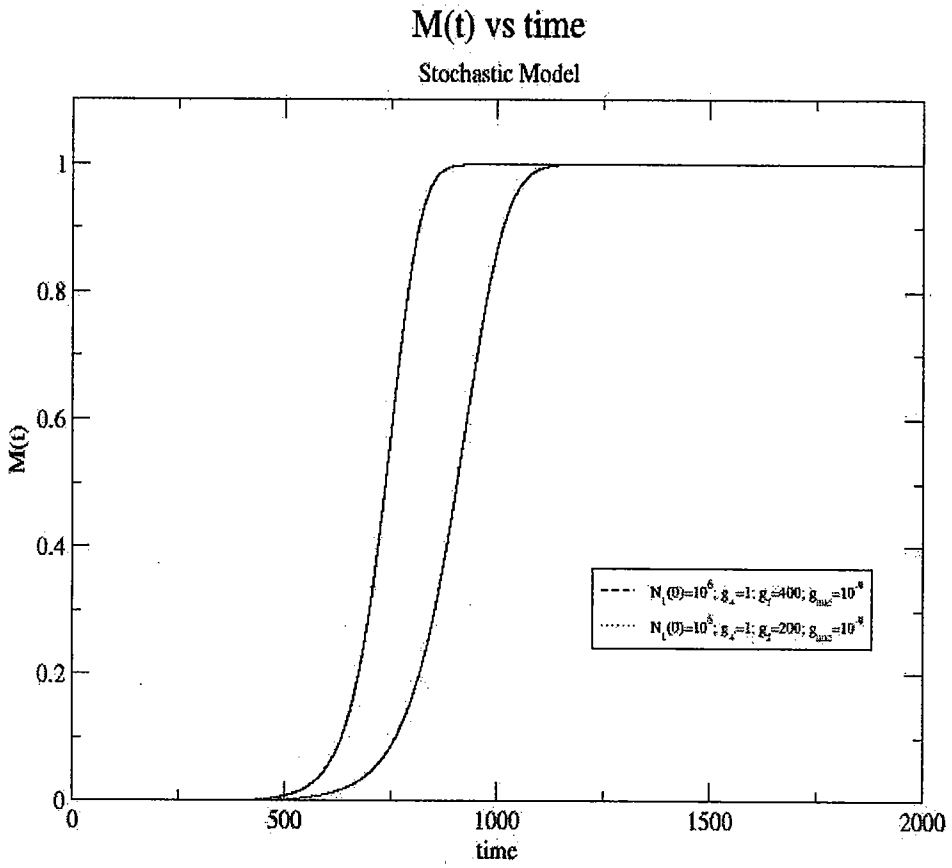

Fig. 2: Dependence of total numbers of prion monomers in aggregate form in 1D aggregation model based upon stochastic Gillespie algorithm. Note that the initial rise is exponential.

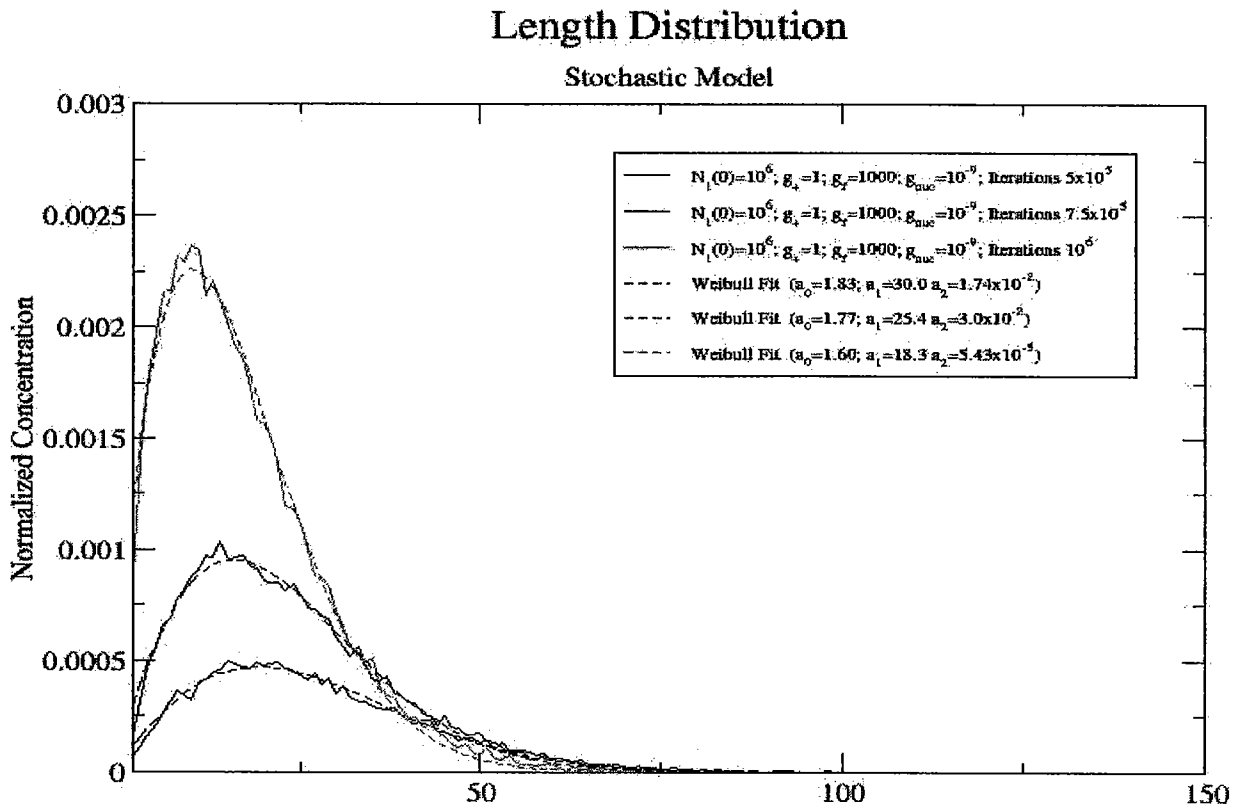

Fig. 3: Distribution of aggregate lengths in stochastic Gillespie model of 1D prion aggregation: comparison to Weibull distribution. The x-axis is length measured in number of monomers; the y-axis is frequency of observation. The three solid curves are for three different sampling times of the aggregates given initial number of monomers N(0) of 10^6, monomer addition propensity $g_+ = 1$ (this sets the time scale), fission propensity $g_f = 1000$, and nucleation propensity $g_{nuc} = 10^{-9}$. The form of the Weibull distribution is

$$f(x) = a_2 (a_0/a_1) (x/a_1)^{a0-1} \exp[-(x/a_1)^{a0}]$$

which are the corresponding dashed curves.

Research Directions for Coming Year

1. ***Extension of peptide Monte Carlo code to allow for beta-sheet interactions.*** This is of direct relevance to two aspects of the prion problems: (1) the hydrogen bonded beta helices of the recently discovered infectious oligomers from Dr. Wille and collaborators at UCSF; (2) the putative beta-sheet binding of PrP^C proteins in the octarepeat regions. The latter suggestion derived from solution NMR studies at pH levels characteristic of the synaptic cleft, is intriguing both for (i) providing explicit candidate oligomeric intermediates related to our published work of App. B, and (ii) providing a plausible approach to fission of infectious aggregates bound to non-hardened oligomers which cross link across the synaptic gap[9]. Our inspiration for this approach comes from the initial successes of coarse-grained discrete molecular dynamics in generating beta-sheet aggregation of model peptides[10]. The PI anticipates collaborating with Profs. J. Onuchic and H. Levine of the Center for Theoretical Biological Physics at UCSD on this problem, as this is a shared interest. Collaboration will continue with current and past associates as well.
2. ***Development of more realistic electronic structure models for transition metal bonding.*** While our previous calculations have correctly captured the binding trend seen in experiments, our binding energies seem excessively large and binding energy differences overamplified. We speculate on three reasons for this problem, which we will explore in the coming year: (i) we probably have the incorrect coordination environment for the unbound ions; rather than arriving coordinated by water, with the possible exception of zinc, they are probably in a chelated organometallic form. (ii) We have so few waters that the Coulomb energies are insufficiently screened. We can add waters to the surroundings of our model complexes and study these on our dual processor, large RAM opteron machines purchased by other funding from the NSF Center for Biophotonics Science and Technology. (iii) We are receiving errors from the nonorthogonal localized basis set upon separation of the molecular pieces. There are standard methods of treating this which will explore. We will also examine binding and stability in the less well understood NON-octarepeat site, which is contained within the minimal sequence of PrP capable of participating in infection (the octarepeats are not!).
3. ***Extension of stochastic kinetic modeling to strains.*** We are close to completion of an extension of our stochastic kinetic modeling code to study strains in one dimensional aggregates. The first goal will be to assess whether the model can generate qualitative morphologies and incubation dynamics characteristic of the yeast prion-like aggregates studied in J. Weissman's lab for which there is considerable data and for which conformation based coding of strains is on strong experimental footing. Subsequently we will extend the modeling to higher dimensional aggregates more likely to describe the mammalian prion problem and

look to quantitatively describe the wealth of existing data on strain incubation time dynamics and inter-generational passage in terms of conformational-only encoding of strains. If successful in this endeavor, we will have helped solidify the most probable answer to one of the open questions in the prion field.

4. ***Exploration of a novel detection scheme for prion infection.*** It has been demonstrated that: (1) copper uptake is suppressed in infected cultured neurons[11]; (2) post-mortem examination of copper concentrations in diseased regions of human brains is suppressed while there is some evidence that manganese concentration is enhanced[12]. These results suggest a novel detection scheme for prion infection, the gist of which is as follows: (i) inject an infected individual with radioactive Cu or Mn species of suitable life times which emit positrons upon decay on a time course; (ii) using positron emission tomography, map the concentration profiles of the radioactive Cu/Mn in the brain of the individual; (iii) in the time series of concentration maps, look for either significantly suppressed Cu levels in those neuronal regions most susceptible for infection, or significantly enhanced Mn levels. While the basic idea seems promising, it is obviously clear that model calculations based upon existing data are important to establish practicality of the method, for knowing, e.g., required dose levels for achieving sufficient spatial and temporal resolution. It is also important to know whether the aforementioned post-mortem studies are actually reproducible. On both counts, the PI and associates have opened some discussions with the Livermore group working on this problem, headed by Dr. Jim DeYoreo.

Reportable Outcomes: Awards, Activities, Presentations and Publications

1. **Awards, Activities, and Presentations** ***(Appendix A)***
2. **Simulations of Oligomeric Intermediates in Prion Diseases** ***(Appendix B)***
3. **Modeling Amyloid Peptide Insertion into Lipid Bilayers** ***(Appendix C)***
4. **Models of Cooperative Dynamics from Biomolecules to Magnets** ***(Appendix D—PhD dissertation of D. Mobley; Apps. B,C are chapters therein, and relevant introductory material from dissertation is included. Full dissertation is available at http://sexton.ucdavis.edu/CondMatt/cox/mobleydissertation.pdf)***

Conclusions

In conclusion, we have successfully modeled oligomeric intermediates of prion aggregates, A-beta peptide insertion (with mutations) in a model membrane, binding energies of divalent transition metal ions in the octarepeat region of the prion protein, and developed a stochastic kinetics algorithm for coarse-grained modeling of prion aggregation and the strain phenomenon. In the coming year we will explore including beta-sheet interactions in our insertion code, extend our electronic structure studies of metal ion binding, tackle quantitative modeling of the strain phenomenon, and investigate a potential detection method based upon uptake of radioactive divalent metal ions.

References

1. *Identification of the Cu2+ Binding Sites in the N-Terminal Domain of the Prion Protein by EPR and CD Spectroscopy,*Eliah Aronoff-Spencer,‡,§,| Colin S. Burns,‡,§ Nikolai I. Avdievich,| Gary J. Gerfen,| Jack Peisach,|William E. Antholine,^ Haydn L. Ball,#,[Fred E. Cohen,X,+,O,[Stanley B. Prusiner,#,X,[and Glenn L. Millhauser*, *Biochemistry* **2000,** *39,* 13760-13771.

2. *Molecular Features of the Copper Binding Sites in the Octarepeat Domain of the Prion Protein,*Colin S. Burns,‡,§ Eliah Aronoff-Spencer,‡,§,| Christine M. Dunham,‡,§ Paula Lario,‡ Nikolai I. Avdievich,|William E. Antholine,^ Marilyn M. Olmstead,# Alice Vrielink,‡ Gary J. Gerfen,| Jack Peisach,|William G. Scott,‡ and Glenn L. Millhauser*, *Biochemistry* **2002,** *41,* 3991-4001

3. http://www.uam.es/departamentos/ciencias/fismateriac/siesta/

4. *Location and properties of metal-binding sites on thehuman prion protein* Graham S. Jackson*, Ian Murray*, Laszlo L. P. Hosszu*†, Nicholas Gibbs‡, Jonathan P. Waltho†, Anthony R. Clarke*‡§,and John Collinge* PNAS **, 2001** , *98* **,8531–8535.**

5. *Copper binding to the octarepeats of the prion protein - Affinity, specificity, folding, and cooperativity: Insights from circular dichroism,* A.P. Garnett and J.H. Viles, *J. Biol. Chem.* **2003,** *278* 6795-6802.

6. *STOCKS: STOChastic Kinetic Simulations of biochemical systems with Gillespie algorithm,* Andrzej M. Kierzek, *BIOINFORMATICS 18,* **2002** 470–481.

7. http://online.kitp.ucsb.edu/online/bionet03/collins/

8. *Quantifying the kinetic parameters of prion replication,* J. Masel, V. Jansen, M. Nowak, *Biophys. Chem.* **1999,** *77,* 139-152; *Silent prions lying in wait: A two-hit model of prion/amyloid formation and infection,* D. Hall, H. Edskes, *J. Mol. Biol.* **2004** *336,*775-786; T. Poschel, N.V. Brilliantov, C. Frommel, *Biophys. J.* **2003** *85,* 3460-3474.

9. *The Octapeptide Repeats in Mammalian Prion Protein Constitute a pH-dependent Folding and Aggregation Site,* R. Zahn, *J. Mol. Biol.* **2003** *334* 477-488.

10. See, e.g., *Thermodynamics and stability of a beta-sheet complex: Molecular dynamics simulations on simplified off-lattice protein models,* H.B. Jang, C.K. Hall, Y.Q. Zhou, *Protein Science* **2004** *13* 40-53.

11. *Prion Infection Impairs CopperBinding of Cultured Cells,* Walid Rachidi‡§, Alain Mange´§¶,Abderrahmene Senator‡, Pascale Guiraud‡,Jacqueline Riondel‡, Mustapha Benboubetra_, Alain Favier**, and Sylvain Lehmann, *J. Biol. Chem.* **2003,** *278* 14596-14598.

12. *Aberrant metal binding by prion protein in human prion disease,* Boon-Seng Wong, Shu G. Chen, Monica Colucci, Zhiliang Xie, Tao Pan, Tong Liu, Ruliang Li, Pierluigi Gambetti, Man-Sun Sy, David R. Brown, *J. Neurochem* **2001** *78* 1400-1408.

APPENDIX A: ACTIVITIES, HONORS, AND PRESENTATIONS ASSOCIATED WITH THIS RESEARCH AWARD

Honors

D.L. Cox, J.S. Guggenheim Memorial Fellowship, for ``Studies in Theoretical Biological Physics'' (emphasizing prion protein research) during sabbatical leave at the Center for Theoretical Biological Physics of the University of California, San Diego, July 2004-June 2005.

D.L. Mobley, Graduate Fellow, Kavli Institute for Theoretical Physics, Aug.-Dec. 2003.

Activities

D.L. Cox, R.R.P. Singh, co-organizers of International Workshop on ``Protein Misaggregation: from Biomolecules to Neurodegenerative Diseases,'' sponsored by the Institute for Complex Adaptive Matter, Boston, Feb. 2004.

Invited Presentations

D.L. Cox:

- *Theoretical Modeling of Prion Disease Incubation Dynamics,* CeresR Forum "Transmissible Spongiform Encephalopathies in Animal and Human Health: The Science and the Policy" sponsored by Virginia Polytechnic Institute, Washington DC, March 2004.

R.R.P. Singh:

- *Prion Diseases,* Colloquium, Tata Institute for Fundamental Research, Bombay India, July 2004

D.L. Mobley:

- "*Modeling Alzheimer's A-Beta Peptide Insertion into Lipid Bilayers*", Vijay Pande group, Stanford Unversity, Dec. 4, 2003
- "*Modeling Alzheimer's A-Beta Peptide Insertion into Lipid Bilayers*", Theoretical and Computational Molecular Biophysics group, The Scripps Research Institute, San Diego, Dec. 11, 2003
- "*Modeling Alzheimer's A-Beta Peptide Insertion into Lipid Bilayers*", St. Jude Children's Research Hospital, Jan. 12, 2004.
- "*Modeling Alzheimer's A-Beta Peptide Insertion into Lipid Bilayers" and "Simulations of Oligomeric Intermediates in Prion Diseases*", Jan. 13, 2004, David Teplow group, Harvard
- "*Modeling Alzheimer's A-Beta Peptide Insertion into Lipid Bilayers*", Jan. 16, 2004, Center for Theoretical Biological Physics, UC San Diego.
- "*Modeling Alzheimer's A-Beta Peptide Insertion into Lipid Bilayers*", Feb. 10, 2004, short talk at Protein Misaggregation: from Biomolecules to Neurodegeneration workshop, Boston, MA, Feb. 9-11, 2004.

- "*Modeling Alzheimer's A-Beta Peptide Insertion into Lipid Bilayers*", Feb. 27, 2004, Biophysics seminar, UC Davis.
- "*The Hunt for the Cause of Cell Death in Alzheimer's Disease*", March 19, 2004, science colloquium, Shasta College, Redding, CA.
- "*Oligomerization and Aggregation in Amyloid Diseases*", April 2, 2004, ICAM workshop on "Lifelike Matter", Santa Fe, N.M.

R.V. Kulkarni,

- *Models of incubation time dynamics in prion diseases,* short talk at Protein Misaggregation: from Biomolecules to Neurodegeneration workshop, Boston, MA, Feb. 9-11, 2004.

Contributed Presentations:

K. Kunes, *Kinetic Model for 1D aggregation of yeast ``prions''*, American Physical Society March Meeting, Montreal, March 2004.

D.L. Mobley, "Modeling Alzheimer's A-Beta Peptide Insertion into Lipid Bilayers", Feb. 17, 2004, poster at Biophysical Society meeting, Baltimore, MD, Feb. 13-18, 2004.

J. Pan, *Ab initio Study of Transition metal binding to the Prion Protein,* American Physical Society March Meeting, Montreal, March 2004.

APPENDIX B

Simulations of Oligomeric Intermediates in Prion Diseases

David L. Mobley, Daniel L. Cox, Rajiv R. P. Singh, Rahul V. Kulkarni, and Alexander Slepoy*
Department of Physics, University of California at Davis, Davis, California; and *Sandia National Laboratories, Albuquerque, New Mexico

ABSTRACT We extend our previous stochastic cellular automata-based model for two-dimensional (areal) aggregation of prion proteins on neuronal surfaces. The new anisotropic model allows us to simulate both strong β-sheet and weaker attachment bonds between proteins. Constraining binding directions allows us to generate aggregate structures with the hexagonal lattice symmetry found in recently observed in vitro experiments. We argue that these constraints on rules may correspond to underlying steric constraints on the aggregation process. We find that monomer-dominated growth of the areal aggregate is too slow to account for some observed doubling-time-to-incubation-time ratios inferred from data, and so consider aggregation dominated by relatively stable but noninfectious oligomeric intermediates. We compare a kinetic theory analysis of oligomeric aggregation to spatially explicit simulations of the process. We find that with suitable rules for misfolding of oligomers, possibly due to water exclusion by the surrounding aggregate, the resulting oligomeric aggregation model maps onto our previous monomer aggregation model. Therefore it can produce some of the same attractive features for the description of prion incubation time data. We propose experiments to test the oligomeric aggregation model.

INTRODUCTION

Prion diseases are a group of neurodegenerative diseases including bovine spongiform encephalopathy (BSE) in cattle, scrapie in sheep and goats, chronic wasting disease in deer and elk, and kuru and Creutzfeldt-Jakob disease (CJD) in humans. These diseases came to the forefront after BSE reached epidemic proportions in Great Britain in the early 1990s, and it was later shown that transmission of BSE to humans can lead to new variant CJD (vCJD) in humans (Bruce et al., 1997; Hill et al., 1997; Scott et al., 1999).

Prion diseases are unusual in that they appear to be caused by infection with some minimal infectious "seed" of misfolded prion protein, which alone may be able to cause disease by catalyzing further misfolding and, in many cases, aggregation of the prion protein. These aggregates are typically amyloidlike fibrils or amyloid plaques (Caughey, 2000). The infectious agent is unusually hard to eliminate by various methods including ultraviolet irradiation, suggesting it contains no nucleic acid and rather only protein, the so-called "protein-only" hypothesis in prion diseases (Weissmann et al., 2002).

In the case of CJD, a sporadic form of the diseases also exists, occurring more or less randomly worldwide with an incidence of about one in a million people per year. It has been suggested that this incidence is due to the very rare event of nucleating the minimal infectious seed by chance in a healthy individual (Come et al., 1993).

Developing an understanding of these diseases is important because, for one, they are invariably fatal. To date, no treatment exists. Additionally, it is not yet clear how large the vCJD epidemic in humans will be; an understanding of the disease process is important to be able to guide the search for treatment ideas.

In many cases, prion diseases result in large, up-to-micron-scale plaques in the brains of people and animals with these diseases. They also involve vacuolization or spongiform change in the brain due to death of neurons (Scott et al., 1996). Additionally, the normal form of the prion protein (known as PrP^{C}) has long been known to misfold and aggregate in vitro when catalyzed by the presence of a misfolded prion protein (PrP^{Sc}) seed (Come et al., 1993). Together, these observations have suggested to some that the aggregation process itself may be important in these diseases (Come et al., 1993; Masel et al., 1999). It has also been suggested that the rate-limiting step in aggregation is nucleation of an appropriate seed, thus the rapid aggregation in the seeded case described above (Come et al., 1993).

Another fact which may be important to this issue is that the prion protein is normally GPI-anchored to the cell surface. Aggregation in vitro as mentioned above is observed in solution rather than in the presence of the GPI anchor on a cell surface, leaving the possibility that the aggregation process in vivo is different.

Aggregation models developed to explore the aggregation process in prion disease include one-dimensional, fibrillar aggregation-and-fission models (Masel et al., 1999; Slepoy et al., 2001), since aggregates grown in vitro are typically seen to be fibrillar. Additionally, our earlier work suggested that an areal aggregation model could explain certain other properties of the diseases (Slepoy et al., 2001). By areal aggregation, we mean two-dimensional aggregation in a relatively regular array, probably on the cell surface due to GPI anchoring, in contrast to the one-dimensional, fibrillar aggregation observed in vitro, and also in contrast to

Submitted April 10, 2003, and accepted for publication July 9, 2003.

Address reprint requests to David L. Mobley, Tel.: 530-752-0446; Fax: 530-752-4717; E-mail: mobley@physics.ucdavis.edu.

Rahul V. Kulkarni's present address is NEC Research Labs, 4 Independence Way, Princeton, NJ 08540.

0006-3495/03/10/2213/11 $2.00

two-dimensional plaques of crossing fibrils which can be observed in vivo. This earlier model is attractive in that it can provide a simple explanation for the long lag phase which is sometimes observed in growth of the amount of infectious material in the brain. This lag phase of little or no growth is followed by a doubling phase with a short characteristic doubling time. Additionally, our earlier model provides a possible explanation of some of the difference between infectious and sporadic forms of CJD (Slepoy et al., 2001). In later work, we used this model to explain and fit experimental dose incubation curves (Kulkarni et al., 2003).

However, there were drawbacks to the earlier aggregation model we proposed. First, no such areal aggregates had so far been observed. Second, the fissioning essential to the model would involve breaking of strong bonds between the proteins, probably bonds between β-sheets (Serag et al., 2002).

More recent experimental work found two-dimensional areal aggregates of prion protein produced during the purification process. These aggregates were examined under electron microscope and found to consist of trimeric or hexameric subunits. These subunits are linked together in a regular array, possibly by their N-terminal sugars or a weak protein-protein interaction (Wille et al., 2002).

This suggested we should modify our earlier model and attempt to reproduce this aggregate morphology. We thought of two basic schemes for growing aggregates of this sort:

1. Growing the aggregate outward, monomer by monomer, from an initial seed, or
2. Oligomeric intermediates (possibly very flexible and of unstable shape), which form on their own in solution and are only catalyzed into stably misfolding in the presence of an existing misfolded seed.

Some evidence in favor of case 2 has already been produced. Monomers of yeast prion can form intermediates if left to stand, which allows aggregation to proceed at an initial faster rate when catalyzed by addition of a seed (Serio et al., 2000). Additionally, the conformation-dependent immunoassay developed by Safar et al. (2002) detects both protease-sensitive and protease-resistant PrP^{Sc}. In hamster brains, sensitive PrP^{Sc} is observed earlier, followed by resistant PrP^{Sc}. This could correspond to case 2 above, where the sensitive PrP^{Sc} is the intermediates that are not yet stably misfolded and the resistant PrP^{Sc} is stably misfolded intermediates.

Work here has been done to further explore these two potential modifications of our earlier model to examine whether they retain the same features and if additional insight can be gained.

It is important to note that even if areal aggregation is not important to the time course of these diseases, the aggregates observed by Wille and co-workers have already provided insight into the structure of the misfolded prion protein (Wille et al., 2002). Theoretical modeling may be able to place further constraints on the protein or subunit structure necessary to reproduce these aggregates, and hence provide valuable information because these aggregates *can* form, even if they are not important to the disease progression.

BASICS OF OUR MODEL

Here we explore the two basic schemes suggested above for growing aggregates like those observed by Wille et al. (2002). To do so, we use a modification of our earlier model. Therefore a recap of common features of these models is useful.

These models are stochastic cellular automata models, meaning that they take place on a lattice with probabilistic interaction and diffusion rules governing the progression of the system. In this case, sites on the lattice are either occupied by individual prion proteins, or water (empty, in the simulation). The protein form at a site can also vary from PrP^{C} to PrP^{Sc}.

Rules vary depending on the model being explored, but the basic procedure is the same. For every simulation step, which represents a small amount of time, we allow proteins and any aggregates to diffuse a small amount on the lattice (each object has a probability $1/(size)^{1/2}$ of moving one lattice site in a given step). Then we look at every protein in the lattice and update its state according to the rules. For example, in our original model, the conformation of an individual prion protein is determined solely by its number of neighboring prion proteins, and this can vary from step to step. After doing this, we add more normal prion monomers to replace any that converted to PrP^{Sc}. This is due to the assumption that this process would be taking place in a small area on a cell, and the normal prion monomers would be added by the cell or diffuse in from other locations on the cell surface to keep the monomer concentration relatively constant.

GROWTH VIA MONOMER ADDITION

First, case 1 from above was explored. Simple rules were developed (Fig. 1) which can reproduce aggregates similar to those observed by Wille et al. (2002). It is important to note that although the rules were designed to reproduce such aggregates, most modifications of these rules could not do so. This means that the rules provide some constraints on the protein-protein interactions necessary to reproduce such aggregates. Also, for the purposes of this model, we are assuming the subunits are hexameric, but the corresponding model for trimeric intermediates is actually much simpler than this model and will produce similar results. Details of the algorithm for this model are covered in Fig. 2.

The rules are as follows. The simulation begins with a single hexagonal subunit consisting of six misfolded monomers (*light gray hexagons* in Fig. 1) which stick some of their residues into an adjacent site, excluding anything else from occupying that site (*black*). Healthy monomers (*light gray spheres*) can then attach via a sugar-bond or other

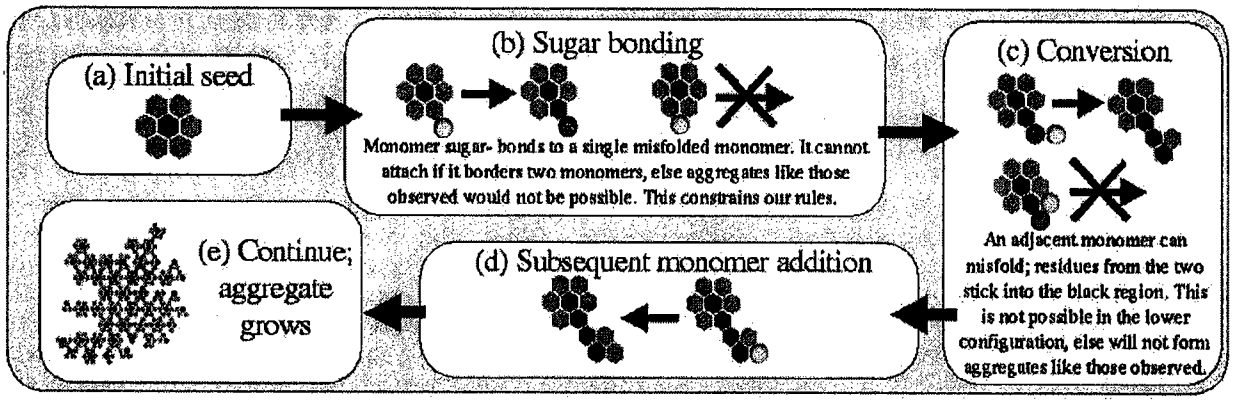

FIGURE 1 Simple rules for monomer-by-monomer growth of aggregates like those observed. Some possible rules can be excluded, thus these rules give insight into how the proteins involved must be interacting with one another. (*a*) The initial seed consists of six misfolded monomers (*light gray hexagons*) surrounding a central region (*black*) which is occupied by some residues sticking into it from the adjacent six sites. (*b*) A healthy monomer (*light gray sphere*) can move adjacent to a misfolded one and attach via a sugar bond or other weak protein-protein interaction (proteins sugar-bonded are colored *dark gray*). This cannot happen if the monomer moves into the site between two misfolded proteins. (*c*) Subsequent monomers can move next to the attached one and misfold and begin to form a new hexamer. Residues from the two stick into the black region, preventing anything else from moving there. This cannot happen if the second monomer is adjacent to the existing hexamer; this would produce irregular aggregates unlike those observed by Wille and co-workers (Wille et al., 2002). (*d*) The forming hexamer can grow and finish via subsequent monomer addition. (*e*) Continue *a–d* for a long time, and an aggregate like the one shown can form.

weak protein-protein interaction to this subunit (*dark gray spheres* to *dark gray hexagons*) but only radially outward from a monomer in the initial hexamer. Additional monomers moving adjacent to the attached monomer can, together with it, misfold but only if the second monomer does not also neighbor the original hexamer. Then additional monomers can attach to this forming hexamer, allowing it to complete. Repeating this process many times can produce mostly regular aggregates with some holes, similar to those observed.

The rules are also probabilistic: above, "can" means that some fraction of the time the event occurs. These probabilities can be changed in the simulation and give different growth rates, but the same essential features and scaling as described below.

If this is in fact how these aggregates are forming, we find out about the orientation of monomers within a hexagonal subunit. We find, as mentioned in the discussion of the rules above, that the N-terminal sugars or attachment sites must stick radially outward from each monomer in a hexagonal subunit (Fig. 1 *b*). This is in agreement with the hexagonal structure proposed by Wille and co-workers (Wille et al., 2002). Additionally, we find that no such regular aggregates can be produced unless the monomer attaching to a previously attached monomer (Fig. 1 *c*) can only attach if it is not adjacent to an existing hexamer. This seems to indicate that the other spaces must be occupied by residues from the existing hexamer, preventing attachment in those sites.

This model can also reproduce gaps in aggregates as observed. In this model gaps are due to variations of the growth rate from average for part of the aggregate, causing several parts of the aggregate to grow apart and then rejoin after leaving a gap.

One reason for developing this model was to see if it would capture the same features of the disease as our original model. Our original model explained the difference between the lag phase and the doubling phase by suggesting that the doubling phase is initiated when aggregates begin to fission, then regrow to a certain fissioning size and break again. Key to this explanation is our result that aggregation speeds up, so that the time for an aggregate to double in size from half its fission size to its fission size is much less than the time for it to get from its initial size to its fissioning size.

To see if this model could produce the same separation of lag and doubling phases, we examined the aggregate growth rate as a function of size in this model (Fig. 3) and found it speeds up only slowly. Naïvely, one would expect the growth rate to be roughly proportional to the square root of the size, as the growth rate is proportional to the circumference of the aggregate, which, assuming a circular aggregate, is $2\pi r$. The size of the aggregate is proportional to the area, πr^2, so the radius is proportional to the square root of the size and thus the rate proportional to the square root of the size. To a good approximation, the growth rate observed here is well-fit by an offset plus a term proportional to $(size)^{1/2}$, as expected.

In this simple picture, one can calculate the ratio of the doubling time to the lag time. The lag time is the time to go from the initial size, say size *0* for simplicity, to size *n*; the doubling time from size *n*/2 to size *n*. Integrating the rate to get the times and taking the ratio we find $t_{doub}/t_{lag} = 1 - 1/\sqrt{2}$ or ~0.293. This means that this model cannot produce such a large separation between lag and doubling times as our earlier model could, at least not without further modification.

This also indicates that if there is a lag phase and if the difference between it and the doubling phase is due to acceleration of aggregation, this picture is not sufficient and

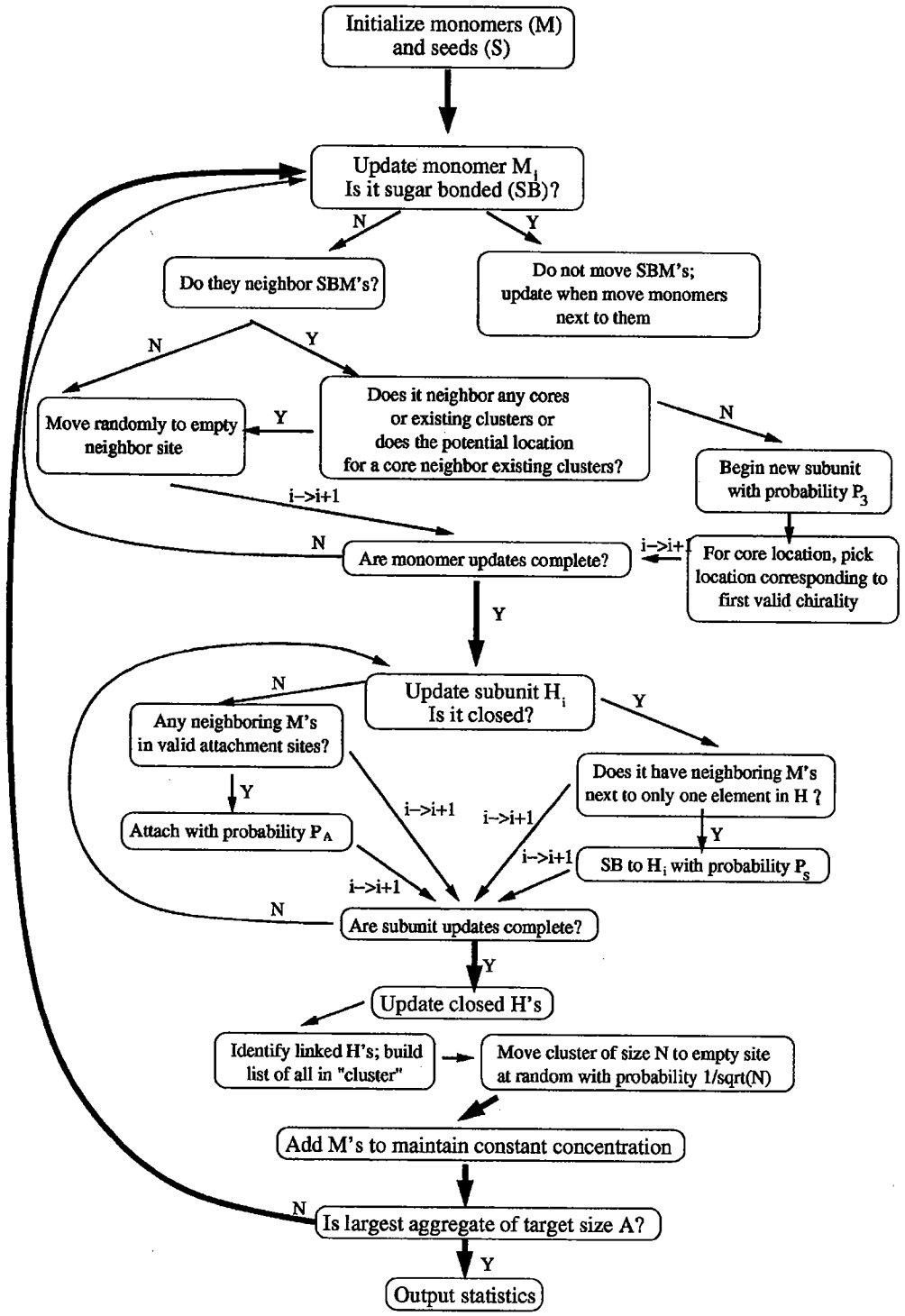

FIGURE 2 Flow chart of simulation for monomer addition model. We typically use $P_3 = 0.2$; we tried a variety of different values for this and values near 0.2 seem to produce the most regular aggregates. We also typically use $P_S = 0.9$. This is not important and roughly sets the simulation timescale. Also, for our statistics, we typically average >1000 such runs as the one described here.

something more like case 2, growth from intermediates, may be a better representation of the disease process.

GROWTH VIA INTERMEDIATES

In this case, aggregation is assumed to be the assembly of independent hexameric intermediates into a larger areal aggregate. The intermediates themselves are not misfolded but only misfold, in this model, when they either aggregate with an existing misfolded seed, or come together in such a way that they can misfold and form a new stable seed. In this way, the model works essentially just like the model of Slepoy et al. (2001), except now hexameric intermediates are playing the role of monomers (Fig. 4). As

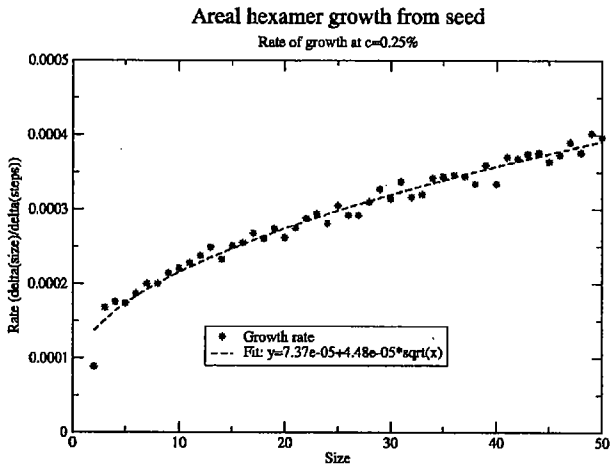

FIGURE 3 Growth rate (change in aggregate size per step) as a function of size for seeded areal aggregation in the monomer growth model. Growth rate goes as the square root of the size with an offset, which was as expected for this model.

mentioned above, there is some evidence that intermediates greatly increase aggregation rate in studies of yeast prions, so this emphasis on the importance of intermediates may be reasonable.

To be able to map this model back into our old model, though, we need to know how the intermediate concentration depends on monomer concentration. And this is not obvious. So a simulation was developed to explore how the concentration of hypothetical hexameric intermediates would depend on monomer concentration. Again, here we are assuming the intermediates are hexameric but we can easily modify the model to accommodate trimers.

To get at the concentration of intermediates, it was assumed that two monomers have a probability P_1 of beginning a new hexameric subunit when they come into contact (see Fig. 5). This new subunit can grow by addition of monomers when they move into appropriate positions (changing this probability does not affect the outcome of the simulation, only the timescale, so it was set to 1). However, this growth process competes with a "dissolving" process by which a monomer that is part of an intermediate but only has one neighboring monomer can break off with a probability P_3. Thus the end destiny of any intermediate that begins is either to form a complete hexameric intermediate, in which case it can persist, or to dissolve completely. Details of the algorithm for this model are shown in Fig. 6.

This dissolving, or reversibility, was included because it was not obvious that at low monomer concentrations, one would expect a reasonable formation rate of intermediates via this mechanism. It was initially thought that at concentrations below something on the order of P_3, breaking would dominate and the formation rate of intermediates would be almost zero. First, the simulation that was developed was used to examine the dependence of time for intermediate formation as a function of monomer concentration (Fig. 7). It was found that at high monomer concentration, the time to form an intermediate scales between $1/c$ and $1/c^2$ (c is concentration). This is because the likelihood of starting an intermediate scales as the dimer concentration ($1/c^2$), whereas the time to add monomers to it scales as $1/c$. On the other hand, at very low monomer concentration, the time asymptotically approaches $1/c^6$. This is due to the fact that at these concentrations, dissolving dominates and it is only in the very rare event that six monomers are in the same place at

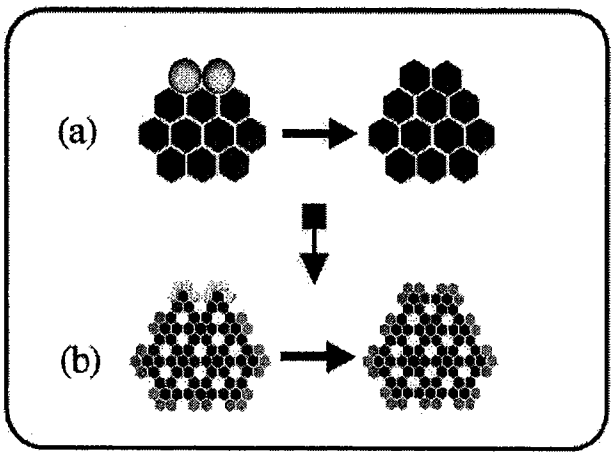

FIGURE 4 (*a*) As in Slepoy's model (Slepoy et al., 2001), subunits were healthy monomers (*light gray spheres*) aggregating with misfolded monomers (*dark gray hexagons*); (*b*), subunits are hexagonal intermediates (*light gray/dark gray*) aggregating with misfolded hexagonal structures (*medium gray/dark gray*). In both cases, the aggregation process and kinetics ought to be, and indeed are, similar.

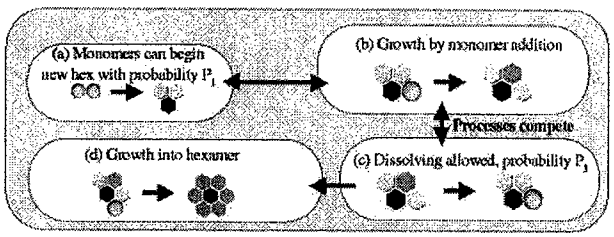

FIGURE 5 Rules for the formation of intermediates. Note that growth and dissolving compete, so that any intermediate eventually either becomes a complete, stable hexagon or dissolves back into monomers. (*a*) Two monomers have a probability P_1 of joining to begin a new intermediate, which is not yet stably misfolded. Black represents a region blocked by some of their residues. (*b*) This can grow by addition of monomers to either "end." After attaching, the monomer sandwiched between the other two has two neighbors and is not allowed to break off, whereas the ones with only one neighbor can. (*c*) A monomer with only one neighboring monomer has a probability P_3 of breaking off in a given step. This competes with the growth process. (*d*) Continuing addition of monomers can result in a finished hexameric intermediate where every monomer has two neighbors and is safe from breaking off.

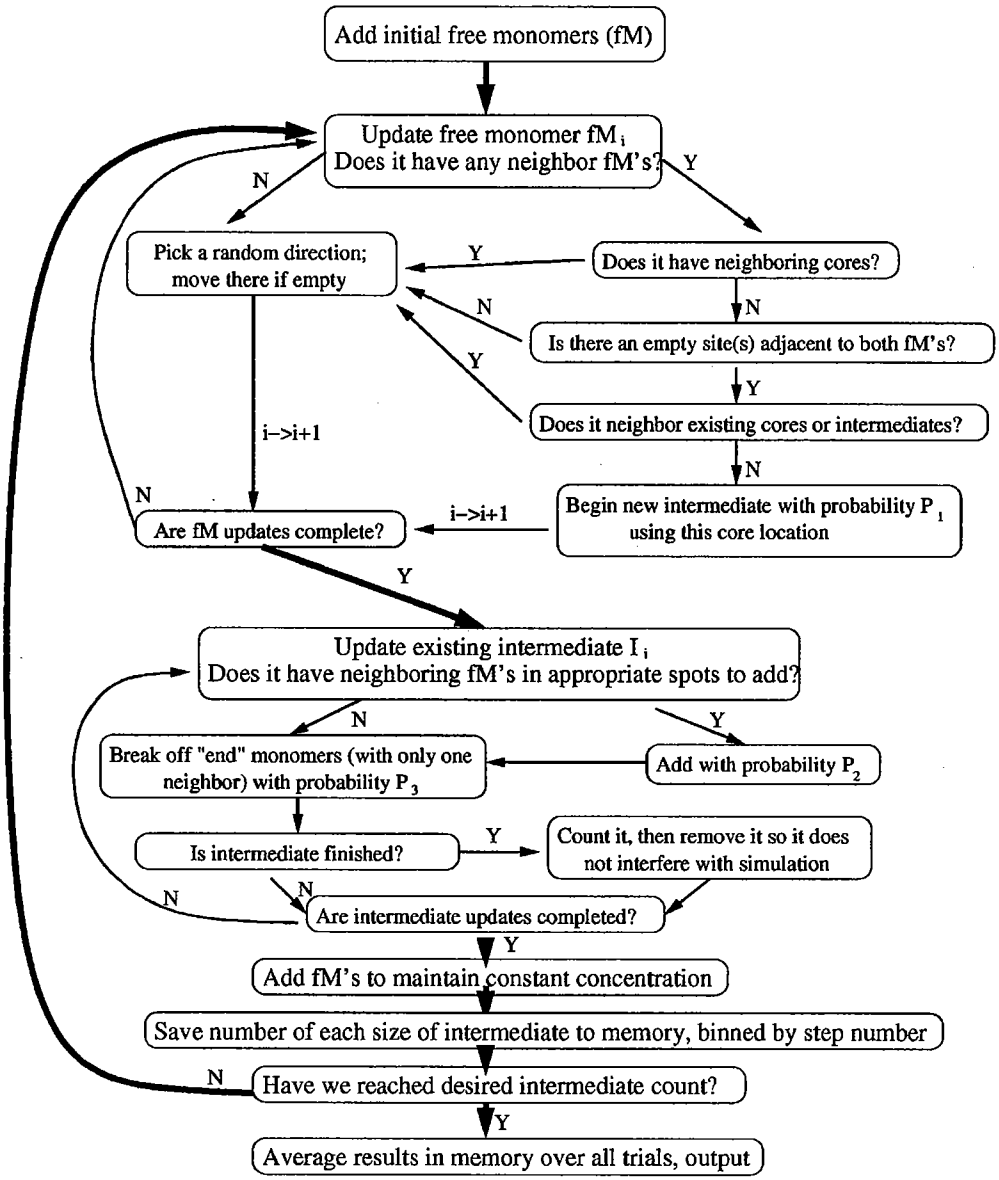

FIGURE 6 Flow chart of simulation for the formation of intermediates. Note that P_1 we vary for different runs, P_2 we typically set to 1 (it sets the simulation timescale and is unimportant), and P_3 we also vary. Finished intermediates are removed so that we can run to a larger number of finished intermediates without the lattice getting clogged. Here, also, we typically average >1000 trials for good statistics.

almost the same time that an intermediate can finish. The probability of that scales as $1/c^6$.

It is interesting to note that the beginning of the transition between high concentration behavior, where most intermediates successfully become complete, and low concentration behavior, where only a lucky few do, begins at a concentration on the order of the breaking probability, P_3. This suggests that if the strength of bonds between intermediates could be weakened somehow, the biological number of intermediates could be drastically decreased by pushing biological monomer concentrations into the $1/c^6$ regime.

The goal, however, was to determine the dependence of the intermediate concentration on monomer concentration. This just provided a formation rate, and the functional form was uncertain. So another sort of result was examined, wherein we began examining behavior of the system as a function of time, and measured the number of different partial intermediates (two monomers, ...five monomers, hexameric intermediates). We first examined the case with no breaking ($P_3 = 0$) to check our results, because it is relatively easy to work out kinetics in that case. A sample of one of these plots is shown in Fig. 8, with symbols as data points and solid lines as approximate kinetics fits. It is important to note that in this case, and in the case of nonzero breaking probability, the number of dimers, trimers, tetramers, and pentamers reaches equilibrium relatively quickly and then the hexamer number begins to grow linearly at a rate equal to the rate of dimer formation.

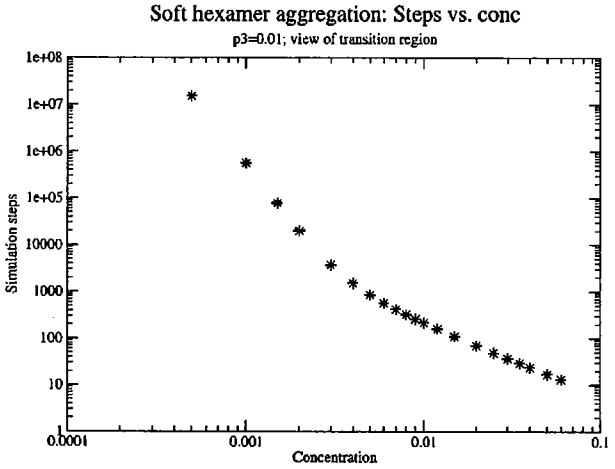

FIGURE 7 Simulation steps (time) to form a hexameric intermediate as a function of monomer concentration. Log-log scale. Note the broad transition to dissolving-dominated behavior at low concentration. The transition actually continues to even lower concentration than can be seen here. At very low concentration the time eventually scales as $1/c^6$. Standard deviations fall within the size of the data points on this plot.

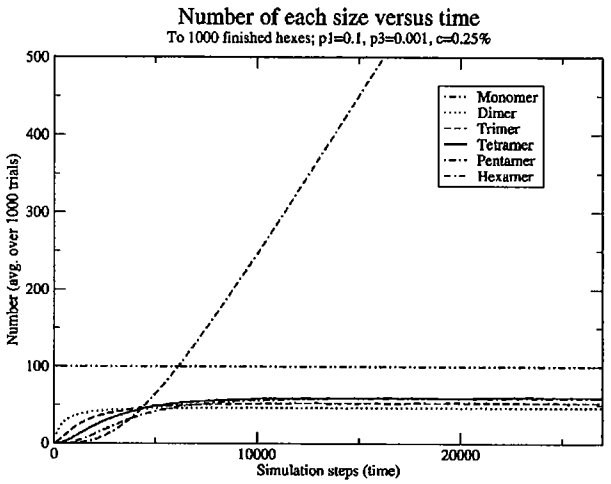

FIGURE 9 Number of each size as a function of time (simulation steps) with nonzero breaking. Compare to Fig. 6; note that the number of intermediates reaches equilibrium faster and at smaller numbers, but that the hexamer number still grows linearly at long times.

Sample results with nonzero breaking are shown in Fig. 9. These results are qualitatively similar, except the number of pre-intermediates that persists is much lower. In the high-breaking limit, the very low level of intermediates demonstrates that either a potential intermediate gets "lucky" and quickly forms an intermediate, or it dissolves back to monomers, leaving few dimers, trimers, and so on.

The kinetics equations we can write down to describe this simulation are relatively simple. With r_{nm} as the rate constant for forming m-mers from n-mers, and b_{nm} as the rate of breaking n-mers into m-mers plus monomers, we can write:

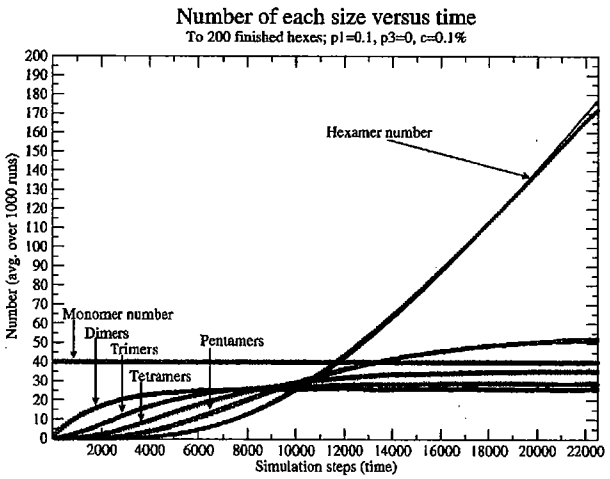

FIGURE 8 Number of each size as a function of time (simulation steps), with zero breaking. Note that, at long times, intermediates reach equilibrium and the hexamer number begins growing linearly with time. Points are simulation data points; solid lines (mostly overlapping points) are approximate kinetics results.

$$[c_1] = c \tag{1}$$

$$\frac{d[c_2]}{dt} = r_{12}[c_1]^2 - r_{23}[c_1][c_2] - b_{21}[c_2] + b_{32}[c_3] \tag{2}$$

$$\frac{d[c_3]}{dt} = r_{23}[c_1][c_2] - r_{34}[c_1][c_3] - b_{32}[c_3] + b_{43}[c_4] \tag{3}$$

$$\frac{d[c_4]}{dt} = r_{34}[c_1][c_3] - r_{45}[c_1][c_4] - b_{43}[c_4] + b_{54}[c_5] \tag{4}$$

$$\frac{d[c_5]}{dt} = r_{45}[c_1][c_4] - r_{56}[c_1][c_5] - b_{54}[c_5] \tag{5}$$

$$\frac{d[c_6]}{dt} = r_{56}[c_1][c_5]. \tag{6}$$

Since we know that the hexamer number grows linearly at steady state and all of the other concentrations are unchanging, we can greatly simplify the above kinetics by looking at the steady state only. We can work backward from the steady-state behavior of the hexamers to find the dependence of the steady-state rate of hexamer formation on the different kinetic parameters and ultimately on the monomer concentration.

This straightforward kinetics analysis produces the equilibrium result

$$m = \frac{r_{12}c^2}{1 + \frac{b_{21}}{r_{23}c}\left\{1 + \frac{b_{32}}{r_{34}c}\left[1 + \frac{b_{43}}{r_{45}c}\left(1 + \frac{b_{54}}{r_{56}c}\right)\right]\right\}}, \tag{7}$$

where m is the slope at equilibrium of the hexamer formation rate.

The constants in our simple result for m, above, can be measured from our simulation. However, our simulation does not necessarily reproduce what these constants would

be in a biological system. So it is difficult to say exactly what the rate of intermediate formation, m, would be in a real system. However, it is nevertheless useful to know the functional form of its dependence on the monomer concentration.

The result that the hexamer number begins growing linearly eventually is independent of monomer concentration. This is important because it means some hexamers can form given these simple rules even if breaking dominates. Given that result, it seems safe to assume that if hexameric intermediates are stable, some will form in biological systems.

In our model, the hexamer number grows linearly indefinitely, which is obviously unrealistic biologically. The reason for this is that we include no mechanism to remove finished hexamers. Realistically, they would be cleared from the body somehow. They could be endocytosed from the cell surface and degraded via the proteasome mechanism or some other pathway. Additionally, any hexamers being taken up into aggregates would reduce this number. Regardless, realistically the number should stabilize at some fixed value determined by the balance of the clearance rate and the formation rate.

With the result that some hexamers form even at low monomer concentrations (and more would form if they are trimers), a model was developed where now hexameric intermediates occupy a single cell on the lattice (equivalently, these could be trimeric intermediates). This model, described below, largely maintains the same attractive features of the original, showing that if areal aggregation is the explanation for these features, as we suggested, this aggregation could be of hexameric intermediates.

Part of our basis for this model is the observation that the intermediates are not yet stably misfolded since formation of intermediates in studies of yeast prions does not lead to a change in circular dichroism results; it is only when they aggregate with a seed that they stably misfold (Serio et al., 2000). This also is justified by observing that if intermediates were stably misfolded, they could act as seeds on their own, without the necessity of an external seed initiating the infection, and thus there would be no difference between sporadic and infectious CJD. Therefore, for aggregates consisting of misfolded oligomers like those observed by Wille et al. (2002), intermediate misfolding must be catalyzed by existing aggregates or few-hexamer misfolded oligomers. We hypothesize that the mechanism for this is intermediates forming bonds to an existing seed. When solvent is excluded locally around these oligomers and their neighbors include a misfolded oligomer or aggregate, they misfold. The important point is that it is solvent exclusion around an intermediate that can cause it to misfold, making this a very rare sporadic event. But a misfolded seed can help this process by providing a place where intermediates bond, helping the solvent-exclusion process. These rules make this model essentially identical in terms of kinetics to our original model. Details of the algorithm for this model and mapping are shown in Fig. 10.

However, from our old model we estimated the sporadic form of the disease could have a peak at ~1000 years, given a biological concentration of 10^{-3}%. In our new model we find that it is very difficult to estimate this number as the scaling of the time as a function of monomer concentration is complicated. It was hoped that this model would give a result for the onset of sporadic disease that could be compared with the time for onset of the infectious form to see if the results were consistent with the roughly 1-in-10^6 incidence of sporadic CJD that we earlier pointed out. Unfortunately, it is difficult for our model to give a concrete answer at this time as the answer depends too much on the value of the biological monomer concentration. We do find, however, that the power law used previously to scale the sporadic data, c^{-3}, is a lower bound on the separation. That is, the actual exponent should be larger, meaning that we previously underestimated the separation of timescales. Thus although we cannot say exactly what the separation of timescales here will be, we can say that it will be greater than the two orders of magnitude that we previously estimated.

This work suggests that a model like our earlier one, modified to involve areal aggregation of hexameric or trimeric intermediates, could maintain the same attractive features of our earlier model in explaining certain aspects of the diseases. However, without precise knowledge of the biological monomer concentration and a way to measure relevant rate constants, it is difficult to make numerical predictions from this model.

DISCUSSION

Our work has shown that both in the case of monomer addition to a seed, and in the case of growth via intermediates, it is possible to produce aggregates like those observed by Wille et al. (2002). This leaves the question of how such aggregates actually grew. If areal aggregation is the cause, or part of the cause, of the difference between lag and doubling times, as suggested by Slepoy et al. (2001), then our work suggests that intermediates are already present in vivo before aggregation.

Our work has also shown that a model can be developed which, with suitable parameters, can reproduce areal aggregates like those actually observed while maintaining the same features of our original model.

Whether or not areal aggregation is actually important in these diseases, we can gain insight from this model. If the aggregates observed are growing via monomer addition, we gain some constraints on the structure simply from our rules. On the other hand, if intermediates are important to aggregation, then our results indicate the intermediate concentration can be quite important. At high intermediate concentrations, intermediates form relatively fast. However, at low intermediate concentrations, intermediate formation

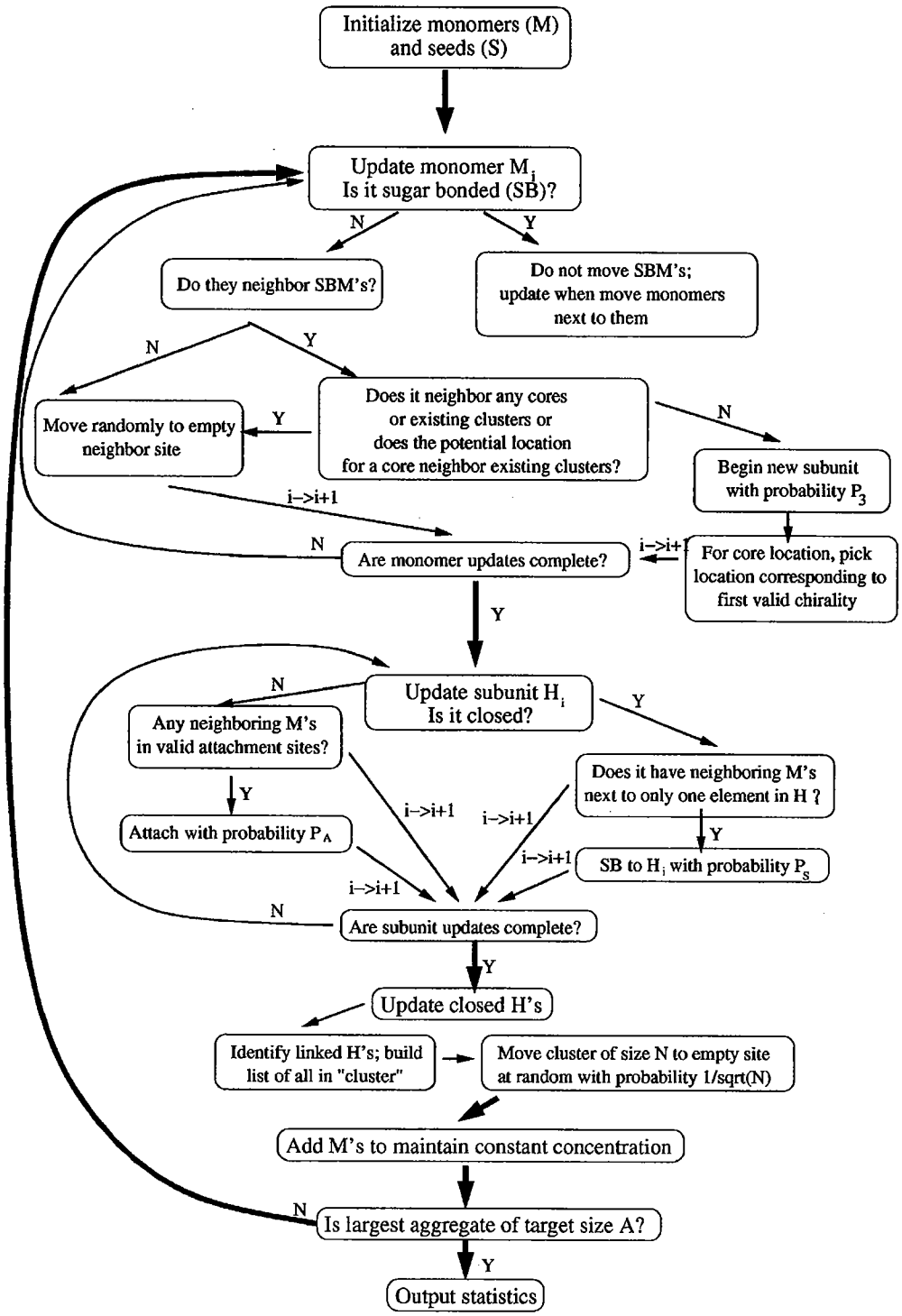

FIGURE 10 Flow chart for simulation mapping back into our original model. Here we basically have free monomers (*fMs*), attached monomers that are not yet stably misfolded (*aM*), and monomers that have stably misfolded and aggregated (*H*). We have some choice of a parameter, $Q_{bc} = m$. This model will capture the features of our original model for m between 3 and 6, and the simulation will proceed in exactly the same way. We compute N_{bc}, the bond coordination number, with $N_{bc} = n_{fM} + n_{aM} + (m - 1) \times n_H$, where the n is the number of neighboring *fMs*, and so on. N_{hc}, the "hardening" or aggregating coordination number, is given by $N_{hc} = n_{fM} + n_{aM} + n_H$. We refer to Q_{bc} as the bonding critical coordination number and Q_{hc} as the "hardening" critical coordination number.

timescales as $1/c^6$. This result is exciting because it suggests the intermediates as a target to prevent aggregation. Simply reducing the monomer concentration by a factor of 2 would decrease the number of intermediates by a factor of 2^6 or 64. Within our model, this would certainly increase the aggregation time, and thus slow down the disease, by at least the same factor. For a disease which can typically incubate for years, this obviously would be a great advantage.

In this case, the location of the transition between low concentration behavior and high concentration behavior is, roughly speaking, set by the probability of monomers breaking off from an intermediate before it becomes a sta-

ble hexamer. Thus if this probability could be increased slightly—that is, the bonds between monomers could be weakened slightly—it would have the result described above. This could provide an explanation for one experimental observation. Humans have a methionine/valine polymorphism at codon 129 of the gene for the prion protein. To date, everyone affected by vCJD has been methionine/methionine homozygous. This effect was also seen in the prion disease Kuru, where the methionine/methionine genotype was associated with increased susceptibility and the shortest incubation time (Goldfarb, 2002). If replacing methionine with valine weakened the monomer-monomer bonds within a forming intermediate and reduced intermediate concentration, this could have exactly the effect described above. This is, however, highly speculative, but as Wille et al. (2002) refine their model of the oligomer structures, it will be interesting to see if this residue falls in the region important to bonding between monomers.

In all, our work shows that our earlier model can be extended to produce aggregates like those observed in vitro while still maintaining its attractive features. Our work also suggests possible mechanisms for formation of these aggregates. If the aggregates form by monomer addition, it constrains protein structure. If they form by addition of intermediates, it highlights the importance of bonds within the intermediates as a target for possible treatment strategies. Our model suggests that an experiment to measure the biological intermediate concentration, if there is such a concentration, would be very useful. That would indicate whether such intermediates are present at a high enough concentration to be important biologically. Additionally, this work suggests that experimentalists should check and see whether reasonably-sized aggregates of prion protein can be found in vivo on the cell surface. This confinement to the cell surface conceivably could make the difference between the one-dimensional fibrillar aggregates typically observed in vitro and two-dimensional areal aggregates like those suggested by the model of Slepoy et al. (2001). Direct measurements, or detailed simulations, giving the strengths of β-bonds between monomers compared to bonds between subunits would be very useful.

One simple way to experimentally discern between growth via monomers or intermediates may be to look at high resolution at the boundary of actual areal aggregates. If growth is by monomers, aggregates will form with monomer-scale roughness at their boundaries (Fig. 1 *e*) while if growth is by intermediates, there will be no such roughness (Fig. 4 *b*). Experimentally, the absence of such roughness would not prove the growth via intermediate hypothesis because incomplete oligomers at the edge of the aggregate could be removed in the purification process, possibly by proteinase K digestion. However, the presence of such roughness would certainly suggest that monomer growth is important.

A more general scheme for experimentally testing the possible role of intermediates and estimating their concentration is via spin labeling (Hubbell et al., 1998; Columbus and Hubbell, 2002). Briefly, a small molecule with a free spin can preferentially react and attach to cysteine residues in proteins. Frequently, these residues are moved around a protein via mutagenesis to then map out structures, but for these purposes a less refined approach is required. Since the PrP protein already possesses cysteine residues at the position of the disulfide bond, the spin labels can attach there (and will not disrupt the disulfide bond). Then the spin-spin interactions will produce a different characteristic spectrum for monomers, incomplete intermediates, and complete intermediates, in particular, with a progressive broadening upon moving from monomers to complete intermediates. Since the spins can have interactions with other spins within a 3-nm sphere, we do not doubt that the broadening will be observable. Of course, since the spin labels will react with *any* cysteines present, it is important to carry this out first by in vitro aggregation experiments with purified prion extracts. This will help to identify the conditions which can lead to areal aggregation as observed by Wille et al. (2000), and serve as an existence proof at least for significant oligomeric intermediate concentrations.

We gratefully acknowledge fruitful discussions on spin labeling with John Voss, and on areal prion aggregates with Holger Wille. R.R.P.S. and D.L.C. have benefited from discussions at workshops of the Institute for Complex Adaptive Matter. Sandia is a multiprogram laboratory operated by Sandia Corporation, a Lockheed Martin Company, for the United States Department of Energy's National Nuclear Security Administration under contract DE-AC04-94AL85000.

This research is supported in part by the Nanophases in the Environment, Agriculture and Technology Integrative Graduate Education, Research and Training program sponsored by the National Science Foundation (IGERT grant DGE-9972741), and by the U.S. Army (Congressionally Directed Medical Research Fund, grant NP020132).

REFERENCES

Bruce, M. E., W. G. Will, J. W. Ironside, I. McConnell, D. Drummond, A. Suttie, L. McCardle, A. Chree, J. Hope, C. Birkett, S. Cousens, H. Frasier, and C. J. Bostock. 1997. Transmissions to mice indicate that "new variant" CJD is caused by the BSE agent. *Nature*. 389:498–501.

Caughey, B. 2000. Prion protein interconversions. *Philos. Trans. R. Soc. Lond. B Biol. Sci.* 356:197–202.

Columbus, L., and W. L. Hubbell. 2002. A new spin on protein dynamics. *Trends Biochem. Sci.* 27:288–295.

Come, J. H., P. E. Fraser, and P. T. Lansbury, Jr. 1993. A kinetic model for amyloid formation in the prion diseases: importance of seeding. *Proc. Natl. Acad. Sci. USA*. 90:5959–5963.

Goldfarb, L. G. 2002. Kuru: The old epidemic in a new mirror. *Microbes Infect.* 4:875–882.

Hubbell, W. L., A. Gross, R. Langen, and M. A. Lietzow. 1998. Recent advances in site-directed spin labelling of proteins. *Curr. Opin. Struct. Biol.* 8:649–656.

Hill, A. F., M. Desbruslais, S. Joiner, K. C. L. Sidle, I. Gowland, J. Collinge, L. J. Doey, and P. Lantos. 1997. The same prion strain causes vCJD and BSE. *Nature.* 389:448–450.

Kulkarni, R., A. Slepoy, R. R. P. Singh, and F. Pázmándi. 2003. Theoretical modeling of prion disease incubation. *Biophys. J.* 85:707–718.

Masel, J., V. A. A. Jansen, and M. A. Nowak. 1999. Quantifying the kinetic parameters of prion replication. *Biophys. Chem.* 77:139–152.

Safar, J. G., M. Scott, J. Monaghan, C. Deering, S. Didorenko, J. Vergara, H. Ball, G. Legname, E. Leclerc, L. Solforosi, H. Serban, D. Groth, D. R. Burton, S. B. Prusiner, and R. A. Williamson. 2002. Measuring prions causing bovine spongiform encephalopathy or chronic wasting disease by immunoassays and transgenic mice. *Nature Biotech.* 20:1147–1150.

Scott, M. R. D., G. C. Telling, and S. B. Prusiner. 1996. Transgenetics and gene targeting in studies of prion diseases. *In* Prions Prions Prions. S. B. Prusiner, editor. Springer-Verlag, Berlin, Heidelberg. pp.95–123.

Scott, M. R., R. Will, H.-O. B. Nguyen, P. Tremblay, S. DeArmond, and S. B. Prusiner. 1999. Compelling transgenetic evidence for transmission of bovine spongiform encephalopathy prions to humans. *Proc. Natl. Acad. Sci. USA.* 96:15137–15142.

Serag, A. A., C. Altenbach, M. Gingery, W. L. Hubbell, and T. O. Yeates. 2002. Arrangement of subunits and ordering of β-strands in an amyloid sheet. *Nat. Struct. Biol.* 9:734–739.

Serio, T. R., A. G. Cashikar, A. S. Kowal, G. J. Sawicki, J. J. Moslehi, L. Serpell, M. F. Arnsdorf, and S. I. Lindquist. 2000. Nucleated conformational conversion and the replication of conformational information by a prion determinant. *Science.* 289:1317–1321.

Slepoy, A., R. R. P. Singh, F. Pázmándi, R. V. Kulkarni, and D. L. Cox. 2001. Statistical mechanics of prion diseases. *Phys. Rev. Lett.* 87: 581011–581014.

Wille, H., M. D. Michelitsch, V. Guenebaut, S. Supattapone, A: Serban, F. E. Cohen, D. A. Agard, and S. B. Prusiner. 2002. Structural studies of the scrapie prion protein by electron crystallography. *Proc. Natl. Acad. Sci. USA.* 99:3563–3568.

Weissmann, C., M. Enari, P.-C. Klohn, D. Rossi, and E. Flechsig. 2002. Transmission of prions. *J. Infect. Dis.* 186:S157–S165. (Suppl.)

APPENDIX C

Biophysical Journal Volume 86 June 2004 3585–3597

Modeling Amyloid β-Peptide Insertion into Lipid Bilayers

David L. Mobley,* Daniel L. Cox,* Rajiv R. P. Singh,* Michael W. Maddox,† and Marjorie L. Longo†
*Department of Physics, and †Department of Chemical Engineering and Materials Science, University of California, Davis, California

ABSTRACT Inspired by recent suggestions that the Alzheimer's amyloid β peptide (Aβ) can insert into cell membranes and form harmful ion channels, we model insertion of the 40- and 42-residue forms of the peptide into cell membranes using a Monte Carlo code which is specific at the amino acid level. We examine insertion of the regular Aβ peptide as well as mutants causing familial Alzheimer's disease, and find that all but one of the mutants change the insertion behavior by causing the peptide to spend more simulation steps in only one leaflet of the bilayer. We also find that Aβ42, because of the extra hydrophobic residues relative to Aβ40, is more likely to adopt this conformation than Aβ40 in both wild-type and mutant forms. We argue qualitatively why these effects happen. Here, we present our results and develop the hypothesis that this partial insertion increases the probability of harmful channel formation. This hypothesis can partly explain why these mutations are neurotoxic simply due to peptide insertion behavior. We further apply this model to various artificial Aβ mutants which have been examined experimentally, and offer testable experimental predictions contrasting the roles of aggregation and insertion with regard to toxicity of Aβ mutants. These can be used through further experiments to test our hypothesis.

INTRODUCTION

Scientific and public interest in Alzheimer's disease has surged in the last several decades. The reason for this is simple: with increasing life expectancy, Alzheimer's disease has emerged as the most prevalent form of late-life mental failure in humans (Selkoe, 2001).

Alzheimer's disease (AD) is a neurodegenerative disease involving progressive memory impairment, altered behavior, decline in language function, disordered cognitive function, eventual decline in motor function, and, finally, death (Selkoe, 2001). In AD, the brain is typically marked by lesions (Selkoe, 2001), neuronal damage, and vascular damage (Durell et al., 1994). These lesions are typically associated with extracellular plaques, called amyloid plaques, and intraneuronal fibrillar tangles (Durell et al., 1994; Selkoe, 2001). The tangles are composed of a protein called *Tau* and are called Tau tangles, whereas the extracellular plaques are largely composed of amyloid β peptide (Aβ) in 40- and 42-residue forms (Selkoe, 2001) (denoted Aβ40 and Aβ42, respectively). These insoluble amyloid plaques composed of Aβ are considered a hallmark of AD. However, they are not specific to AD (Dickson and Vickers, 2001) and have been observed in older patients free from AD symptoms (Jarrett et al., 1993). It has been pointed out that correlations between amyloid plaque density and severity of dementia are weak, whereas there are stronger correlations between soluble Aβ levels and severity of dementia (Walsh et al., 2002). This is one reason for the suggestion that oligomers of Aβ may be more important to toxicity than large insoluble aggregates or plaques. Evidence for this idea has been provided in vivo (Walsh et al., 2002) and in vitro (Hartley et al., 1999; Lambert et al., 1998).

One mechanism by which oligomers can damage cells is formation of pores or ion channels through the cell membrane. Early work in this area showed that Aβ can insert into planar lipid bilayers and allow a calcium current upon insertion, and further that these channels can be blocked (Arispe et al., 1993), suggesting that the calcium current is really due to channel formation, not just bilayer permeabilization by the peptide. Theoretical modeling based on predicted secondary structures for membrane-bound Aβ has suggested that the Aβ peptide can form channels with four or six Aβ subunits in each leaflet of the bilayer (for a total of 8 or 12 per channel; Durell et al., 1994). More recent work has been done using atomic force microscopy to look at the structure of Aβ inserted in planar lipid bilayers and has found what appear to be channels consisting of four or six visible subunits around a central pore, consistent with the theoretical picture described above. The monomers oligomerize after insertion into the bilayer. Furthermore, in the presence of these oligomers, current can flow (Lin et al., 2001). Lin et al. (2001) also show that, under similar conditions, Aβ42 induces neuritic degeneration and death in cell culture and that this toxicity is calcium-dependent and blocked by zinc. Imaging work by another group has also shown that *A*β40 oligomers with the E22G mutation (where glutamate, *E*, at residue 22 is replaced with glycine, *G*), which causes a form of familial AD, can form pore-like structures (Lashuel et al., 2002). These pore-like structures actually could be intermediates which, when not membrane-bound, build up into the amyloid plaques observed in the brain of AD patients (Lashuel et al., 2002).

Based on these suggestions, and the observation of Lin et al. (2001) that oligomers in the membrane form after insertion of monomers, we model insertion of the Aβ peptide

Submitted July 30, 2003, and accepted for publication March 5, 2004.

Address reprint requests to David Lowell Mobley, Physics Department, University of California at Davis, One Shields Avenue, Davis, CA 95616. Tel.: 530-752-0446; E-mail: mobley@physics.ucdavis.edu; web: http://asaph.ucdavis.edu/~dmobley.

0006-3495/04/06/3585/13 $2.00

doi: 10.1529/biophysj.103.032342

into the cell membrane. We first examine the regular Aβ40 and Aβ42 peptides, then the 40- and 42-residue versions of all of the mutations in the Aβ peptide that are known to cause familial AD (FAD) and reduce the average age of onset for the disease compared to people with sporadic AD (Selkoe, 2001). We believe FAD mutants provide a tool for assessing proposed toxicity mechanisms, in that the biological toxicity mechanism should explain why these mutants cause FAD. Our reasoning in looking at these mutants is that if the insertion behavior of the FAD mutant peptides is different, this could make a difference in the prevalence of oligomers in the membrane and thus have an effect on toxicity, if membrane-associated oligomers are indeed important for toxicity in vivo. Although some earlier modeling work has dealt with the structure of Aβ40 in a lipid bilayer (Pellegrini-Calace et al., 2003), we believe this work is the first to compare insertion of FAD mutants.

This system is modeled using a Monte Carlo (MC) code which has been developed to study insertion behavior of peptides into lipid bilayers. This model, which is specific at the amino acid level, allows us to simulate larger peptides and longer timescales than traditional molecular dynamics simulation studies. The configurational steps are sufficiently small that it has been used successfully to suggest insertion mechanisms, as well as to describe insertion conformations for some peptides (Maddox and Longo, 2002a,b). Here, we find that in all cases the peptide inserts relatively easily. However, we find differences in the conformations the peptide adopts once inserted. These differences in the prevalence of conformations are our central result. Relative to the normal Aβ peptide, most of the FAD mutant peptides are more likely to insert only partially in the bilayer. We point out similarities between this partially inserted conformation and the predicted channel structures (Durell et al., 1994). Thus we suggest that FAD mutants may, in this way, facilitate formation of harmful channels. Moreover, the Aβ42 peptide, with additional hydrophobic residues, has a greater tendency than Aβ40 to hang up in this conformation, and this may correlate with the increased toxicity of Aβ42.

INTRODUCTION TO THE MODEL AND METHOD

Model energy function

The Monte Carlo model used here has been described in detail in an earlier publication in this journal (Maddox and Longo, 2002a). Accordingly, we give a brief overview of the essentials here and direct the interested reader to the earlier reference for greater detail.

The model follows previous work from the past decade, most notably and closely that of Milik and Skolnick (1992, 1993) and Baumgaertner (1996). Each amino acid residue is treated as a sphere of identical 1.5 Å radius. There are three contributions to the potential energy function which are residue-independent: 1), U_s, which is a hard-core steric interaction preventing residue-residue overlap; 2), U_T, an energy measuring the cost of rotating the peptide planes of successive residues, which is periodic in the torsional angle ϕ between successive residues and has a shallow minimum at $\phi = 52.1°$; and 3), U_A, characterizing the energy of distortion of the angle θ between adjacent bonds, with a shallow minimum at $\theta = 89.5°$.

The lipid bilayer with surrounding water is modeled as a medium without molecular specificity, but with three different spatial regions. The bilayer's normal is taken to lie along the z axis, so these regions are invariant in the x–y plane. The bilayer has overall thickness $2(z_0 + z_h)$, where z_0 is the length of the acyl chains of a given leaflet, and z_h is the width of the headgroup region. We have used $z_h = 4.5$ Å and $z_0 = 13.5$ Å. We have also tried different chain lengths z_0 but we do not present the results here as they were not significantly different except for reductions in the amount of the transbilayer conformation of the inserted peptide when the membrane is sufficiently thick, as we discuss in Results.

The water-lipid medium is characterized by three dimensionless functions, two of which couple linearly to residue specific parameters we discuss in the next paragraph. These functions are (as shown in Fig. 1):

1. $w(z)$, which measures the fractional water content; this is modeled as a step function with exponentially rounded edges (decay length of 2 Å) that is zero in the hydrophobic acyl chains, one in the water region, and varies smoothly through the head region.
2. A polarity function $p(z)$, also exponentially rounded with the same decay length, and chosen to be one in the lipid head regions and water while falling to some small value $1-f_q$ (where f_q, the polarity factor, determines the polarity of the tail region, with larger f_q corresponding to a less polar tail region) after approximately one residue diameter into the tail region.
3. A hydrophobicity function $y(z)$, which is the sum of two exponentially rounded step functions: one which is zero in the water region and saturates in the head region, proportional to the total gain of hydrophobic energy in the head region, and a second which saturates in the tail region after approximately one residue diameter and accounts for the hydrophobic energy gained for residues penetrating the acyl tail region.The water content $w(z)$ couples linearly to the external hydrogen bonding energy of each residue, which is residue independent in form. The net hydrogen bonding energy is taken as U_H given by a sum over residues i as

$$U_H = \sum_i (w(z_i)H_0 + (1 - w(z_i))H_{int}(i)), \qquad (1)$$

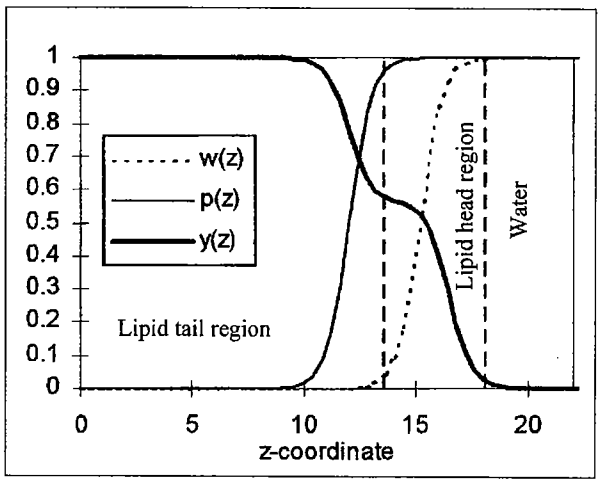

FIGURE 1 Functions characterizing bilayer properties. The lipid bilayer is described by three functions, $w(z)$ for the fractional water content, $p(z)$ for the polarity, and $y(z)$ for the hydrophobicity. Here the z axis is perpendicular to the plane of the bilayer, and the functions (and the bilayer) are symmetric at $\sim z = 0$.

where $H_0 = -6.12$ kcal/mol is the transfer energy of an unbonded peptide group to water and $H_{int}(i)$ the internal hydrogen bonding energy associated with α-helix formation given by

$$H_{int}(i) = \frac{H_0}{4} \sum_{n=-4,-3,3,4} V_H(|\vec{r}_{n+i} - \vec{r}_i|). \quad (2)$$

V_H is a nearly hard-core function of the separation between residue i and the potential helical hydrogen bonding partners along the peptide chain, as proposed by Milik and Skolnick (1993).

Residue specificity is included in two energies associated with polarity and hydrophobicity. First, a potential energy term $U_Q = \sum_i q_0(i)p(z_i)$ is included, where $q_0(i)$ is the residue-specific polar energy associated with charged or partially charged functional groups. Second, a hydrophobic energy $U_B = \sum_i B(i)$ is included, where

$$B(i) = y(z_i)b_0(i) + (1 - y(z_i))\frac{b_1(i)}{4} \times \sum_{n=-4,-3,3,4} V_H(|\vec{r}_{n+i} - \vec{r}_i|). \quad (3)$$

Here, $b_0(i)$ is residue-specific and measures the water-to-alkane Gibbs hydrophobic transfer energy for residue i, and $b_1(i)$ is the maximum reduction in hydrophobic energy due to helical folding. The value $b_0(i)$ is taken to be proportional to the stochastic accessible area of the residue. The helical-folding related term derives from the loss of accessible surface area associated with helix formation. Values for $q_0(i)$, $b_0(i)$, and $b_1(i)$ for all residues are tabulated in the previous work (Maddox and Longo, 2002a). Note that because the model treats the lipids and water only as media, the hydrophobic energy must be included explicitly in our model energy function.

Because of the way the hydrophobic and hydrogen bonding energies are calculated—simply based on local helicity—the simulation is biased toward α-helices, as β-structure involves longer range interactions and is not taken into account by the model. Therefore, the model will not accurately describe insertion behavior of any peptide that inserts while in a conformation rich in β-structure. Fortunately, the monomeric Aβ peptide is predicted, based on secondary structure, to be α-helical between residues 15 and 40 or 42 (Durell et al., 1994; Pellegrini-Calace et al., 2003) when membrane-bound. Experimental NMR work in aqueous sodium dodecyl sulfate micelles, which to some extent resemble a water-membrane medium, confirms this for Aβ40 (Coles et al, 1998). Thus the model's bias away from β-structure should not play a significant role here. Indeed, we find that the region mentioned above inserts into the membrane in a largely helical structure, as described below.

Our total energy is then taken as the sum $U = U_S + U_T + U_A + U_B + U_Q + U_H$. All of our modeling presented below is done at pH 7.0 with temperature 305 K, and uses a polarity factor $f_q = 0.85$, corresponding to a polarity between that of octanol and hexadecane. The choice of this value is based on experimental studies (Griffith et al., 1974; Roseman, 1988) and earlier simulation work (Maddox and Longo, 2002a).

Monte Carlo simulation details

The simulation method is the canonical MC method. We use periodic boundary conditions in all three directions, and in the case where the peptide runs across the boundary, interactions are calculated using the minimum separation between the two residues in question (the minimum image convention). New peptide conformations are generated using three different sorts of moves:

1. Peptide translation: The whole peptide is randomly translated a small distance (between 0 and 0.2 Å) along each Cartesian axis.
2. Spike move (two sorts): (*a*), For an end residue, the virtual bond connecting it to the chain is rotated slightly, first in the x–y plane, and then in the y–z plane. The angle of rotation is random, between 0° and 20°. (*b*), For a central residue, the residue is rotated a random (between 0° and 20°) amount around an axis joining the centers of its nearest neighbors, while keeping all virtual bond lengths fixed.
3. Slide move: A random virtual bond is selected and all residues on one side (selected randomly, either up or down the chain) of it are moved a small, random amount (between 0 and 0.2 Å), while remaining fixed relative to one another. The move leaves the initial virtual bond the same length but rotated relative to the residues it connects.

One MC step consists of one modification of each type 1, 2, and 3, where the choice of residue is random for moves 2 and 3. Modifications are accepted or rejected with a probability given by the usual Boltzmann factor $p = e^{-\frac{\Delta U}{kT}}$ so that favorable moves, with a negative ΔU, are always accepted, and some unfavorable moves are accepted.

In our work, we wanted to capture insertion behavior without biasing results by initial peptide conformations. We have done two groups of simulations to accomplish this. First, we have started the peptide outside the bilayer in the aqueous phase in a random conformation. Second, we have started the peptide in an initially helical, fully inserted conformation.

MC simulations can be used to investigate nonequilibrium properties (e.g., insertion mechanisms) or equilibrium properties (e.g., inserted conformations) of a system. When these simulations are used to study equilibrium properties, it is important to ensure that the system has fully equilibrated before data collection begins. If this is not done carefully, one consequence is that the so-called equilibrium state might depend on the initial conditions. To establish an appropriate period of equilibration, we monitored the average energy of the peptide as a function of simulation steps. As the peptide equilibrates (reaching its energetically preferred conformation(s)), the average energy decreases from an initially higher value. Thus we can get a reasonable idea how many simulation steps it takes for this to happen simply by plotting energy versus step number.

Using this method, we find that for insertion from an initial conformation outside the bilayer, a 30-million-step equilibration period is usually sufficient, whereas for an initially inserted and helical conformation, 30 million steps is *always* sufficient. Although both initial conformations eventually produce the same equilibrated state, the inserted helical conformation converges more rapidly and is used, with an equilibration period of 50 million steps, in all our simulations (unless otherwise noted).

As a further test that our equilibration period is sufficient, we have also used conformations from peptides at the end of an entire simulation run as starting points for new simulations, and the results at the end of both simulations are within our error bars of one another.

It is worth pointing out that no equilibration would be required if the insertion mechanism is being studied. However, in this work, we find that in every case insertion is fairly easy, as we discuss in Results. Thus we focus on peptide conformations at equilibrium.

Data collection

Every MC simulation run employs a unique set of random numbers, resulting in a slightly different result each trial (similar to the way in which no two experimental measurements are identical). More accurate data are therefore generated by averaging multiple runs. Here, we have run a minimum of 10 trials for every peptide: five beginning in initially helical and inserted conformations, and five with initially random conformations outside the bilayer. Following equilibration (discussed above), data is collected for 50 million steps. In this article we report the results of the initially inserted conformations, thus our results are averaged over a minimum of five such trials. However, as we will discuss in the appendix on data analysis, in some cases we use more trials.

RESULTS

Overview

Overall, we simply input the sequence of Aβ40 and Aβ42 and various mutants and run the simulations. As discussed above, we do multiple trials for each peptide and average the results. What we find, briefly, is that the peptides all insert relatively easily into the bilayer if they begin initially outside the bilayer, and we do not find that the FAD mutations significantly effect this ease of insertion. However, we find that the mutations do influence the conformation the peptide adopts once inserted into the bilayer. Therefore, our focus in this work is not on details of how the peptide inserts, though we believe it is likely that insertion proceeds via one of the two main insertion mechanisms described previously (Baumgaertner, 1996; Maddox and Longo, 2002a).

One of our fundamental results is that the peptide appears to exhibit multiple possible inserted conformations which have nearly the same energies, thus allowing the peptide to switch between conformations often in the course of a simulation. We have previously described such behavior as conformational partitioning (Maddox and Longo, 2002b). We find that that the Aβ peptide and its mutants can always adopt the same small set of conformations. However, the mutations alter the number of MC steps the peptide spends in each of these conformations (which, in a real system, would correspond to the number of inserted peptides in each conformation). These conformations are shown in Figs. 2 and 3.

Essentially, it is quite easy to distinguish three conformations: the first has the last several residues anchored in the lower head region. We call this conformation *transbilayer*. The second conformation is similar, but usually much more prevalent since the last residues are hydrophobic and prefer to remain in the tail region. This is especially true in the case of Aβ42. In this conformation, the essential difference is that the tail of the peptide is not anchored and thus is fairly floppy and able to change the angle it makes with the z axis easily. We call this conformation *fully inserted*. The third conformation is different in that in the first two, only residues 1–15 or so remain in the upper lipid head region, while in the third conformation, the polar residues 22–23 and/or 26–28 also remain in the upper head region (along with some of their neighbors), where there is still some water content. As a result, the C-terminus (residue 40 or 42) does not stick down into the lipid tail region nearly as far as in the other two conformations. We call this conformation *partially inserted*. In this case all, or almost all, of the peptide is only in the upper leaflet of the bilayer.

This third, partially inserted conformation can be divided into two conformations simply by distinguishing whether it is residues 22–23 that remain in the upper head region, or residues 26–28. This separation of conformations is shown in Fig. 3. Some of our analysis is done grouping these together, and some by separating them, as we will discuss below.

Briefly, we find that when the FAD mutations have an effect on the insertion behavior, it is usually by causing the mutant peptides to favor the partially inserted conformation more than wild-type. The E22G mutant is an exception, as it essentially eliminates this conformation. We refer the reader to the Appendix for detailed discussion of our data analysis procedure. Overall, however, the basic output of the simulation is the number of steps, or percentage of steps, each residue in the peptide spends at each z-coordinate. We can plot this for all residues (Fig. 4) or particular residues (Figs. 5–7). With some analysis of these (the data analysis is explained in the Appendix) we are able to get accurate measurements of increases or decreases in the number of steps the peptide spends in a given conformation, relative to wild-type. We are able to do this whether we choose to separate the peptide's conformations into three or four groups. Results obtained using these methods are presented in Table 1 and Table 2.

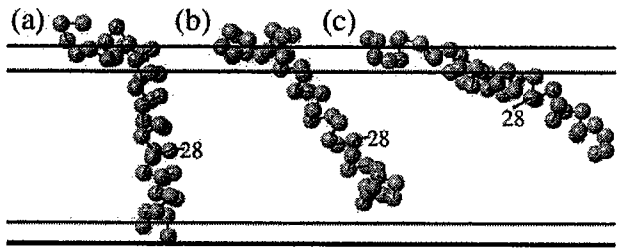

FIGURE 2 Primary inserted conformations of the Aβ peptide. We find that in every case, the inserted peptides can adopt essentially three different conformations. Mutations appear to alter the percentage of steps the peptide spends in each conformation but do not fundamentally change the conformations. (*a*) Transbilayer. The peptide inserts with the last several residues near the C-terminus in the lower lipid head region; the portion crossing the bilayer is roughly helical. (*b*) Fully inserted. Just like *a*, except the last several residues are not anchored in the lower head region, meaning that the conformation is fairly flexible. (*c*) Partially inserted. Like *b*, except now much more of the peptide is tethered to the upper head region by the polar residues 22–23 and 26–28, whereas before only residues 1–15 or so were in the upper head region. The conformations shown are for Aβ40, but Aβ42 has similar conformations with two additional residues (isoleucine and alanine) at the C-terminus.

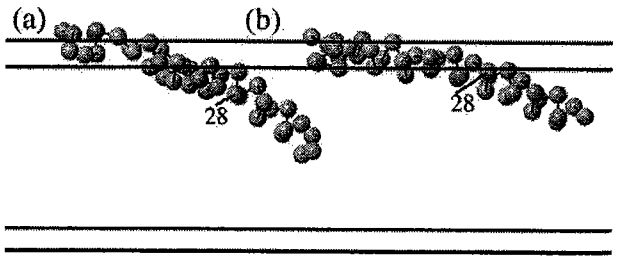

FIGURE 3 Subconfigurations associated with locations of the polar residues. We can further break up the partially inserted conformation, from Fig. 2 *c*, into two conformations: (*a*) a conformation where only residues 22–23 remain in the upper head region, and (*b*) a conformation where both residues 22–23 and 26–28 remain in the upper head region.

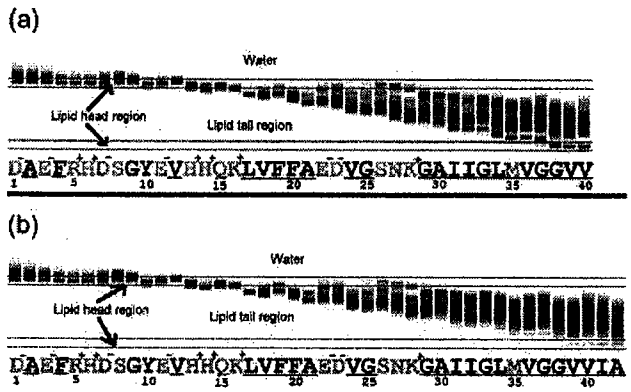

FIGURE 4 Number of steps at each z-coordinate (vertical axis is z axis; darker means more steps) plotted versus residue number (sequence shown), from 1–40 for Aβ40, *a*, and from 1–42 for Aβ42, *b*. Note that on residue 30, there appear three dark regions, corresponding to three peaks, whereas residues 26 and 28, for example, have four peaks. This result is important for our data analysis. Note also that the transbilayer conformation for Aβ42 is less common than for Aβ40 (compare the darkness, or number of steps, of the lowest peak on residue 40 for Aβ40 and Aβ42). The sequence of Aβ has polar residues shaded, hydrophobic residues underlined, and charged residues with charges indicated.

Normal Aβ peptide insertion

As detailed in the Appendix, some results for Aβ40, Aβ42, and various mutants, are shown in Figs. 5–7. We have also extracted the number of steps in each conformation and present these (measured as percentages of total steps) in Table 1, along with standard deviations. As we discuss in the Appendix, the percentages for conformations (*b*) and (*c*) are not completely accurate as absolute measures of the number of steps in those conformations, but the change relative to wild-type is accurate.

It is important to note that there is a fundamental difference between Aβ40 and Aβ42. While both can adopt all the conformations of Fig. 2, Aβ42 spends many fewer steps in conformation (*a*). This is because the last two residues of Aβ42 add significantly to the hydrophobicity of the C-terminus (see sequence in Fig. 4), as both are nonpolar and isoleucine is strongly hydrophobic. One might well ask, however, why Aβ40 has its last three residues in the lower head region at all, especially the final two valines, which are nonpolar and strongly hydrophobic. To understand this effect, it is worth noting that in this conformation, the transbilayer helix begins after, or around, residue 16, lysine, which is the final charged and polar residue before a number of nonpolar, hydrophobic residues, beginning with leucine. To remove residues 39 and 40 from the lower head region would require either the peptide to insert at a more shallow angle so that these residues do not make contact with the lower head region, or putting a kink in the helix (as in Fig. 2 *b*) so that they do not make contact. In the first case, changing the insertion angle would move lysine, and possibly residues after it (it is immediately followed by

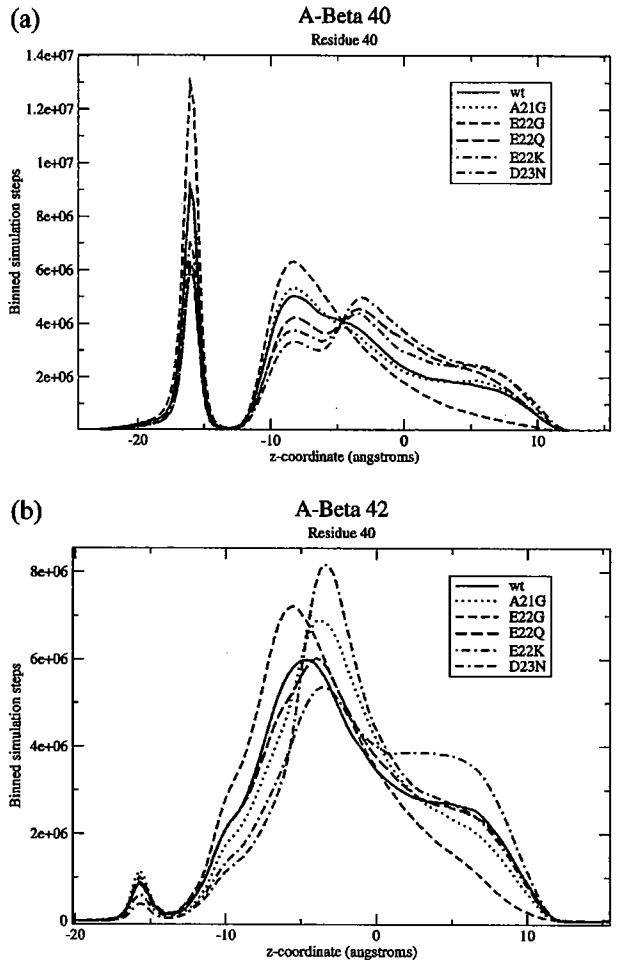

FIGURE 5 Binned numbers of steps spent at each z-coordinate for residue 40 of (*a*) Aβ40 and (*b*) Aβ42. Each plot also shows various FAD mutations. It is easily apparent that Aβ42 spends significantly fewer steps in the fully inserted conformation (*leftmost peak*) compared to Aβ40. It is difficult to tell much about the other conformations by looking at this distribution for residue 40, but the prevalence of these can be extracted from other residues. Note that the lipid head regions are from $z = 13.5$ Å to $z = 18$ Å (and similarly for negative z).

valine), into the upper head region where there is still some water. This would be costly energetically. So is putting a kink into the helix. Thus we believe that, in the case of Aβ40, the energy cost of either putting a kink in the helix, or imbedding K16 and V17 in the upper head region, is comparable to the energy cost of imbedding V39 and V40 in the lower head region, thus the conformation in Fig. 2 *a* does occasionally happen. On the other hand, for Aβ42, the additional I41 makes this conformation so costly that it almost never happens. This reduction in the transmembrane conformation results in an increase in the prevalence of the other two conformations relative to Aβ40 which, if correct, could help explain why Aβ42 is typically more toxic.

It is probably important to point out that our results do not necessarily mean Aβ40 would be biologically

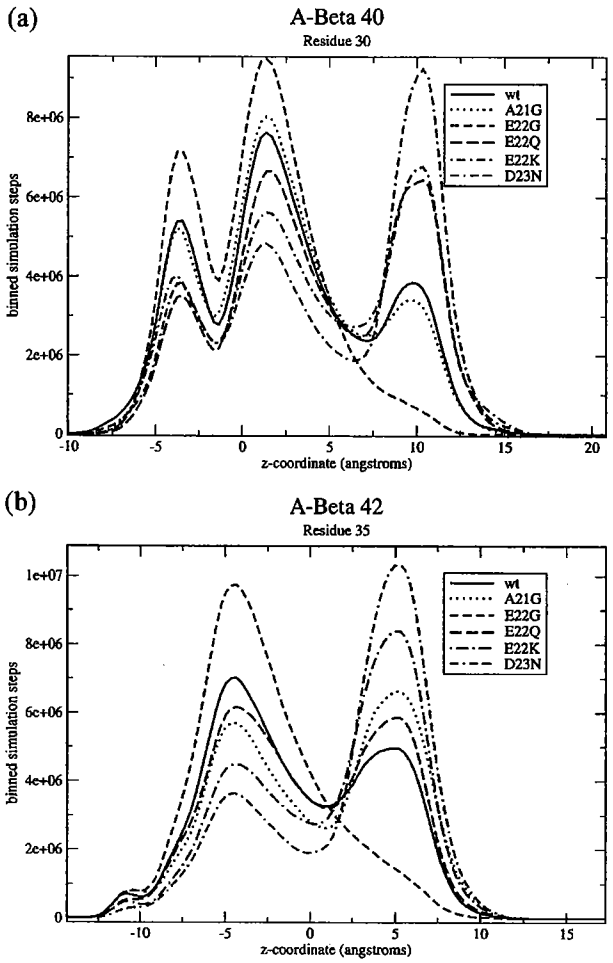

FIGURE 6 Binned number of steps spent at each z-coordinate for (a) residue 30 of Aβ40 and (b) residue 35 of Aβ42. These are the residues we picked which best distinguish three groups of conformations. The leftmost group on both, which is very small for Aβ42, is in conformations that appear nearly transbilayer. The middle group is in conformations that are inserted and fairly floppy, as in Fig. 2 b, and the rightmost group is in the partially inserted conformation. It can be clearly seen that for Aβ40, all of the mutations but E22G and A21G result in an increase in this last peak relative to wild-type, and for Aβ42 all of them except E22G do, as well.

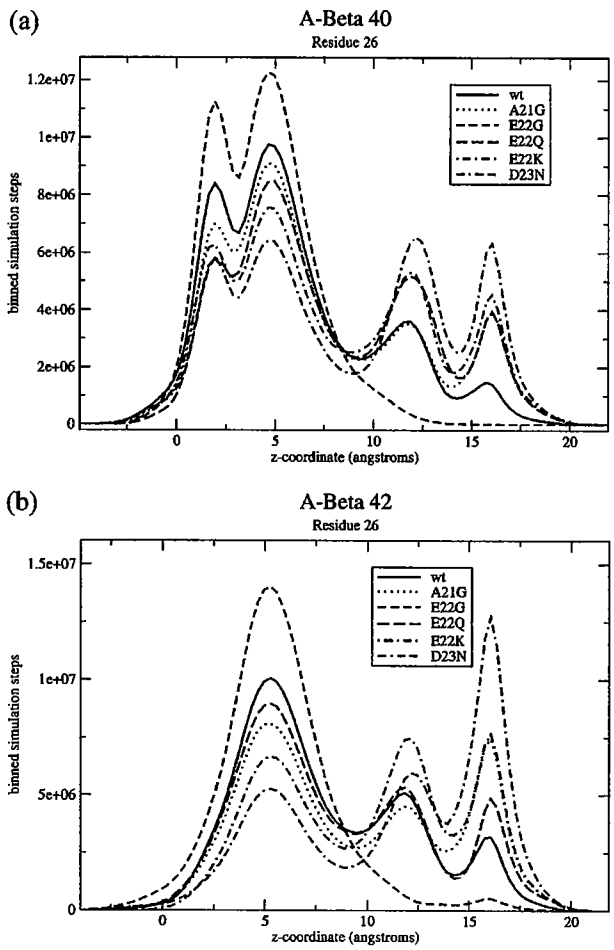

FIGURE 7 Binned number of steps spent at each z-coordinate for residue 26 of (a) Aβ40 and (b) Aβ42. For this residue, there are four apparent peaks, corresponding to the conformations of Fig. 2, a and b, and Fig. 3. For Aβ42, the transbilayer conformation is so small that there is no apparent peak. For Aβ40, it is the leftmost peak, followed by the fully inserted peak, then the partially inserted peaks: the peak of Fig. 3 a, and then the peak of Fig. 3 b. Notice that for both Aβ40 and Aβ42, the FAD mutants increase the weight of the rightmost conformations (those of Fig. 3) relative to wild-type, except for the E22G mutant.

transmembrane. We have tried making the bilayer slightly thicker (by 5 Å) and the transbilayer conformation essentially disappears. This means the transmembrane insertion is due to the limited space between head regions, as we argued above. Biologically, the membrane could be slightly thicker than our model, or the peptide might cause a small bulge in the membrane to accommodate a fully inserted, rather than transbilayer, conformation. So, although the simulation does produce this transbilayer conformation, we have no reason to believe that this conformation would be distinct from the fully inserted conformation in biological systems. On the other hand, this conformations does exist in our model. Here, it is the reduction in the prevalence of this conformations that makes the other two conformations more prevalent for Aβ42 than Aβ40.

FAD Aβ peptide insertion

FAD mutations

There are a number of known FAD mutations, including some involving Aβ (as well as others involved in other aspects of the disease including Aβ production). These are named by the populations they were first found in and include Flemish (A21G), Arctic (E22G), and Iowa (D23N) (Murakami et al., 2002). Murakami et al. also include Dutch (E22Q) and Italian (E22K) but there is some dispute about whether these are properly to be considered AD mutations (Melchor et al., 2000; Nilsberth et al., 2001; Wattendorff et al., 1995). To understand this, it is important to note that AD is often accompanied by cerebral amyloid angiopathy

TABLE 1 Frequency of each conformation for native and FAD Aβ peptides

Peptide form	Onset	% Trans.	Three-peak analysis		Four-peak analysis	
			% Fully ins.	% Partially ins.	Δ% Upper(*a*)	Δ% Upper(*b*)
WT Aβ40	72.8	15.6 ± 3.8	48 ± 5.2	36.3 ± 6.8	—	—
Aβ42		2.1 ± 0.5	58.5 ± 5.6	39.4 ± 5.8	—	—
A21G Aβ40	52	17.6 ± 3.0	48.3 ± 6.8	34.1 ± 8.0	0.5 ± 1.8	2.9 ± 8.4
Aβ42		1.9 ± 0.7	44.4 ± 5.4	53.7 ± 5.4	−2.8 ± 3.2	14.8 ± 6.9
E22G Aβ40	57	27.4 ± 7.5	67.4 ± 7.0	5.13 ± 7.0	−11.8 ± 1.6	−13.2 ± 6.2
Aβ42		2.3 ± 1.7	94.8 ± 7.0	1.29 ± 1.0	−16.8 ± 3.7	−9.6 ± 5.6
E22Q Aβ40	?	13.6 ± 4.6	43.6 ± 5.5	42.8 ± 5.5	6.4 ± 3.5	2.8 ± 11.0
Aβ42		2.0 ± 0.3	55.8 ± 6.9	42.2 ± 7.0	4.5 ± 3.4	−1.8 ± 8.7
E22K Aβ40	?	15.5 ± 9.6	37.9 ± 5.2	46.6 ± 6.0	9.9 ± 2.3	2.2 ± 10.0
Aβ42		1.3 ± 0.8	34.2 ± 10.5	64.5 ± 9.4	9.4 ± 8.0	14.6 ± 17.1
D22N Aβ40	69	13.1 ± 9.2	30.0 ± 8.8	56.8 ± 10.2	8.6 ± 7.2	10.8 ± 16.2
Aβ42		1.2 ± 0.5	41.1 ± 16.3	57.7 ± 16.7	0.6 ± 5.8	16.0 ± 11.4

Ages of onset (where known) (Grabowski et al., 2001; Li et al., 2002; Nilsberth et al., 2001; Roks et al., 2000) and simulation results: percentage transbilayer, percentages in the fully inserted (Fig. 2 *b*) and partially inserted (Fig. 2 *c*) conformations as calculated from the three-peak analysis on residue 30. The last two columns measure the change in percentage of the conformations of Fig. 3, *a* and *b*, relative to wild-type (from the four-peak analysis). For each mutation, one row represents Aβ40 and the next Aβ42. Onset age is not specific to the 40- or 42-residue forms. Here, the only consistent trend that we find is that most of the FAD mutants, with the exception of E22G, appear to increase the percentage of the partially inserted conformation relative to wild-type. This appears to be true for both Aβ40 and Aβ42. By way of comparison, the FAD mutations increase fibrillar aggregation of Aβ42 in vitro in every case except the A21G mutant (Murakami et al., 2002) and increase soluble Aβ levels in every case but the E22G mutant (Lashuel et al., 2002; Nilsberth et al., 2001). To improve statistics, wild-type Aβ40 results are the average of 25 trials rather than the usual 5; wt Aβ42 are the average of 20; A21G Aβ40 20 trials; A21G Aβ42 10 trials, and Aβ42 E22Q and D23N 10 trials each. All the rest are five trials, as described in Appendix: Data Analysis.

(CAA), deposition of Aβ in blood vessels of the brain potentially leading to vessel rupture and stroke, especially in FAD cases (Murakami et al., 2002). Wattendorff et al. (1995) point out that classic Alzheimer's plaques are rarely found in the Dutch CAA case and dementia and death are due to cerebral hemorrhage involving damage to blood vessels, as is also the case in the Italian E22K mutant (Melchor et al., 2000). But the fact that AD also involves amyloid angiopathy leaves open the possibility that the Dutch and Italian forms are vascular forms of AD (Wattendorff et al., 1995).

Here, we set aside the issue of whether or not the Dutch and Italian Aβ mutations are actually AD mutations or whether they should be regarded as something different and simply model insertion of these peptides into cell membranes. It is known that even the Dutch E22Q and Italian E22K mutant peptides interact with cell surfaces of cerebral vascular smooth muscle cells and cause cell death in vitro (Melchor et al., 2000). Thus, it is conceivable that the mechanism may be similar to that described by Lin et al. (2001) and the type of cells being damaged may simply be different—either cerebral vascular smooth muscle cells (Melchor et al., 2000) or brain pericytes (Verbeek et al., 1997) rather than neurons. For simplicity, we will call all of these FAD mutations.

It is also important to note that these Aβ mutations are autosomal-dominant (Nilsberth et al., 2001) and, in addition to lowering the age of onset for AD compared to sporadic cases, cause AD in all subjects with the mutations who live long enough. Many of these mutations also lead to increased Aβ levels, but that cannot be the sole cause, as at least the Arctic mutation (Lashuel et al., 2002) leads to decreased levels. The cause of disease also cannot be simply the increased propensity to form fibrils or aggregates, because at least the Flemish mutation does not increase fibril formation (Murakami et al., 2002).

FAD mutation results

Results for these mutations are shown in Figs. 5–7, and presented in reduced form in Table 1. We find that the most consistent difference in results relative to wild-type, for both Aβ40 and Aβ42, is that four of the five FAD mutants increase the number of steps the peptide is in a conformation like that of Fig. 2 *c*. The E22G mutant, however, results in a huge decrease of this conformation.

To understand our results, consider the changes in polarity and hydrophobicity the mutations involve. The polarity and hydrophobicity values used in this model have been tabulated before (Maddox and Longo, 2002a) and will not be repeated here, but it is worthwhile to discuss the mutations briefly. The A21G mutant involves a decrease in hydrophobicity, hence should cause residue 21 to more strongly prefer to be in the upper head region and thus result in an increase in the prevalence of the partially inserted conformation (Fig. 2 *c*). This is what we find, at least for Aβ42 (for Aβ40, the percentage stays about the same). The E22Q mutant involves a fairly large increase in polarity and slight increase in hydrophobicity, thus the polarity should dominate and cause

TABLE 2 Frequency of each conformation for artificial Aβ mutants

		Three-peak analysis		Four-peak analysis	
Peptide form	% Trans.	% Fully ins.	% Partially ins.	Δ% Upper(*a*)	Δ% Upper(*b*)
WT Aβ40	15.6 ± 3.8	48 ± 5.2	36.3 ± 6.8	—	—
Aβ42	2.1 ± 0.5	58.5 ± 5.6	39.4 ± 5.8	—	—
E22QD23N Aβ40	15.5 ± 5.0	30.0 ± 6.4	54.6 ± 6.9	4.4 ± 6.3	13.9 ± 16.2
Aβ42	0.9 ± 0.7	24.6 ± 11.4	74.4 ± 11.4	4.0 ± 10.5	30.9 ± 19.0
E22A Aβ40	23.1 ± 7.6	71.7 ± 7.1	5.2 ± 0.7	−10.8 ± 2.3	−13.3 ± 6.3
Aβ42	2.0 ± 0.4	85.6 ± 2.1	12.4 ± 2.0	−13.8 ± 7.0	−11.4 ± 4.2
E22D Aβ40	22.9 ± 8.9	64.9 ± 7.6	12.2 ± 2.0	−3.9 ± 2.6	−13.1 ± 6.2
Aβ42	1.9 ± 1.1	62.9 ± 6.6	35.2 ± 6.6	−5.9 ± 3.4	−0.4 ± 10.7
A2S Aβ40	17.6 ± 9.1	49.3 ± 6.4	33.1 ± 5.0	−1.2 ± 9.9	−3.2 ± 9.7
Aβ42	2.2 ± 1.3	60.4 ± 3.4	37.4 ± 3.3	2.4 ± 3.3	−5.3 ± 8.7
F19S Aβ40	1.6 ± 2.4	5.3 ± 4.4	93.1 ± 4.9	4.9 ± 10.3	57.9 ± 16.1
Aβ42	0.1 ± 0.1	10.8 ± 5.2	89.1 ± 5.2	7.8 ± 13.6	43.6 ± 14.9
I32S Aβ40	14.2 ± 7.0	34.7 ± 8.7	51.1 ± 10.7	−1.7 ± 3.2	17.0 ± 12.6
Aβ42	1.5 ± 0.7	49.5 ± 13.9	49.1 ± 14.1	−1.1 ± 4.5	10.2 ± 11.5
I32V Aβ40	16.0 ± 3.9	58.8 ± 2.8	25.3 ± 1.3	4.4 ± 1.6	−10.8 ± 6.8
Aβ42	2.5 ± 1.2	63.2 ± 2.1	34.4 ± 2.0	−0.1 ± 3.7	−5.7 ± 5.6
V36E Aβ40	83.0 ± 13.9	10.6 ± 9.3	6.4 ± 6.2	−12.7 ± 3.0	−5.3 ± 13.3
Aβ42	16.7 ± 11.9	36.2 ± 19.5	47.1 ± 10.5	1.6 ± 5.1	5.6 ± 11.8
H6R Aβ40	17.3 ± 4.8	47.7 ± 7.7	35.0 ± 8.4	2.2 ± 2.5	−1.2 ± 8.8
Aβ42	2.0 ± 0.6	52.9 ± 8.2	45.1 ± 8.4	1.8 ± 3.7	2.5 ± 7.3

Shown are results for artificial Aβ mutants mentioned in the literature: percentage transbilayer, percentages in the fully inserted (Fig. 2 *b*) and partially inserted (Fig. 2 *c*) conformations as calculated from the three-peak analysis on residue 30. The last two columns measure the change in percentage of the conformations of Fig. 3, *a* and *b*, relative to wild-type (from the four-peak analysis). The Aβ40 E22QD23N mutant is more toxic to HCSM cells than either mutant alone (Van Nostrand et al., 2001), whereas the E22D mutant of Aβ40 is not toxic to HCSM cells and the E22A mutant is (Melchor et al., 2000). The A2S, F19S, I32V, I32S, and V36E mutants are known to reduce aggregation of Aβ42 (Wurth et al., 2002), and the H6R mutant has been suggested as an FAD mutant (Janssen et al., 2003).

residue 22 to strongly prefer the upper head region, as we find. The E22K mutant is quite similar, but involves an even larger increase in polarity, and should also cause residue 22 to prefer the upper head region, as we find. And the D23N mutant involves a similar increase in polarity and slight increase in hydrophobicity, so again the polarity should dominate and increase this conformation, as we find. On the other hand, the E22G mutant replaces a polar, charged residue with a neutral, nonpolar residue and thus residue 22 is now mostly indifferent. This results in the observed huge decrease in the partially inserted conformation.

On one hand, the different behavior of the E22G mutant could be taken as evidence that there is no consistent change in insertion behavior, and thus suggest that this may not be the toxicity mechanism, or at least that oligomerization, not insertion, is important. That is certainly a possible meaning of these results. However, we would suggest that the reader compare the conformation of Fig. 2 *c* with the channel structure of Durell et al. (1994), specifically in Fig. 4 of that article. Note that there are two helices predicted, from residues 15–24, running near the upper head region, and from 25–40 or 25–42, inserted. In Fig. 2 *c*, we have a nearly helical region from around residues 14–24 or 25 that is near the upper head region, and one from 25–40 which hangs down inserted. Thus it resembles the predicted structure more than either of the other conformations. In the structure prediction, the part of the chain before residue 15 folds down inside the oligomer and forms a β-barrel, which we obviously do not capture here because we do not have oligomers necessary to stabilize such a structure, and because the model is not designed to capture β-structure. With the similarity of Fig. 2 *c* to the predicted channel structure in mind, we form the hypothesis that the partially inserted conformations (Fig. 2 c, or Fig. 3, *a* and *b*) are more likely to form channels, simply because of their resemblance to the structure of the monomers making up the channels. Below, in the subsection "Insertion of other mutant Aβ peptides", we test this hypothesis against some experimental data for artificial Aβ mutants, and present predictions for further tests. One might argue that the observed changes in the prevalence of different conformations are relatively small and thus would be unlikely to result in a large difference in the toxicity of the different mutants. However, these channels consist of eight or twelve monomers. If one thinks of a large number of monomers inserted in a bilayer, some will be in each conformation at any given time, so we can think of the concentration of each conformation. Consider, then, the concentration of the conformation that can form channels.

The time it takes for 12 monomers within a bilayer to find each other, or the probability, should scale as c^{12}, where c is this concentration. Thus a small difference in the amount in the proper conformation could make a big difference in the likelihood of forming channels.

Insertion of other mutant Aβ peptides

A variety of other data is available on mutant Aβ peptides. Some reduce aggregation in vitro (Wurth et al., 2002), some might cause FAD (Janssen et al., 2003), and some have various effects on cultured cerebrovascular smooth muscle cells (Melchor et al., 2000; Van Nostrand et al., 2001). Here, we examine some of the mutations which have been mentioned in the literature as a test of our hypothesis—if it is right, and toxicity depends in part on the relative prevalence of the partially inserted conformation, our results ought to correlate with the experimental toxicity measurements.

First, we address the E22Q,D23N Aβ40 double mutant created by Van Nostrand et al. (2001). This mutation's effect has been examined on human cerebrovascular smooth muscle cells (HCSM cells) because the E22Q mutation causes especially pronounced cerebral amyloid angiopathy and patients with this mutation typically die of hemorrhage, as discussed above. HCSM cells are known to degenerate in CAA in a manner that is associated with Aβ deposition (Melchor et al., 2000). Van Nostrand et al. (2001) found that the E22Q,D23N double mutant is even more toxic to HCSM cells than E22Q or D23N alone. Our idea was that the mechanism for this toxicity also involves insertion of the peptide and formation of channels, so we modeled this mutant as well. Results for this mutant are shown in Table 2; we find that the prevalence of the partially inserted conformation does increase relative to wild-type. Relative to the D23N mutant, which we would predict would be the more toxic of the E22Q and D23N mutants, we observe an increase in the partially inserted conformation only for Aβ42. Again, however, we would argue simply based on the residue properties that since both the E22Q and D23N mutants increase preference of those residues for the upper head region, the double mutant should have a stronger effect on this than either alone, and thus we expect that, given better statistics, we would agree with Van Nostrand et al. (2001) and predict that the double mutant is more toxic than either alone.

Melchor et al. (2000) have found that an artificial E22D mutant of Aβ40 does not effect HCSM cells, in contrast to biological E22Q and E22K mutants. They also observed that the Aβ40 E22A mutant is toxic to HCSM cells. Therefore we model insertion of E22D and find (Table 2) that the E22D mutant results in a decrease in the partially inserted conformation (as one would expect due to the decrease in polarity), especially for Aβ40. The E22A mutant results in a large decrease in the partially inserted conformation for both Aβ40 and Aβ42 (again, as one would expect due to the decrease in polarity). Thus, based on our hypothesis, we would agree that the E22D Aβ40 mutant would not be toxic, but disagree that the E22A mutant would be toxic. This could be taken as evidence against our hypothesis or evidence that the toxicity mechanism is different for HCSM cells.

Janssen et al. (2003) recently identified a previously unknown mutation in the Aβ peptide in two early-onset AD patients in the same family. This mutation, H6R, produced ages of onset ~55. We have here tried this mutation (results in Table 2) and find that it produces insertion behavior that is within error bars of wild-type. Given the position of the mutation, this is what we would expect, as it is within the range of amino acids (1–14 or more) that are firmly anchored in or near the upper head region, where there is some water content. Replacing histidine with arginine, which is even more polar, does not have a strong effect on this as both try to remain where there is water, i.e., the surface of the upper head region. Thus, if toxicity depends only on insertion conformation, we would suggest that this is indeed *not* a FAD mutation. Thus we would suggest testing toxicity of this mutant in cell culture, particularly as already done for Aβ42 by Lin et al. (2001).

Some in vitro work has been done to find artificial mutants that can reduce aggregation of Aβ42 (Wurth et al., 2002). Unfortunately, this has not yet been extended to include Aβ40. However, we selected some of the point mutations which are known to reduce aggregation of Aβ42 and modeled the insertion of these. We tried A2S, F19S, I32V, I32S, and V36E. Results are shown in Table 2. We find that F19S and I32S strongly increase the prevalence of the partially inserted conformation for both Aβ40 and Aβ42. For F19S, this is due to the substitution of polar serine for strongly hydrophobic phenylalanine, causing residue 29 to prefer the upper head region; for I32S, the reason is similar. In this case, the conformation is actually different from normal in that residue 32 also sticks in the upper head region. In contrast, the I32V mutant does not result in a large change relative to wild-type, consistent with the relatively small change between isoleucine and valine. Unsurprisingly, the A2S mutant makes no change to insertion behavior (residue 2 is firmly in the upper head region, so changing it to polar makes little difference). The V36E mutant, however, as one might expect, drastically increases the number of steps that the peptide is transbilayer, as the polar and charged glutamic acid strongly prefers to be in an environment with more water. Thus it decreases the prevalence of the partially inserted and fully inserted conformations. Thus we would predict that, if our hypothesis is correct, F19S and I32S should be the most toxic, I32V and A2S should be comparable to wild-type, and V36E *might* be much less toxic than wild-type. We say *might* because this probably depends on the thickness of the bilayer; if the bilayer is too thick it will probably behave just like wild-type since the E36 could not reach the lower head region. Thus a testable experimental prediction of our hypothesis is that toxicity of these mutants would be related to their insertion behavior as just described.

We can make a second prediction which is simply based on the observed insertion behavior of Aβ42. Looking at the insertion behavior of the Aβ42 versions of the Wurth et al. (2000) mutants, we find that I32V, A2S, and possibly V36E insert more like natural Aβ42, whereas F19S, I32S, and possibly V36E insert differently. The reduction in aggregation splits the group differently—I32S aggregates most, then A2S, V36E, and F19S are similar to one another and intermediate, and I32V aggregates least (Wurth et al., 2002). So if fibrillar aggregation primarily causes toxicity, experiments looking at toxicity should see the latter grouping, whereas if insertion behavior is of much more importance, toxicity experiments should see the former grouping.

DISCUSSION AND CONCLUSIONS

We have here presented work applying a model of peptide insertion to Aβ, a peptide implicated in Alzheimer's disease. Specifically, we have examined the effect of FAD mutations on the peptide's insertion behavior, with the idea that any successful hypothetical toxicity mechanism should be able to explain why FAD mutations are toxic. Thus if FAD mutants do not affect peptide insertion into, or oligomerization within, membranes, the ion channel toxicity mechanism proposed previously (Arispe et al., 1993; Durell et al., 1994; Lin et al., 2001) is probably not relevant biologically.

What we find is that the FAD mutations do affect peptide insertion. Four of these five mutations involve an increase in polarity or decrease in hydrophobicity and thus cause the peptide to prefer (relative to wild-type) a conformation where those residues are in the upper lipid head region (i.e., Fig. 2 *c*). It is interesting to note that a channel structure suggested previously (Durell et al. (1994), see Fig. 4) has these residues laying along the surface of the bilayer. Thus we find that four of the five FAD mutations increase the resemblance to this configuration.

Based on this similarity, we develop the hypothesis that causing the peptide to hang up in the upper leaflet (the partially inserted conformation) facilitates formation of harmful channels. We test this hypothesis on several artificial mutations examined in vitro and find that it can explain the change in toxicity of two and is wrong on a third. As a further test of our hypothesis, we can offer some testable predictions. For example, if the hypothesis is right, we would suggest that the F19S mutant would increase toxicity of Aβ relative to wild-type. Additionally, there are several mutations known to reduce aggregation of Aβ42 that we predict would promote the insertion behavior that would facilitate channel formation. Thus, it would be simple to distinguish between the channel formation toxicity mechanism and the aggregation toxicity mechanism by looking at the toxicity of these mutants. Even more evidence could be provided by replicating the work of Lin et al. (2001) but using various FAD mutants and looking at how these effect the abundance of channels. Additional information could also be gained from theoretical work along the lines of that by Durell et al. (1994) to see what effect these FAD mutants would have on channel structures.

Overall, this approach of modeling peptide insertion provides a simple way of making concrete predictions to distinguish the proposed mechanism of channel formation from others. The limitation of this approach, however, is that we can only look at insertion of single peptides, and not interaction between these. This is fine if formation of channels depends on having peptides initially in the correct conformations, which seems reasonable. However, it is also possible that interaction between inserted peptides causes them to adopt conformations appropriate for channel formation. If this is the case, then insight into channel formation would require a more sophisticated model that can include interaction between peptides. Even if this is not the case, including interaction between peptides will certainly answer the question of whether FAD mutants affect channel formation in a consistent way much more thoroughly than we are able to do here. Therefore, this would be a logical continuation of this work and is something we hope to do in the future.

Even if our hypothesis proves to be wrong, we have shown that the FAD mutants affect insertion behavior of the Aβ peptide into lipid bilayers, and provided an understanding as to why the FAD mutants affect insertion in the way they do.

In conclusion, our work shows that most FAD mutations have a significant effect on the insertion of the Aβ peptide in lipid bilayers in this theoretical model, and this effect can easily be understood by looking at the change in polarity and hydrophobicity accompanying the mutations. The effect of FAD mutations on insertion has not been studied previously, and may be significant. Additionally, we offer a hypothesis based on promoting channel formation by causing peptides to insert less fully that can help explain toxicity of Aβ FAD mutants, as well as several artificial mutants studied in vitro. While this hypothesis is unproven, it is based on the observation that these peptides do insert into cell membranes and form ion channels (Lin et al., 2001), and similarities to theoretically predicted channel structures (Durell et al., 1994). We provide testable predictions based on this hypothesis. It should be simple for experimentalists to disprove this hypothesis, if it is false, or to offer additional evidence for it, if they follow the experimental suggestions we offer above. Additionally, our work suggests the value of further modeling work to describe the full formation of these channels, rather than just single-peptide insertion.

APPENDIX: DATA ANALYSIS

The basic output of the simulation is the binned number of steps—essentially the frequency with which each residue is found at each z-coordinate. This can be plotted across all residues and illustrates, as in Fig. 4, that there are multiple conformations that the peptide can switch between.

In terms of data analysis, it is more useful to plot z-distributions of specific residues which can be used to distinguish between the conforma-

tions described above. For example, residue 40 has a well-defined peak in the lower head region that can be used to distinguish the transbilayer conformation from the other conformations. A plot of residue 40 z-distributions for various mutations is shown in Fig. 5.

It is somewhat more difficult to distinguish exactly how many steps the peptide spends in the fully inserted and partially inserted conformations (Fig. 2, *b* and *c*). To understand this, it is important to recognize that each conformation results in a peak for a given residue. That is, from Fig. 2, one can easily see that the position of residue 28 has three significantly different locations depending on which conformation the peptide is in. As it turns out, it also has a fourth, which is not very different from the third, as can be seen in Fig. 3. Unfortunately, these peaks tend to overlap with each other quite significantly—that is, residue 28 can sometimes have similar locations whether it is in the partially inserted conformation or the fully inserted conformation. This means that, to extract the number of steps in a given conformation from the data, it becomes necessary to fit some function to the peaks and then calculate the number of steps from that.

To do this, we select residues where the peaks appear to be particularly well separated. For one, we choose residue 30 (for Aβ40), because at that residue, the peaks corresponding to the two partially inserted conformations actually overlap—that is, residue 30 has the same average location no matter whether it is residues 22–23 alone that are stuck in the upper head region, or 22–23 and 26–28. This means that we can extract the weight of conformation from Fig. 2 *c*—the conformation grouping these two together—by looking at this residue. For Aβ42, the two peaks of the partially inserted conformation do not quite overlap for residue 30, but do for residue 35, so we do the same analysis, but for residue 35. A plot of the number of steps at each z-value for these residues is shown in Fig. 6.

To separate the two partially inserted conformations of Fig. 3, we choose three residues that have four peaks that are the most well-separated (unlike residue 30 or 35, where these two peaks merge into one). These are residues 26, 28, and 31. Plots of the number of steps at each z-value for different mutations for one of these residues, residue 26, are shown in Fig. 7.

Our goal was to find the number of steps in each conformation. Having chosen the residues where the peaks are the best separated, it is necessary to find the number of steps under each peak. Since they overlap, we find that the best way to do this is to use the least-squares method to find fits to each peak that best describe the whole function. This is probably best understood using a concrete example, for which we choose residue 26.

For residue 26, we know there are four peaks, and, as seen in Fig. 7, the locations of these are fairly clearly visible. To fit these peaks, we begin by averaging all of our results for the wild-type form of Aβ40. We assume that the peaks are Gaussian. Since the peaks are reasonably well separated, we assume initially that the center of each Gaussian is at the maximum. Then, we perform a least-squares fit of the standard deviation and amplitude of each Gaussian. Particularly, we perform our fit by looping through the peaks and suggesting changes first to the standard deviation and then to the amplitude. Each time, we try both increasing and decreasing the standard deviation by a specified step size, and check whether this improves the quality of the fit. We then move on to the next peak and do the same thing, then repeat the process for the amplitude. Then we reduce the step size and repeat the whole process. We do this until the fit can no longer be improved by further iterations of the process. Having done all that, we also then try altering the locations of the centers of the Gaussians slightly to see if it improves the fit. Having then selected optimal standard deviations and center locations, we store those, and assume that the shape and location of each peak will remain the same for other simulations, and that simply the amplitudes will vary. A sample such fit is shown in Fig. 8. As is apparent from the figure, the fit is good. Therefore, we concluded that assuming the peaks are Gaussian is sufficient, at least to get a reasonable estimate of the number of steps in each conformation.

Having done this, we are able to then perform a four parameter fit for every other data set for every Aβ40 mutation data set, simply by fitting the amplitudes while keeping the standard deviations and peak locations fixed. We have also tried allowing the standard deviations to vary when doing these subsequent fits but this does not substantially improve the quality of the fit, and it seems reasonable that the shape of a given peak for a given residue should be constant.

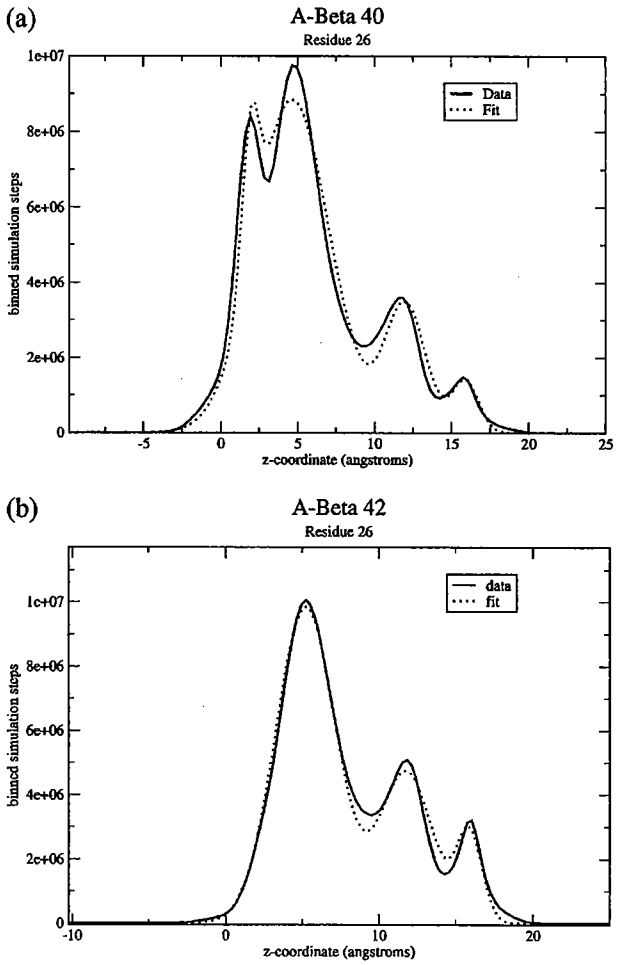

FIGURE 8 Binned number of steps spent at each z-coordinate for residue 26 of (*a*) Aβ40 and (*b*) Aβ42, along with fits used for data analysis. Shown here are the data for wild-type, compared to fits of Gaussians, as described in Appendix: Data Analysis. The Gaussians appear to provide fairly good fits and thus we use these in this work to calculate the number of steps in each conformation.

We apply a similar technique to fitting residues 28 and 31, and residue 30, but we fit residue 30 using only three peaks, and we do the same for Aβ42. Additionally, using this technique, we are able to calculate standard deviations for a given peptide or mutant. For example, for the D23N mutant, where residue 23 is changed from aspartate (D) to asparagine (N), we perform a fit separately for each of our five MC runs and calculate the area under each peak. Then, we average the results over all five trials and calculate the standard deviation.

For the four-peak case, it is somewhat difficult to accurately separate the third and fourth peaks, thus it helps that we are able to separately perform fits to four peaks on residues 26, 28, and 31. We are thus able to take the apparent change of steps under each of these three peaks relative to the wild-type and average over all three residues. This significantly reduces our error.

There is one more factor which complicates issues. Going back to our earlier example of the location of residue 28 in Fig. 2, it appears in very different positions along the z axis depending on which conformation the peptide is in. However, it is also possible to have conformations where residue 28 may, for example, be quite low, like it is in the transbilayer

conformation (Fig. 2 *a*) but residues 38–40 are not in the lower leaflet. This effect gets worse the further the residue being examined is from residue 40, and is apparent in Figs. 6 and 7 as the area under the transbilayer peak on those residues is obviously much larger than the area under the same peak on residue 40, simply because more conformations look similar to the transbilayer conformation.

This means that the calculated number of steps under each peak for residues 26, 28, 30, and 31, while accurate, are not really to be taken as a measure of how many simulation steps the peptide spends in each of those conformations. Since the peak shapes remain constant over the different mutations, however, these *do* accurately describe the change relative to the wild-type. That is, an increase in the prevalence of the conformation of Fig. 2 *c* relative to wild-type for a given mutation is correct, while the absolute number of steps in that conformation may not be accurate, except for the conformation of Fig. 2 *a*, which we can extract accurately from residue 40.

As we discussed above, for many of the peptides we have studied results are averaged over five trials. However, for some we have used significantly more trials. Specifically, for wild-type of Aβ40 and Aβ42, we used more trials, as it was particularly important to have a good average for those results since we compare all of our other results to those. For Aβ40 we used 25 trials; for Aβ42 we used 20. Additionally, for mutants with particularly small changes relative to wild-type, or particularly large standard deviations, we also used more runs. We did 20 trials for A21G Aβ40; 10 for A21G Aβ42; and 10 each for Aβ42 E22Q and D23N. Of the artificial mutants, we did 10 trials for Aβ40 and Aβ42 of both I32S and H6R.

We are grateful to R. Lal and G. Millhauser for useful discussions, and W. Pickett for a donation of computer time.

We acknowledge support of the National Science Foundation (Integrative Graduate Education and Research Traineeship Program grants DGE-9972741 and PHY99-07949 to D.L.M.), the U.S. Army (Congressionally Directed Medical Research Fund, grant NP020132 to D.L.C.), the Materials Research Science and Engineering Center Program of the National Science Foundation (under award number DMR-0213618 to M.L.L.), and the Nanoscale Interdisciplinary Research Teams Program of the National Science Foundation (under award number 0210807). M.L.L. acknowledges the generous gift of Joe and Essie Smith for endowing part of this work.

REFERENCES

Arispe, E., E. Rojas, and H. B. Pollard. 1993. Alzheimer disease amyloid β protein forms calcium channels in bilayer membranes: blockade by tromethane and aluminum. *Proc. Natl. Acad. Sci. USA.* 90:567–571.

Baumgaertner, A. 1996. Insertion and hairpin formation of membrane proteins: a Monte Carlo study. *Biophys. J.* 71:1248–1255.

Coles, M., W. Bicknell, A. A. Watson, D. P. Fairlie, and D. J. Craik. 1998. Solution Structure of the amyloid β-peptide (1–40) in a water-micelle environment. Is the membrane-spanning domain where we think it is? *Biochemistry.* 37:11064–11077.

Dickson, T. C., and J. C. Vickers. 2001. The morphological phenotype of β-amyloid plaques and associated neuritic changes in Alzheimer's disease. *Neuroscience.* 105:99–107.

Durell, S. R., H. R. Guy, N. Arispe, E. Rojas, and H. B. Pollard. 1994. Theoretical models of the ion channel structure of amyloid β-protein. *Biophys. J.* 67:2137–2145.

Grabowski, T. J., H. S. Cho., J. P. G. Vonsattel, G. W. Rebeck, and S. M. Greenberg. 2001. Novel amyloid precursor protein mutation in an Iowa family with dementia and severe cerebral amyloid angiopathy. *Ann. Neurol.* 49:697–705.

Griffith, O. H., P. H. Dehlinger, and S. P. Van. 1974. Shape of the hydrophobic barrier of phospholipid bilayers (evidence of water penetration). *J. Membr. Biol.* 15:159–192.

Hartley, D. M., D. M. Walsh, C. P. Ye, T. Diehl, S. Vasquez, P. M. Vassilev, D. B. Teplow, and D. J. Selkoe. 1999. Protofibrillar intermediates of amyloid β-protein induce acute electrophysiological changes and progressive neurotoxicity in cortical neurons. *J. Neurosci.* 19:8876–8884.

Janssen, J. C., J. A. Beck, T. A. Campbell, A. Dickinson, N. C. Fox, R. J. Harvey, H. Houlden, M. N. Rossor, and J. Collinge. 2003. Early onset familial Alzheimer's disease: mutation frequency in 31 families. *Neurology.* 60:235–239.

Jarrett, J. T., E. P. Berger, and P. T. Lansbury, Jr. 1993. The carboxy terminus of the β amyloid protein is critical for the seeding of amyloid formation: implications for the pathogenesis of Alzheimer's disease. *Biochemistry.* 32:4693–4697.

Lambert, M. P., A. K. Barlow, B. A. Chromy, C. Edwards, R. Freed, M. Liosatos, T. E. Morgan, I. Rozovsky, B. Trommer, K. L. Viola, P. Wals, C. Zhang, C. E. Finch, G. A. Krafft, and W. L. Klein. 1998. Diffusible, nonfibrillar ligands derived from $A\beta_{1-42}$ are potent central nervous system neurotoxins. *Proc. Natl. Acad. Sci. USA.* 95:6448–6453.

Lashuel, H. A., D. Hartley, B. M. Petre, T. Walz, and P. T. Lansbury, Jr. 2002. Amyloid pores from pathogenic mutations. *Nature.* 418:291.

Li, Y.-J., W. K. Scott, D. J. Hedges, F. Zhang, P. C. Gaskell, M. A. Nance, R. L. Watts, J. P. Hubble, W. C. Koller, R. Pahwa, M. B. Stern, B. C. Hiner, J. Jankovic, F. A. Allen, Jr., C. G. Goetz, F. Mastaglia, J. M. Stajich, R. A. Gibson, L. T. Middleton, A. M. Saunders, B. L. Scott, G. W. Small, K. K. Nicodemus, A. D. Reed, D. E. Schmechel, K. A. Welsh-Bohmer, P. M. Conneally, A. D. Roses, J. R. Gilbert, J. M. Vance, J. L. Haines, and M. A. Pericak-Vance. 2002. Age at onset in two common neurodegenerative diseases is genetically controlled. *Am. J. Hum. Genet.* 70:985–993.

Lin, H., R. Bhatia, and R. Lal. 2001. Amyloid β protein forms ion channels: implications for Alzheimer's disease pathophysiology. *FASEB J.* 15:2433–2444.

Maddox, M. W., and M. L. Longo. 2002a. A Monte Carlo study of peptide insertion into lipid bilayers: equilibrium conformations and insertion mechanisms. *Biophys. J.* 82:244–263.

Maddox, M. W., and M. L. Longo. 2002b. Conformational partitioning of the fusion peptide of HIV-1 gp41 and its structural analogs in bilayer membranes. *Biophys. J.* 83:3088–3096.

Melchor, J. P., L. McVoy and W. E. Van Nostrand. 2000. Charge alterations of E22 enhance the pathogenic properties of the amyloid β-protein. *J. Neurochem.* 74:2209–2212.

Milik, M., and J. Skolnick. 1992. Spontaneous insertion of polypeptide chains into membranes: a Monte Carlo Model. *Proc. Nat. Acad. Soc. USA.* 89:9391–9395.

Milik, M., and J. Skolnick. 1993. Insertion of peptide chains into lipid membranes: an off-lattice Monte Carlo dynamics model. *Proteins Struct. Funct. Genet.* 15:10–25.

Murakami, K., K. Irie, A. Morimoto, H. Ohigashi, M. Shindo, M. Nago, T. Shimizu, and T. Shirasawa. 2002. Synthesis, aggregation, neurotoxicity, and secondary structure of various Aβ1–42 mutations of familial Alzheimer's disease at positions 21–23. *Biochem. Biophys. Res. Commun.* 294:5–10.

Nilsberth, C., A. Westlind-Danielson, C. B. Eckman, M. M. Condron, K. Axelman, C. Forsell, C. Stenh, J. Luthman, D. B. Teplow, S. G. Younkin, J. Näslund, and L. Lannfelt. 2001. The "Arctic" APP mutation (E693G) causes Alzheimer's disease by enhanced Aβ protofibril formation. *Nat. Neurosci.* 4:887–893.

Pellegrini-Calace, M., A. Carotti, and D. T. Jones. 2003. Folding in lipid membranes (FILM): a novel method for the prediction of small membrane protein 3D structures. *Proteins.* 50:537–545.

Roks, G., F. Van Harskamp, I. De Koning, C. De Jonghe, S. Kumar-Singh, A. Tibbel, H. Tanghe, M. F. Niermeijer, A. Hofman, J. C. Van Swieten, C. Van Broeckhoven, and C. M. Van Duijn. 2000. Presentation of amyloidosis in carriers of the codon 692 mutation in the amyloid precursor protein gene (APP692). *Brain.* 123:2130–2140.

Roseman, M. A. 1988. Hydrophilicity of polar amino acid side chains is markedly reduced by flanking peptide bonds. *J. Mol. Biol.* 200:513–522.

Selkoe, D. J. 2001. Alzheimer's disease: genes, proteins and therapy. *Physiol. Rev.* 82:741–766.

Van Nostrand, W. E., J. P. Melchor, H. S. Cho, S. M. Greenberg, and G. W. Rebeck. 2001. Pathogenic effects of D23N Iowa mutant amyloid β-protein. *J. Biol. Chem.* 276:32860–32866.

Verbeek, M. M., R. M. W. de Waal, J. J. Schipper, and W. E. Van Nostrand. 1997. Rapid degeneration of cultured human brain pericytes by amyloid β protein. *J. Neurochem.* 68:1135–1141.

Walsh, D. M., I. Klyubin, J. V. Fadeeva, W. K. Cullen, R. Anwyl, M. S. Wolfe, M. J. Rowan, and D. J. Selkoe. 2002. Naturally secreted oligomers of amyloid β protein potently inhibit hippocampal long-term potentiation in vivo. *Nature.* 416:535–539.

Wattendorff, A. R., B. Frangione, W. Luyendijk, and G. T. A. M. Bots. 1995. Hereditary cerebral haemorrhage with amyloidosis, Dutch type (HCHWA-D): clinicopathological studies. *J. Neurol. Neurosurg. Psychiatry.* 698:699–706.

Wurth, C., N. K. Guimard, and M. H. Hecht. 2002. Mutations that reduce aggregation of the Alzheimer's Aβ42 peptide: an unbiased search for the sequence determinants of Aβ amyloidogenesis. *J. Mol. Biol.* 319:1279–1290.

APPENDIX D

Dr. David Mobley's dissertation includes chapter versions of the articles appearing in Apps. A, B, as well as an extensive review of prion proteins and disease in its introductory chapter. We have attached a copy of the introductory chapter in this appendix. Dr. Mobley graduated in June and is now a postdoctoral researcher in the group of Prof. Ken Dill at UC San Francisco. The entire dissertation is available for downloading at

http://sexton.ucdavis.edu/CondMatt/cox/mobleydissertation.pdf

Models of Cooperative Dynamics from Biomolecules to Magnets

By

David Lowell Mobley
B.A. (University of California, Davis) 2000
M.S. (University of California, Davis) 2002

DISSERTATION

Submitted in partial satisfaction of the requirements for the degree of

Doctor of Philosophy

in

Physics

in the

OFFICE OF GRADUATE STUDIES

of the

UNIVERSITY OF CALIFORNIA
DAVIS

Approved:

_____

_____

_____

Committee in Charge

2004

Acknowledgements

I want to thank my committee, and especially my advisers Daniel Cox and Rajiv Singh, who have encouraged me to pursue interesting ideas and helped me to stay focused and finish quickly. I also want to thank my Pastor, P.G. Mathew, for his faithful teaching of the Bible. I work hard and do my best at my research because I know, because of my Pastor's teaching, that it matters to God, and my work should bring glory to God.

I also want to acknowledge financial support from the National Science Foundation (IGERT grant DGE-9972741 and Grant No. PHY99-07949), the U.S. Army (Congressionally Directed Medical Research Fund, Grant NP020132), and the U.S. Department of Energy office of Basic Energy Sciences Division of Materials Research.

Abstract

Models of Cooperative Dynamics from Biomolecules to Magnets

by

David Lowell Mobley

This work details application of computer models to several biological systems (prion diseases and Alzheimer's disease) and a magnetic system. These share some common themes, which are discussed.

Here, simple lattice-based models are applied to aggregation of misfolded protein in prion diseases like Mad Cow disease. These can explain key features of the diseases. The modeling is based on aggregation being essential in establishing the time-course of infectivity. Growth of initial aggregates is assumed to dominate the experimentally observed lag phase. Subsequent fission, regrowth, and fission set apart the exponential doubling phase in disease progression. We explore several possible modes of growth for 2-D aggregates and suggest the model providing the best explanation for the experimental data. We develop testable predictions from this model.

Like prion disease, Alzheimer's disease (AD) is an amyloid disease characterized by large aggregates in the brain. However, evidence increasingly points away from these as the toxic agent and towards oligomers of the Aβ peptide. We explore one possible toxicity mechanism – insertion of Aβ into cell membranes and formation of harmful ion channels. We find that mutations in this peptide which cause familial Alzheimer's disease (FAD) also affect the insertion of this peptide into membranes

in a fairly consistent way, suggesting that this toxicity mechanism may be relevant biologically. We find a particular inserted configuration which may be especially harmful and develop testable predictions to verify whether or not this is the case.

Nucleation is an essential feature of our models for prion disease, in that it protects normal, healthy individuals from getting prion disease. Nucleation is important in many other areas, and we modify our lattice-based nucleation model to apply to a hysteretic magnetic system where nucleation has been suggested to be important. From a simple model, we find qualitative agreement with experiment, and make testable experimental predictions concerning time-dependence and temperature-dependence of the major hysteresis loop and reversal curves which have been experimentally verified. We argue why this model may be suitable for systems like these and explain implications for Ising-like models. We suggest implications for future modeling work.

Finally, we present suggestions for future work in all three areas.

Chapter 1

Introduction

This dissertation is concerned with several diverse systems in which interactions, dynamics, and cooperative behavior are important, and details the application of different models to these different systems. Specifically, in prion disease, large-scale aggregation of the prion protein may be important to disease progression, and may be linked to a simple nucleation and growth model that will be presented in this work. Alzheimer's, like prion disease, involves protein aggregates, but smaller aggregates may be more important biologically. Here, work evaluating a possible toxicity mechanism – interaction with cell membranes – is detailed. As in prion disease, nucleation may also be important in establishing the shape of hysteresis loops in some magnetic systems, and a lattice-based model for describing this is presented here.

A brief overview of the current thinking on prion diseases is given in Sec. 1.1, Alzheimer's disease in Sec. 1.2, and hysteresis loop shape and dynamics in Sec. 1.3. The present work on these topics is described in Chapters 2–4, and questions this work leaves unanswered and ideas for future work in each of these areas are given

in Chapter 5. In addition to this introduction, some brief introductory material of more immediate relevance to the work at hand is also presented at the beginning of each of Chapters 2–4.

1.1 Prion Diseases

1.1.1 General Introduction

Prion diseases, also known as transmissible spongiform encephalopathies (TSEs) [1], are a group of degenerative central nervous system (CNS) diseases which received relatively little public attention until the widespread outbreak of Bovine Spongiform Encephalopathy (BSE), or mad cow disease, in Great Britain in the 1990s [2]. These diseases lead to loss of motor function (inability to move), dementia, and finally death [1] and are invariably fatal [3]. There are no treatments, and unlike other neurodegenerative diseases like Alzheimer's disease (AD) and Parkinson's disease, progress is extremely rapid [3]. In some cases, patients may progress from health to death within as little as several weeks [3].

Prion disease is also unusual in that there are three different forms – sporadic, infectious, and genetic or inherited [3, 4]. These different forms will be described in detail below under the Historical Background section, below.

Prion diseases, or TSE's, are interesting from a physics point of view in several regards. First, it has been suggested that a simple nucleation and growth model can provide an explanation for key features of the diseases [4, 5] including previously unexplained features concerning disease incubation times [6]. In addition, the problem of protein folding is a physically interesting one, and how the prion protein, which

is responsible for these diseases, can adopt the multiple conformations necessary to encode multiple different strains or varieties of the disease [1] (as will be discussed below) is a mystery of fundamental interest in this area. In particular, how can a protein be capable of folding quickly to a stable native state, yet also have many other stable structures it can adopt? Finally, the term prion has also been used more generally for any protein that is able to infect, or convert the normal form of the protein into itself [7], raising the physical question of what general properties of proteins are necessary for this to be possible. Most of these issues are as yet unresolved, but the nucleation and growth model will be explored in further detail in this work in Chapter 2, and the others are mentioned briefly here and below as areas in which modeling work from a physics perspective may be helpful.

Below we provide a historical background of prion diseases in general, address some of the recent research concerning the function of the prion protein, and give an overview of some of the previous modeling work that has been done in this area.

1.1.2 Historical Background

TSEs or prion diseases are a group of transmissible neurodegenerative diseases which include scrapie in sheep, bovine spongiform encephalopathy (BSE) in cattle, and, in humans, Creutzfeldt-Jakob disease (CJD), Gerstmann-Sträussler-Scheinker syndrome (GSS), Kuru, fatal familial insomnia, and new-variant CJD (nvCJD) [1, 3]. Scrapie was the first recognized of these diseases and was identified in sheep in the 18th century [7]. The name scrapie, and other early names from the disease, resulted from the symptoms observed in sheep, such as ataxia (incoordination), metabolic wasting, and rubbing or scraping against trees or posts [7].

Scrapie

In 1936, Cuille and Chelle found that scrapie could be transmitted to sheep by injection of spinal cord material from diseased animals into the eyes of healthy sheep [8]. They subsequently found that the disease could be transmitted similarly to goats [9]. These findings were reproduced in England and subsequent work also demonstrated unusual features of the scrapie agent such as resistance to inactivation by heat or formaldehyde, which would be sufficient to inactivate most viruses [7]. This was actually discovered in the 1930s and 1940s when it was found that a batch of vaccine for louping-ill which was created from the brain, spinal cord and spleen of sheep, along with formaldehyde, was able to cause scrapie in healthy sheep inoculated with the vaccine. One of the sheep from which the vaccine was created had scrapie [10]. In this situation, it also was found that the scrapie infection had an incubation time, during which time the disease was unobserved in the infected sheep, of more than two years. This long incubation time is another unusual feature of these diseases that will be discussed below. The incubation time was found to be shortest when inoculated intracerebrally (in the brain) and longest subcutaneously (under the skin) [10]. Subsequent work showed that large doses of infectious material, especially material from the brain, can greatly decrease incubation times [3].

These unusual facts about scrapie, especially its resistance to formaldehyde, provided an early hint of more perplexing discoveries to come. In the germ model of disease, infection is carried by a virus or a bacteria, both foreign to the body. Bacteria are single-celled organisms which are capable of replicating themselves, while viruses are a protein capsid containing genetic information in the form of nucleic acids (DNA or RNA) which is subsequently inserted into the cells of a host

and replicated using the cell's genetic machinery. Viruses and bacteria would typically be deactivated or killed by formaldehyde. Here, the remaining infectivity of formaldehyde-exposed scrapie perplexing.

Still more perplexing were several other results. First, researchers worked to separate out the infectious agent from brain and spinal cord extracts, filtering these through smaller and smaller filters and testing each fraction to see if it was infectious. Using this method, it was found that the infective particle probably has a diameter slightly larger than 30 nm, small even for a virus (bacteria are always on the micron scale, as they are single-celled organisms) [3]. Viruses typically range in size from around 30 nm in diameter and spherical, to long, thin tubes around 15 nm wide and 300 nm long [3]. Secondly, researchers found no immune response to the infectious agent [3], even though the immune system is designed and trained to recognize foreign molecules [11]. The third group of unusual results (perhaps better described as unusual lack of results) came in the 1950s and 1960s with the advent of electron microscopy (EM) which was able to observe viruses exiting cells after using the cellular machinery to make copies of themselves. No scrapie virus has ever conclusively been observed, despite much searching [3], although there have been various unreproducible or unexplained observations. The final body of evidence concerns the nucleic acids that bacteria and viruses use to store their genetic information. Nucleic acids are sensitive both to specific enzymes which degrade them, and to irradiation with ultraviolet light, which damages them. Both these approaches have been tried and the scrapie agent is resistant to both [3]. A classic result in this area is that by Alper et al. [12] who showed that under ultraviolet irradiation far above that which would inactivate a bacteriaphage, a bacteria (which

was particularly selected for effective DNA repair mechanisms to resist this damage), and a virus, the activity of the scrapie agent was not reduced at all. This was the case even when the wavelength of ultraviolet light was selected to be at the peak wavelength for damaging nucleic acids. This suggests that the scrapie agent does not inactivate like nucleic acid and that it possibly might be devoid of nucleic acid [12].

The suggestion that the scrapie agent might be devoid of nucleic acid was a revolutionary concept, and a controversial one, because proteins, the basic cellular building blocks and machinery, are produced from nucleic acid. Nucleic acids and DNA are the blueprints and code providing cellular instructions. How can an infectious disease be infectious without this information? One suggestion was that the infectious agent could be a protein, but no mechanism was known for proteins to replicate without nucleic acid, and foreign proteins of such a large size should be recognized by the immune system easily [13]. At this point, J. S. Griffith suggested several mechanisms by which a protein could replicate itself without violating the rule that nucleic acids are required for creation of proteins. He suggested that the infectious agent could be a gene that encodes a protein that induces its own expression. Thus the gene could become spontaneously turned on in the sporadic forms of the disease, or turned on by the similar protein from another individual in the infectious form. A second suggestion he offered was that it might self-associate and change conformation, requiring a critical nucleus of infectious material to start off the process. He likened the process to nucleated condensation of a gas [14]. This idea was thought very unlikely at the time and most continued to believe that the infectious agent was an unusually difficult to deactivate, slow virus. Only following

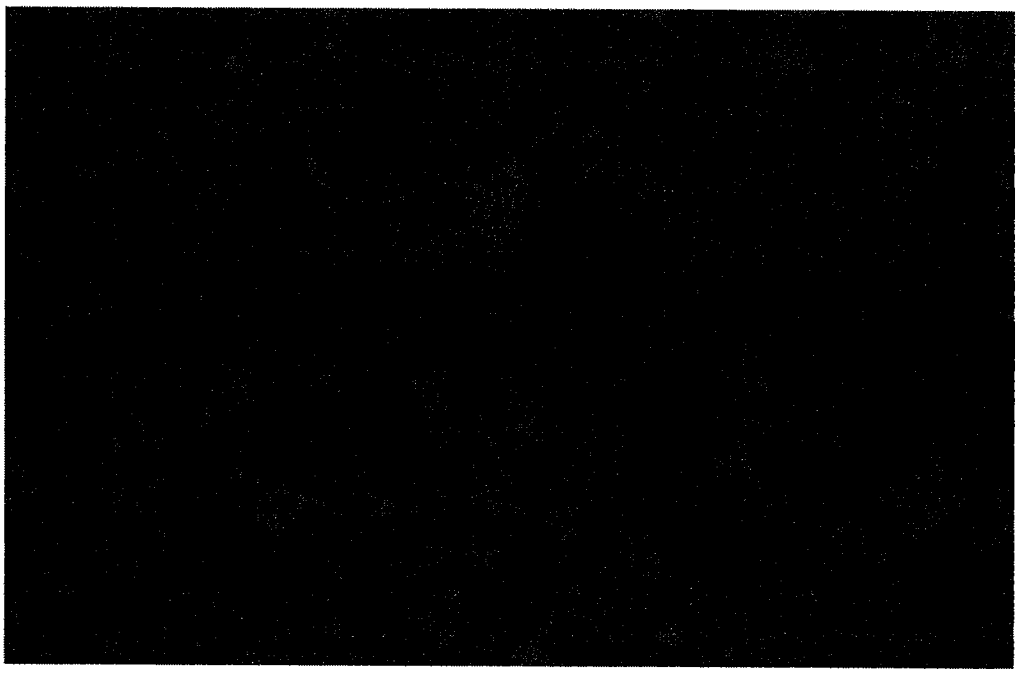

Figure 1.1. An image of a brain slice shows characteristic amyloid plaques (dark staining) in CJD, as well as spongiform change (light regions). Image from "http://www-sop.inria.fr/epidaure/Collaborations/QAMRIC/Overview/sld008.htm".

the later work of Prusiner, discussed below, did this idea resurface.

In scrapie, pathologically, disease is confined to the nervous system, although infectious material can also be found in other parts of the body [7]. The prominent findings are vacuoles, or small bubbles, within neurons, and, on a larger scale, loss of neurons and large-scale "spongiform change" (see Fig. 1.1. Spongiform change describes large-scale holes or bubbles within the brain which appear not to be simply due to neuronal loss [3, 7]. There are also often large aggregates of several proteins observable in the brain, but this will be discussed below as they only began to receive attention somewhat later.

Kuru

Meanwhile, in 1957, a neurological syndrome among the Fore people, natives of New Guinea, was first described [15, 16]. It is now called Kuru, the term the Fore used for it, which literally means trembling. In this disease, interval from clinical onset to death was typically only about three months. The disease was rare in adult males, but common (20 times more likely than males) in adult females, and had a ratio of close to one male per female in children [7]. Relatives were often affected, but also people who had married into the family, or who had moved away from the family [3]. Many possible origins of the disease were considered, but it was perplexing that there were no pathologic changes indicating infection, and no elevation of cells or protein in the cerebrospinal fluid, as typical in infections. Like in scrapie, intracellular vacuoles and spongiform change were observed.

William Hadlow had spent significant time studying scrapie and, when he encountered a display describing features of Kuru, saw the similarities to scrapie [17]. His observation led to the inoculation of monkeys with brain material from Kuru patients and Kuru was found to be infectious in this way, much like scrapie in sheep [7]. Early researchers had also noticed similarities to the pathological findings in sporadic Creutzfeldt-Jakob disease (CJD) patients (a randomly-occurring human prion disease occurring worldwide) so they also tried inoculating CJD brain material into monkeys and it also led to infection with similar pathological findings and incubation period, as did Gerstmann-Straüssler-Scheinker syndrome (GSS) brain matter (a genetic form of CJD) [7]. This link to CJD made the study of Kuru and scrapie more relevant to human health on a larger scale.

This work helped lead to the realization that Kuru was due to ritual cannibalism

that had been practiced by the Fore, as well as many other surrounding native peoples. Specifically, the Fore believed that consuming ancestors or relatives was a sign of respect, thus they typically consumed respected family members. Men typically ate the fleshy parts of the body, leaving the brain and some internal organs for women and children. Since infectious material is especially concentrated in the central nervous system, this meant that women and children were eating the potentially infectious body parts [3, 7]. Considerable effort has been made into tracking back the Kuru epidemic to several specific funeral feasts which occurred among the Fore and an overview of some of this work is given by Ridley and Baker [3], but will not be presented in more detail here. It is worth noting, however, that it is believed that Kuru originated from a case of sporadic CJD which probably caused the death of one of the Fore early on. Ritual cannibalism must have allowed this to spread to the family members and close friends, and thus the epidemic started [3]. One further fact we have learned from Kuru is that incubation times for the disease in humans ranged from as little as several years to likely more than 30 years [3, 7], and this could be relevant for variant CJD incubation times, as the diseases are similar.

Scrapie Part II

Another breakthrough in the study of scrapie came in the early 1960s with the finding that scrapie could be transmitted to mice and hamsters, drastically reducing the cost of experiments relating to transmissibility of scrapie – now it was no longer necessary to sacrifice an entire herd of sheep to the disease to do these sorts of experiments [7]. This work also helped to highlight another interesting feature of

these diseases, the species barrier. Brain extract from infectious sheep can cause scrapie in sheep after an incubation period around five months, while the same extract takes 18 months to cause disease in goats. But extract from goat brain after infection via this method takes only eight months to cause disease in goats, as do subsequent transmissions from goat to goat. This also occurs in mice, in that sheep brain extract takes 12 months to cause disease in mice but is faster (around five months) from mouse to mouse. In addition, transmission from mouse to sheep takes longer – 24 months. Thus the species barrier is not symmetric [7].

Around this same time, Dickinson studied the genetics of scrapie extensively in mice, and a particular locus was identified as controlling the incubation period, while the effects of other loci were minor [7]. This provided further hints that these diseases might be very different from typical viral diseases.

The Protein-Only Hypothesis and the Prion Protein

Much more work on scrapie and these other diseases occurred over the next two decades, but we now fast forward to 1982, when S. B. Prusiner published work arguing, based on a variety of lines of evidence, that scrapie and similar diseases are unique and require a protein for infectivity. Prusiner suggested naming the infectious agent a prion, for *pro*tinaceous *in*fectious agent [18]. He suggested two possibilities for the infectious agent: (1) It is a small nucleic acid surrounded by a tightly packed protein coat. If a nucleic acid, it would be too small to code for a protein, so the mechanism of infectivity would need to be identified. (2) The prion is a protein devoid of nucleic acid – an infectious protein. We refer the reader to Prusiner's paper for a complete discussion of the evidence, but a brief

summary of the multiple lines of evidence he offers for the necessity of a protein for infectivity follows: (1) proteinase K, which degrades proteins, inactivates the scrapie agent if applied following denaturation. (2) Diethyl pyrocarbonate, which chemically modifies and inactivates proteins in a reversible manner, is effective to reversibly inactivate the scrapie agent. (3) SDS, which is used to denature proteins and isolate nucleic acids, denatures the scrapie agent. (4) Chaotropic ions, which especially inactivate proteins, inactivate the scrapie agent. (5) Phenol, which is used in the isolation of nucleic acids, inactivates the scrapie agent. (6) Urea, at concentrations which would probably denature proteins but not nucleic acids, inactivates the scrapie agent [18]. In his work, Prusiner also detailed a vast amount of data suggesting that the scrapie agent does not contain nucleic acid, including UV inactivation data mentioned above, and the fact that it is resistant to nuclease digestion [18]. He also pointed out that its small size – data suggested 50 kD or less – showed that it could not contain enough nucleic acid to code for its coat protein, as viruses typically do, while still being encased in a protein coat – which it would need to do to resist nuclease digestion [18]. This was the origin of the term prion diseases for this group of diseases.

Around this same time, the Prusiner group developed a purification scheme which concentrated the prion by a factor of around 1,000. Furthermore, they found that in this fraction, after proteinase K digestion, was a 27-30 kilodalton (kD) protein which was not present in material prepared in a similar way from the brains of healthy animals [19, 20]. This provided evidence that (1) this protein is important to the disease, possibly a structural component of the prion, and (2) the protein is either not present in healthy animals (in this case, hamsters) or has an altered

conformation that makes it protease resistant in the case of diseased animals [19]. Additional evidence that it is an altered conformation making it protease resistant is provided by the fact that the prion agent can be inactivated by proteinase K following denaturation, as discussed above [18, 19] but not prior to denaturation [20]. This work provided additional evidence that the prion might actually be a protein with an altered conformation.

Prusiner's work was extremely controversial, but eventually led to his receipt of a Nobel prize in 1997 for his work on prion diseases, and there is now compelling evidence that he was right in that the infectious agent is a protein, as we will discuss below. Interestingly, the mechanism for the protein's infectivity now appears to be the mechanism first suggested by Griffith [14] much earlier – a protein with an altered conformation which is capable of converting the normal form of the protein in healthy individuals or regions into this altered form [7]. This idea has come to be known as the protein-only hypothesis.

It is also worth noting that the highly infectious purified prion fractions obtained by Prusiner's group and others also contained what were called scrapie-associated filaments (SAF), long, fibrillar aggregates, apparently consisting of some protein. These appeared to be especially common in samples with high infectivity, although smaller numbers were occasionally observed in samples with no infectious material [7, 20].

Following the Prusiner group's work on purifying this protein (which came to be known as the prion protein, or PrP, for reasons that will become apparent; the disease associated (often protease resistant) form of the protein is known as PrP^{Sc} for scrapie- or disease- associated, and the normal form PrP^{C} for cellular (normal)),

they were able to sequence part of the protein from infected hamsters [7]. Charles Weissmann's lab then found that this protein is coded for by the hamster DNA [7]. This was important because it showed that PrP is a normal protein even in healthy individuals, unlike the case of viral capsid proteins, which are coded for by the viral nucleic acids. It also lent additional credence to the earlier idea of Griffith [14] that the infectious agent might be a protein with altered conformation. Further evidence in favor of this came with the result that the amount of PrP is similar in infected and uninfected animals, but is only protease resistant in animals with the disease [7]. The identification of the sequence of PrP in hamsters quickly led to location and sequencing of the homologous protein in mice, and soon humans and sheep [7]. Subsequently, many mammalian PrP genes have been sequenced, and are highly conserved. Indeed, more recently, the protein has been compared across 26 different mammalian species [21]. The strength of the species barrier correlates roughly with differences in sequence, although some sequence differences are more important than others [7, 22]. The shortest incubation times are achieved by intracerebral inoculation of prions with a sequence identical to that of the host animal. This procedure also achieves the most reproducibility in incubation times [22].

An interesting result which further highlights the importance of PrP is the fact that inherited forms of CJD, GSS, and fatal familial insomnia (FFI) all involve mutations in the prion protein [7]. The E200L (residue 200 is changed from glutamate (E) to leucine (L)) mutant is the most common inherited CJD mutation, and D178N causes FFI or CJD [7]. This strongly suggests that this protein, on its own, is able to cause disease and that perhaps the mutations more easily allow a conformational change which is associated with disease. How exactly this could occur is a subject

of active research and will be discussed below in the section on modeling work and in Chapter 2. It is also worth noting that humans have a common polymorphism in the prion gene, so residue 129 can be either methionine or valine. Some 37% of the normal caucasian population are Met/Met homozygotes, 51% Met/Val, and 12% Val/Val homozygotes [7]. This appears to have some effect on disease, in that 95% of patients with sporadic CJD are homozygotes [7]. To date, everyone affected by vCJD (which will be discussed more below) is Met/Met homozygous, and in Kuru, the Met/Met genotype was associated with increased susceptibility and the shortest incubation time [23]. One idea for why this might happen will be discussed in Chapter 2. A final point on familial diseases is that all of the familial (genetic) forms which have been sufficiently tested have been found to be infectious in animals, as have the sporadic forms of the disease [7].

Iatrogenic CJD

Before discussing a bit more about the current state of prion knowledge and current research, there are three more major historical developments on prion diseases to cover. First, unfortunately, the transmissibility of CJD from human to human has been accidentally confirmed. In 1974, a middle-aged woman died from CJD after receiving a corneal transplant two years earlier. Corneal transplant is a common procedure where the corneas are removed from a donor after death and used to replace those of someone who has damaged corneas. This death in itself was unusual since CJD is typically a disease that occurs at older ages. However, it was found that the corneal donor had died of CJD, thus leading to the conclusion that CJD in the transplant recipient was iatrogenic, or physician-caused [3]. This conclusion

was reasonable because CJD is normally very rare and the chances of it occurring in two individuals connected by such a surgery are very low, but it was subsequently confirmed by other cases of iatrogenic transmission. A further example was shortly (1977) provided by two cases in young patients (17 and 23) who had been examined electroencephalographically (EEG). EEG involves inserting electrodes into the brain to record electrical signals. In this case, the EEG used electrodes that had been earlier used to study a CJD patient but had been sterilized with alcohol and stored in formaldehyde vapor for two months after use. The patients had incubation periods of about 17 months and 18 months, respectively [24, 25]. Incidentally, this incident further highlights the unusual properties of the infectious agent, as the sterilization procedure used had previously been sufficient to prevent any sort of infection [24]. The results were later confirmed by transmission of CJD to a chimpanzee by implantation of the same electrodes, after storage of two years in formaldehyde vapor [25]. A variety of other iCJD cases have been documented over the years – some 267 as of July, 2000 – and a review is given by P. Brown *et al.* [26]. Following these early cases, it was shown that, aside from corneal transplant (3 cases) and EEG (2 cases), iatrogenic CJD has also been caused by dura mater graft (114 cases), human growth hormone treatments (139 cases), gonadotropin (4 cases) and neurosurgery (5 cases) [26]. Average ages of onset appear to be shorter in cases where there would have been close contact intracerebrally or to the central nervous system and longer in the cases of human growth hormone, gonadotropin, and dura mater, with a very wide spread of incubation periods – from as little as 16 months for corneal transplant and EEG, to 30 years for a human growth hormone case [26]. This could have implications for vCJD as will be discussed below. One might hope

to be able to extract data about the course of the disease in humans to compare with laboratory animals from this data by plotting the distribution of incubation times. However, this procedure would certainly be complicated and to be done well might require much more data than is available. Dose data is also not available, and since increasing doses of infectious material typically shortens incubation times, the overall distribution of incubation times then is the convolution of several different distributions. However, this data is available, as is shown in Figure 1.2 for some of the dura mater transplants (data taken from the review by Lang et al. [27]) and may potentially be useful for comparison with models of the disease if the appropriate factors can be accounted for.

Bovine Spongiform Encephalopathy and New Variant CJD

Another important historical development, which has made prion diseases the subject of much more research and public interest, is the epidemic of bovine spongiform encephalopathy (BSE) in Great Britain. This epidemic ultimately led to about 180,000 diagnosed cases in cattle [1], and probably a great deal more had been infected but were slaughtered for consumption prior to showing symptoms [3] due to the disease's long incubation time in cattle (2-6 years) [2]. The BSE epidemic provided yet another example of the transmissibility of prion diseases. In the United Kingdom, and many other countries (including, before this epidemic, the United States), dead cattle and sheep unsuitable for consumption have typically been rendered, or essentially cooked to produce meat and bone meal (MBM) and tallow. MBM was often used in animal feed, including that fed to cattle, as a protein supplement. What apparently happened in the U.K. was that some cattle first came

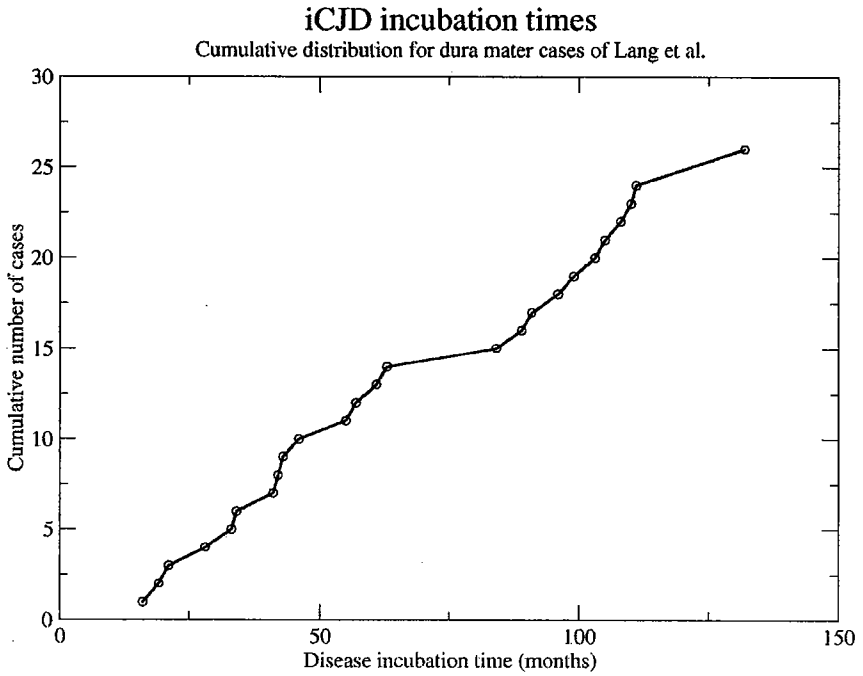

Figure 1.2. The cumulative distribution of iCJD cases caused by dura mater graft plotted versus incubation time in months. Data are from the cases reviewed by Lang *et al.* [27]. The disease incubation time obviously varies widely.

down with a prion disease, possibly a form of scrapie as a result of the disease crossing over from sheep used in their food. Then, these cattle were rendered and their protein used in cattle food, spreading the disease to more cattle, and so on [2]. At each stage, as more and more cattle became ill due to the disease, more and more cattle became with Mad Cow disease were rendered into protein products, amplifying the problem. It is worth noting that the start of the epidemic came around the same time as a change in the rendering process – a decrease in prolonged exposure to organic solvents at high temperatures, and a decrease in treatment of the material with superheated steam. Apparently, enough infectivity was allowed to survive to start the epidemic [2]. As mentioned above, it is possible that the disease first arose as a result of scrapie crossing the species barrier to cattle, but it also could have been that a few cows naturally get BSE, much like a few humans sporadically get CJD, and the change in rendering process simply allowed this to start an epidemic [2]. Further evidence that the disease was indeed caused by consumption of contaminated protein by cattle is the fact that, when the British government banned such material from feed, the disease gradually subsided [3]. In addition, it has been shown that mice, sheep, calves, and primates can be experimentally infected with BSE by the oral route [1]. Thus it is clear that the disease was caused and maintained by consumption of infectious material from rendered protein, but it is not certain how the disease originated in the first case or cases [3]. A great deal of data is available on this epidemic, perhaps more so than any of the natural prion diseases mentioned so far, because it became so prevalent in the U.K. and subsequently cost the British government so much money (the equivalent of about $5 billion, not to mention costs to the associated industries [3]).

The BSE epidemic, though under control in the U.K. and Europe, is important for two other reasons. First, it appears that BSE has been able to cross the species barrier and infect humans as vCJD, new-variant Creutzfeldt-Jakob disease [1]. This is not terribly surprising in hindsight, since, as mentioned above, BSE can be transmitted orally to mice, sheep, calves, and even primates [1, 28]. But at the time it was shocking, since previously the British government had held that there was no risk to humans based on the reasoning that despite extensive consumption of scrapie infected sheep, there was (and is) no evidence that these caused disease in humans [3]. Since the BSE epidemic, spongiform encephalopathies have been found in a variety of other species of pets and zoo animals which had eaten feed containing beef-derived protein, or meat, including housecats, cheetahs, pumas, tigers, antelope, and kudu, as well as several primates, especially lemurs [3, 28, 29]. Bons et al. have experimentally infected lemurs and compared with spontaneously affected zoo lemurs and results support the fact that the zoo lemurs contracted prion disease from infection by BSE-contaminated meat [28]. This evidence suggests a risk of the disease crossing over to humans via the oral route, but there is compelling evidence that it *has* done so. In particular, a new form of CJD arose in the U.K. around this time and was first described in 1996 [30]. This form was unusual in that it occurred primarily in young people with a consistent and unique clinicopathological pattern [30]. A new form pointed to a new cause, which suggested BSE [3]. Molecular evidence quickly showed that vCJD is caused by the same strain of the disease as that causing BSE [31]. Strains are different forms of the disease which can have distinct incubation times, lesion patterns in the brain, and physicochemical properties of the PrP^{Sc} generated [1]. Different strains can even have different symptoms

(i.e. hyper and drowsy strains in goats) [22]. Here, it was shown that sporadic CJD has two typical strains as identified by banding pattern of PrP in Western blot, and iatrogenic CJD typically has one of these two strains, except in some cases related to pituitary hormone, where it has a third. BSE and vCJD alone share a fourth pattern, called type 4 [31]. These patterns correspond to different glycosylation levels – PrP can have varying numbers of sugars attached to it, and the frequency of diglycosylated, monoglycosylated, and unglycosylated is often characteristic of the strain [31]. This initially occurred in 12 CJD cases in the U.K., and Collinge *et al.* describe their results in the following way: "The spontaneous occurrence of a novel human PrP^{Sc} type, that is the same in twelve individuals in the United Kingdom, over the last two years, seems extraordinarily unlikely as an explanation for 'new variant' CJD" [31]. It is worth noting that all of the vCJD patients were Met/Met homozygotes at codon 129, unlike in other CJD cases [32],providing further evidence that vCJD is unique. Ultimately, around 130 vCJD cases have been identified in the U.K. (as of March 2004) with the yearly incidence now apparently decreasing (see Fig. 1.3) [33].

It is fortunate that now the yearly vCJD incidence appears to be decreasing, as initially the trend was simply upwards and it was not clear how long this would continue. However, this is not necessarily the whole story. A further point relating to this on the susceptibility of the Met/Met homozygotes is that, since cattle have no such polymorphism, this may (as *in vitro* experiments suggest) have led to their prion protein being more easily converted by the bovine prion protein to a harmful form [32]. It is therefore possible that the disease may cross over to humans who are not Met/Met homozygotes but with a much longer incubation time [32] similar

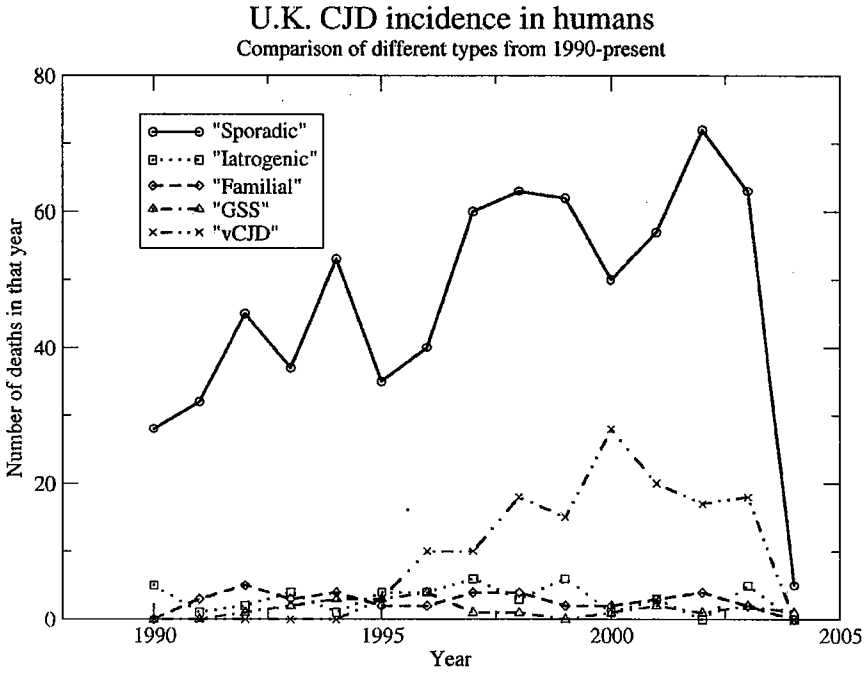

Figure 1.3. Current statistics for the incidence of CJD in humans from the British government [33] as of March 2004. Data for 2004 is only through March 1. Deaths due to sporadic CJD, iatrogenic CJD, GSS, familial CJD, and vCJD are shown. vCJD increased markedly during and following the BSE epidemic; initially, it was not clear how far this trend would continue, but as of 2002-2003, the trend now appears to be downwards again. Iatrogenic CJD deaths have been relatively constant, as have familial and GSS deaths, but sporadic cases appear to have increased substantially. Several possible reasons for this will be discussed in the text.

to how the Met/Met homozygotes had the shortest incubation times and highest susceptibility in Kuru [23]. This is of potential importance since only some 37% of people are homozygotes for methionine [7, 32]. If this is the case, we might see that Val/Val or Met/Val patients will contract vCJD after much longer incubation times, possibly even bringing second or third peaks in the number of deaths annually. In Kuru, some had incubation times as long as 30 years, so it is possible we may see something similar.

Another curious point is that in Fig. 1.2 the number of deaths annually due to sporadic CJD has also apparently increased during the increase in vCJD cases. There are several possible explanations for this. One is that, prior to the start of the BSE/vCJD scare, CJD was quite rare and sCJD cases – where there is no history of the disease in the family – were simply misdiagnosed as something else. With the increased public awareness of CJD associated with the incidence of vCJD, diagnoses of CJD may have become more accurate and thus some cases which were previously misdiagnosed are now correctly diagnosed as sCJD [34]. This is certainly possible; several studies have indicated that some CJD cases are misdiagnosed as Alzheimer's (in 6 of 42 cases examined in one study [35], 3 of 54 in another study [36]), and it seems reasonable that as awareness of CJD increases, diagnoses should more frequently be correct. A more disturbing explanation of the increase in SCJD cases is that BSE may occasionally look, biochemically and pathologically, like sCJD, both in cattle [37], and when transmitted experimentally to mice [38]. If these results prove to be right, then it is also possible that the extent of the epidemic in humans might so far have been underestimated due to misdiagnosis of sCJD cases as Alzheimer's cases. This is of course at this point speculative, but nevertheless a

disturbing possibility. As an aside, frequent misdiagnosis of sCJD could also explain another curious fact about CJD: The peak incidence of the sporadic form appears to be between 60-64 [7]. It is not clear why the incidence should fall off with increasing age, but it is worth noting that AD prevalence increases from around 1% at age 60 to 25% by age 85 [39]. Misdiagnosis as AD would probably be unlikely until incidence of AD is significant because patients would seem to young for the disease. So misdiagnosis as AD beginning around age 60-65 could provide an explanation for the observed falloff in sCJD cases after age 65. Given all these factors, including possible misdiagnosis, BSE transmitted to humans may still pose a risk, and the degree of risk is relatively unknown, especially considering the fact that hundreds of thousands or perhaps millions of people have potentially eaten meat from infected cattle [3].

One final reason BSE is still important, despite declining incidence in the U.K. and Europe, is recent discovery of BSE in the U.S. [40]. This has had significant impacts on the U.S. beef industry already, with other countries banning imports of U.S. beef. In addition, the U.S. has been criticized for failing to test enough cattle for the disease. The U.S. has tested about 20,000 cattle (out of about 200,000 annual downers, or cattle too sick to walk) annually the last two years and now plans to increase testing to about 120,000 of the 35 million cattle slaughtered annually. In comparison, Europe tests every cow over 30 months and Japan tests every cow that is slaughtered [41]. Following the discovery of BSE in the U.S, the USDA convened an advisory panel consisting of a number of European experts and they found significant problems with the U.S.'s current testing strategies and regulations concerning the use of high-risk material from cattle, and suggested that cattle in

the U.S. have been indigenously infected with BSE [42]. Obviously, BSE and mad cow disease are currently very important issues to the U.S. government and beef industry.

Chronic Wasting Disease

The final important historical development to cover is the recent incidence of chronic wasting disease (CWD) in deer and elk. This has recently been recognized as a prion disease and plaques in the brains of afflicted dear and elk are daisy-shaped, a characteristic previously unique to vCJD. The disease was first found in the 1960s in captive mule deer in a wildlife research facility in Colorado. Since, it has been identified in several neighboring states and Canada. Recent surveillance shows it spreading into more of Colorado, Wisconsin, Minnesota, New Mexico, and Utah [43]. This disease will not be discussed in detail here, but a review is provided by Salman [43]. Two points are worth mentioning, however. First, this disease, too, is having significant economic impact, because of its impact on states where hunting is a large industry. Some states, in an effort to keep the disease from spreading, are exterminating significant portions of their wild deer. Secondly, CWD is interesting because it appears to be demonstrating horizontal transmission – that is, infected deer are able to spread the disease to one another without consumption of contaminated brain matter, unlike the human diseases and BSE [43, 44]. An interesting side point is that horizontal transmission likely happened in a herd of kudu at the London Zoo who contracted BSE after one had contracted the disease from eating feed containing protein derived from (presumably) BSE-infected cattle [3]. It is also generally thought that naturally occurring scrapie is a result of horizontal transmis-

sion (see Wickner [7], Weissmann *et al.* [1], Hourrigan *et al.* [45], and Miller and Williams [44], for example) but some favor genetic predisposition to the disease and can make a fairly compelling argument in favor of this [3]. In both scrapie and CWD the means of transmission remains uncertain, although in CWD, PrP^{Sc} occurs in the alimentary tract, suggesting that it may be shed in feces and saliva [43, 44]. This has also been suggested for scrapie [44] as has contact with placental material after birth [3, 7]. Regardless, the point is that some strains of prions, in some species, may be much more infectious than in other species. It is unclear what allows some species to support horizontal transmission, while not others.

This concludes the historical discussion of prion diseases. While there is much more work that has been done, it is now more useful to give a brief overview of current knowledge relating to these diseases rather than continuing to follow historical development of work in these areas.

1.1.3 Current Knowledge about Prion Diseases

Here, it is worthwhile to discuss briefly several important aspects of current research and thought on prion diseases, including (1) how proteins might be infectious and produce different strains, (2) experimental incubation time and dose features, (3) route of CNS invasion, (4) propagation of infection.

Infectious proteins and strains

As discussed in the section on Historical Background, above, it is thought that the infectious agent, PrP^{Sc}, is a protein alone (lacking nucleic acid) – the "protein-only hypothesis". Some fairly convincing evidence of this was provided above, but

there is even more compelling evidence for this that has been provided more recently. If PrP^{Sc} is the infectious agent and works by converting normal host PrP^{C} to PrP^{Sc}, then eliminating host PrP^{C} should protect against the disease. Büeler *et al.* have done this experiment by creating transgenic mice lacking PrP^{C} (knockout mice) and found that the mice develop normally, without unusual behavior, but are resistant to scrapie infection [46]. This was confirmed [47] and it was later shown that susceptibility can be restored by introducing transgenes (reintroducing a PrP gene) and that incubation times are dependent on PrP^{C} levels [48] as one would expect if the protein-only hypothesis is right. Curiously, total PrP^{Sc} levels are decreased [48] or constant [49] at the final stages of the disease in mice overexpressing PrP relative to wild-type, perhaps because there is less time for accumulation [48]. It has also been demonstrated that, if normal (PrP^{C}-containing) brain tissue is grafted into a mouse not expressing PrP^{C}, only the ingrafted tissue will be infected following intracerebral inoculation [50], further supporting this point. It has been suggested that this last result also implies that it is the process of conversion that proves toxic to cells, rather than the presence of PrP^{Sc}, since presumably PrP^{Sc} would spill out of the graft region [3] but this interpretation is open to debate and is a side issue at this point.

How exactly a protein can be infectious is a subject of active research, both in this work and others which will be discussed below in the section on previous modeling work. However, it is worth summarizing briefly what is known about this. To begin with, it is important to point out that the normal form of the protein, PrP^{C}, is expressed in healthy individuals and has a function which is as yet unknown. Some suggestions will be provided below in the section on function of

the prion protein. However, it is known that the protein is normally found primarily on the outer surface of neurons anchored by a glycosylphosphatidyl inositol anchor (GPI anchor) [1]. Apparently, PrP^{Sc} is able to catalyze misfolding of this normal form into an abnormal form [1], which is unique to infected animals/people [49]. The evidence that this involves a conformational conversion is compelling. For example, circular dichroism shows that PrP^{Sc} and PrP^{C} have different levels of β-sheet content (PrP^{Sc} is high in β-sheet and PrP^{C} is low, as shown in Fig. 1.1.3), and the diseased form of the protein can become protease resistant [1]. When the prion protein is called protease resistant, this actually means that a significant fraction of the protein is protease resistant, but the flexible N-terminal domain is still protease sensitive. Interestingly, the size of this protease-resistant fragment can vary from one strain to another, providing evidence that strain information is also encoded in the conformation of the protein [49]. Further evidence is provided by work looking at the amount of protease-resistant PrP produced by different strains. This work found that different strains produce varying amounts of protease-resistant protein, suggesting different conformations, and furthermore that these amounts (as a ratio of total PrP) correlate with variation in the incubation time. In other words, increased incubation time corresponds to less protease-resistant PrP^{Sc} produced [51]. Furthermore, experiments with an antibody binding to PrP^{Sc} find that the amount of PrP^{Sc} that is protease-sensitive varies from one strain to another and, furthermore, there is a linear relationship between the amount of PrP^{Sc} that is protease sensitive and the incubation time [52]. Not only does this suggest that strain information may be encoded in the conformation, but that the difference in incubation times may also be due simply to conformation. A final point suggesting

the change is conformational is that studies have shown that conversion of PrP^C to PrP^{Sc} occurs post-translationally, after PrP^C has reached its normal extracellular location [49, 53].

Prion strains are interesting in that they breed true. In other words, propagation of a strain from one species to another and then returning to the original species again produces the original strain. For example, propagation of a strain from a mouse in a hamster will produce the original strain when returned to mouse. However, the incubation time on the first passage in a new species is typically longer due to the species barrier (i.e. the first passage after infecting a mouse with prions from the hamster) and it is only when another mouse is infected with material from this first mouse that the original strain properties (such as incubation time) are fully manifest [22]. Presumably, this is because the infectious PrP^{Sc} has to overcome some obstacles in templating conversion of host PrP^C when it does not have the same sequence. The interesting part, however, is that when (in the case of infecting hamster) the hamster prion protein is converted, somehow it is still able to maintain the original strain information [22]. If indeed the strain information is encoded in the conformation of PrP^{Sc}, this means that the effects of the *strain* of the infecting PrP^{Sc} dominate over the effects of the *sequence* of the host PrP^C [22]. So not only is the strain encoded by the conformation, but it is able to template folding of host prions with a different sequence into that same conformation! An interesting side point on strains is that it is actually possible for a host to be infected by more than one strain of prion disease simultaneously, as observed (for example) by Kimberlin and Walker [55].

While modeling as to how the prion protein might be caused to adopt altered

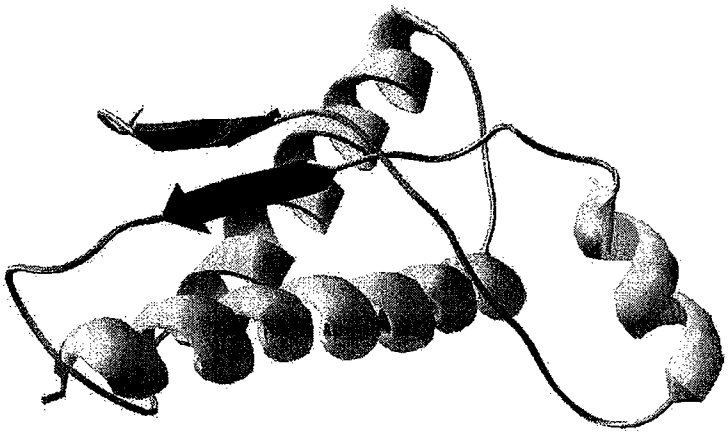

Figure 1.4. The NMR structure for residues 23-230 of the Bovine prion protein in its PrP^C form from the Protein Data Bank (code 1DX0 [54]). There is not yet an NMR or crystal structure for the PrP^{Sc} form, although some suggestions have been provided and will be discussed in Chapter 2.

conformations (or re-fold) will be discussed below, it is worth noting that the idea that a protein can adopt several different biologically relevant conformations has been a controversial one, but is now well established. It has typically been thought that the primary sequence sets a unique fold, and no other folds will be stable [49]. The fact that the prion protein can adopt other stable conformations may have broad implications for the study of many other proteins [49]. In fact, the term prion has been defined more generally a protein which imparts and propagates variability through multiple stable conformations. Several proteins which behave this way are known from studies of yeast [7, 49].

While on the subject of the prion protein itself, it is worth pointing out that this protein often forms large aggregates in the brains of people and animals with these diseases (see Fig. 1.1). These aggregates have the staining properties of amyloid – staining like starch – meaning prion diseases are part of the broader category of amyloid disease [49]. PrP^{Sc} is a major component of these plaques [3, 49]. While this may be important, it is also important to note that only 15% of CJD cases have amyloid plaques in the brain [3]. Furthermore, in human prion diseases, patients with the most severe spongiform encephalopathy, who typically died quickly after diagnosis, were the least likely to have amyloid plaques, yet the most likely to have disease that was experimentally transmissible to primates [3]. One interpretation of these results would be that the large plaques are actually a means of protecting against damage from PrP^{Sc} [3]. Another interpretation is that they are late-stage disease products.

Another point relating to plaques and aggregates is that the prion protein can form what are called Scrapie-associated filaments (SAFs) [3, 49], and also prion

rods which are often produced during the purification process [49]. Both are long, slender rod-shaped aggregates of the prion protein which are several nanometers in diameter. Sometimes, a spiral-like structure can be observed with AFM. There is some debate as to whether these two should be called by the same name [3, 49], and initially it was thought that these might be the infectious agent [49], but subsequent research has shown they are not required for infectivity [49]. However, they have been the subject of considerable research, especially since they may be a component of the large plaques of PrP^{Sc} found in the brain, and because PrP^{Sc} seems to easily assemble into these rod-like structures or amorphous aggregates *in vitro* [56]. In fact, in GSS, plaques appear to fibrillar – that is, consisting of long, thin rod-like structures resembling these [57].

While there is compelling evidence that the infectious agent does not include nucleic acid and involves PrP^{Sc}, infectivity has yet to be produced *in vitro*, so it is clear that we do not yet know the whole picture [1, 49, 56]. It is possible that there is another protein, called Protein X, which acts in production of infectivity (see Prusiner's Nobel lecture [49] for a discussion of the evidence for this; the suggestion is that it may play the role of a chaperone or catalyst) based on some molecular genetic data [49] but it is also possible that the mechanism suggested by Slepoy *et al.* [4] could explain this data. Another possibility is that the protein aggregates produced *in vitro* lack the environmental chemical conditions which work passively to help produce the infectious conformations that occur *in vivo*.

Experimental incubation time and dose features

As mentioned above, incubation time in laboratory animals depends on the level of PrP^C expression and on the strain of the disease, but it also depends on the dose of infectious material and on genetic factors [58]. For high doses inoculated intracerebrally, disease incubation time is remarkably precise (see, for example, Manuelidis and Manuelidis [35], Table 4 of Prusiner's Nobel lecture [49], and Prusiner *et al.* [58]), with the onset of symptoms coming inside a range of several days after months of incubation. The molecular mechanism(s) behind this precision are unknown [58].

Various routes of infection have been tried in laboratory animals. The most efficient is intracerebral inoculation [58] but, as previously mentioned, oral ingestion also works, as does injection in various other areas of the body. Spread of infectivity from other parts of the body to the central nervous system (CNS) will be discussed below under the subsection on invasion, but the thinking is that once the prions reach the brain and begin replicating there, disease progresses as if the prions had been inoculated intracerebrally, except dose may be different. So here, we discuss experimental results following intracerebral inoculation.

Inoculated doses are typically measured in ID_{50} units – the logarithm of the (I)nfectious (D)ose for which (50)% of animals get sick. One ID_{50} unit is thought to correspond to around 10^5 PrP^{Sc} molecules [22]. Large doses, like 10^7 ID_{50} units [58] lead to the synchrony described above, while smaller doses lead to lengthening incubation times – a mean of 65-69 days in hamsters in the high dose limit, 120-130 days for doses of around 10 ID_{50} units [58] – and more variation in incubation time from one animal to another [58]. At very high doses, the incubation time saturates at some value which is independent of dose. At lower doses, the incubation

times depend logarithmically on the dose and show deviations from this at very low doses [6]. Kulkarni *et al.* have done some theoretical modeling of experimental dose-incubation curves to try and understand these phenomena [6].

Following infection, the amount of infectious material (also known as the titer) in the brain increases dramatically over time. Prusiner *et al.* point out that in the case mentioned above, with inoculation with 10 ID_{50} units, titer increases by a factor of 10^8 over 130 days [58]. This is a huge amount. The time course of this increase can vary between strains and species. In hamsters, for example, at high doses exponential growth in the titer is observed for about 50-60 days, followed by a plateau in the amount of infectious material [58]. This has also been observed in some experiments on mouse [59]. However, as others have pointed out, there is occasionally a lag phase or zero phase [6, 55, 59] preceding this exponential growth phase. This lag phase can occur even following intracerebral inoculation, although sometimes the origin of this lag phase may be in replication in the spleen prior to entry into the brain [59] (see below under propagation of infection for a discussion of the role of the spleen). Whether this is common or not is a matter of debate, and its origin is even more uncertain. Kimberlin and Walker have pointed out there appear to be two sorts of lag or zero phases – one due to crossing a species barrier, and one which occurs even for passage within the same species [55]. It has been pointed out that this lag phase may be a feature that is more common in longer incubation period models [59]; models with short lag phases are the easiest to study in the lab since results arrive the quickest, so this could mean cases where the lag phase is easily apparent will be ignored [60]. Nevertheless, it is clear that from the time of infection to the onset of disease, the amount of infectious material in the brain must increase

tremendously, and this happens in a fairly exponential fashion [58, 61]. How exactly this increase occurs is unresolved and is of tremendous importance in the study and, hopefully, the treatment of prion diseases. The emerging consensus is that fission of aggregates may be essential to producing this exponential increase [4, 62]. Some modeling work relating to this will be discussed in Chapter 2.

Route of invasion

Since, biologically, prion diseases are not typically transmitted by intracerebral inoculation, how prions enter the body and reach the brain before beginning to cause damage is a question of key importance. As mentioned previously, there have been some cases of iatrogenic transmission of CJD in humans following brain surgery, and this is perhaps the closest to intracerebral inoculation. However, that certainly was not the case in the BSE epidemic, scrapie, Kuru, and variant CJD.

A classic experiment was done in 1967 by Eklund *et al.* who looked at the distribution of infectious material in mice following subcutaneous (under the skin) inoculation [63]. They found that infectivity first appeared in the spleen after one week, then in other lymph organs (the lymphoreticular system) at 4 and 8 weeks, then after 12 weeks appears in other internal organs and the spine, and only after 16 weeks was it apparent in the brain. This also appears to be the case for intraperitoneal inoculation [7], although in some strains, infectivity levels in brain and spleen appear to rise concurrently [59]. In the mouse, and many animals, initial events in replication after intraperitoneal inoculation do appear to take place in the lymphoreticular system (LRS) [64], which includes the spleen. Of different inoculation methods, intraperitoneal inoculation probably most closely resembles

oral transmission [64]. This result is intriguing because, as already pointed out, the body does not mount a classical immune response against the scrapie agent since it is a host protein, yet involvement of the LRS suggests involvement of the immune system. Evidence indicates that follicular dendritic cells (FDCs), which are involved with antigen presentation, are involved in prion accumulation in the spleen. For example, PrP^{Sc} colocalizes with FDCs in the spleen [64]. Impairment of the immune system inhibits not just accumulation of prions in the spleen but also propagation to the CNS [64] following intraperitoneal (IP) inoculation, while intracerebral (IC) inoculation remains effective [64]. It also appears possible for the disease to spread via neuronal connections from the periphery even if the immune system is impaired, but in a less efficient manner [64], or perhaps there is simply less infectious material if it is not amplified in the spleen. Interestingly, infectivity is found in B and T lymphocytes from the spleen, but not in circulating lymphocytes [64]. Weissmann *et al.* have also shown that infectivity is replicated in the spleen of PrP knockout mice expressing PrP only in the spleen, further highlighting the importance of the spleen [64]. PrP expression in T or B cells alone is not sufficient to replicate infectivity [64]. It is important to again point out, however, that invasion of the CNS can occur even without FDCs, so other routes are probably also important [1]. Indeed, Bartz *et al.* give a brief overview of some of the additional evidence that infection and neuroinvasion can be independent of the LRS [65]. This will not be discussed here, but the interested reader is referred to their work. The main point, here, is that the LRS is sometimes involved.

The question remains, how do prions make their way from the digestive tract to the central nervous system? This is the most typical route of infection in these

diseases. As has already been pointed out, PrP^{Sc} is protease resistant, probably allowing it to survive passage through the digestive tract [1]. Presumably, prions then reach the peripheral nervous system – either by way of the LRS or another, less efficient route – and then move along nerves to reach the brain [1]. Other work demonstrates that PrP expressing brain grafts in knockout mice cannot be infected by IP or intravenous inoculation even if normal PrP expression in the LRS is restored, suggesting that another PrP expressing compartment is required for efficient infection of the CNS [66]. Presumably this other compartment is what becomes infected when the LRS is bypassed in the less-effective route of invasion following IP inoculation. This may be the peripheral nervous system [64], although an interesting result relating to this is that occasionally, prions appear to be transmissible through the blood [1]. In particular, infectivity appears *not* to be transmissible by leukocytes or in the blood of BSE-infected cattle, but the blood of hamsters appears to be reproducibly infectious, and there is only preliminary data on sheep [1].

From the LRS and other sites, the idea is that prions proceed along the peripheral nervous system (PNS) to reach the brain, either via the vagus nerve or the spinal cord [1]. Intranerval injection of prions bypasses the need for secondary replication in the LRS or other compartment, suggesting transport along peripheral nerves [67]. While it is known that PrP^{C} is subject to fast axonal transport, mice with impaired fast axonal transport do not have extended incubation times relative to wild-type mice, suggesting that PrP^{Sc} is transported in some other way [67]. Perhaps PrP^{Sc} is transported by infecting consecutive PrP^{C} expressing nerve cells in the PNS, a "domino" route of infection [67, 68]. This would be consistent with the earlier work suggesting that another PrP expressing compartment is required for CNS

invasion [66] – in this case the compartment would be the PNS. On the other hand, in the experiment, impairment of fast axonal transport is not perfect, so perhaps some PrP^{Sc} can still infect the brain and cause disease, perhaps with slightly longer incubation times. There has also been some suggestion that prion infectivity can move in a pattern consistent with retrograde transport [49], so the issue of entry mechanism is not yet resolved. A review of issues related to propagation of prions to the CNS is provided by Aguzzi *et al.* [68].

An additional suggestion as to the route of infection is provided by Bartz *et al.*, who demonstrated that infection through inoculation into the tongue is more efficient than infection by ingestion. Furthermore, topical application to the tongue in the presence of a superficial wound is more effective than delivering a comparable dose by oral ingestion. In addition, infectivity arrives in the brain via this method more rapidly than any other experimental model involving peripheral inoculation, including ocular inoculation. This suggests that inoculation of peripheral tissues that have nerves projecting into the brain stem, like the tongue, can result in rapid infection of the brain [65]. This work also suggests that this may be a biologically relevant method for infection in the case of tongue lesion [65]. Furthermore, PrP^{Sc} was shown to accumulate in the tongues of hamsters following intracerebral inoculation with each of six different strains, suggesting that the tongue (which, from cattle, is included in products for human consumption) may also be a risky tissue to consume [65]. The very rapid invasion of the brain in the case of inoculation into the tongue probably demonstrates that in this case the LRS is not important [65].

Propagation of infection

The idea that prions may reach the brain by infecting cells one after another in a domino-like manner was discussed above in the section on the route of invasion. In contrast to axonal transport, this would essentially mean sequential infection of each cell, rather than just transport by the cells. This is a hypothetical method of transport through the PNS, but something like this must be the case in the brain, as individual cells are able to infect other nearby cells. How exactly cells do this is of crucial importance.

Since brain homogenate of infected brain material is able to cause disease after IC inoculation, a simple hypothesis would be that, once in the brain, cells secrete PrP^{Sc} which is able to infect other nearby cells in a similar fashion to the initial infection. However, some work on cell culture experiments finds that infected cells are much more efficient at converting neighboring cells to express PrP^{Sc} than the initial infection from brain homogenate [69]. Furthermore, if infected cells are cultured and then removed and healthy cells are cultured in the medium, they are not infected, suggesting they secrete no PrP^{Sc}. In addition, healthy cells cultured near, but not in contact with, infected cells are not infected, while those in contact with (or close enough to adhere to) infected cells become infected. Moreover, infected cells which are killed with aldehyde, washed, and then placed in culture in contact with healthy cells infect the healthy cells [69]. These results strongly suggest that it may be something – perhaps PrP^{Sc} itself – that templates conversion of PrP^{C} on neighboring cells to PrP^{Sc} in a contact-dependent manner, at least in these experiments. The fact that this works for cells that have been killed strongly suggests the mechanism is not facilitated by the host cell. A facilitated mechanism would be, for

example, the vesicle exocytosis mechanism that has been suggested [69].

Some interesting work by Flechsig *et al.* further provides some insight into the mechanism of propagation. Earlier, the iatrogenic CJD cases caused by use of prion-contaminated electrodes were discussed. These provided the motivation to look at transmission of prion disease via electrodes. Flechsig *et al.* [70] looked at infectivity of wires exposed either to infected brain homogenate, or temporarily inserted into infected brain, and found that those temporarily inserted into infected brain were the most infectious. Furthermore, they found that these could cause disease with as little as 30 minutes of insertion into healthy mice following 5 minutes of contact with infected mice. These wires were sufficiently small that they could bind far less infectious material than would be present in a typical injected brain homogenate, yet they were more infectious. Furthermore, when they attempted to wash PrP off of the wire, they detected none released, with a detection limit of 15 pg. Assuming one ID_{50} unit corresponds to 10^5 molecules or infectious subunits, one wire released less than 3000 ID_{50} units yet led to an incubation time similar to that following injection of 20,000 ID_{50} units [70]. Perhaps the localization of the infective material makes it more infectious than via intracerebral inoculation, where infectivity is distributed over much of the brain and much of it is cleared from the brain within 4 days [70] or perhaps the PrP^{Sc} bound to the wires is able to easily template conversion of PrP^{C} in neighboring cells as in the cell culture experiments above. Another possibility is that many of the 10^5 units in one ID_{50} unit may be ordinarily in large, noninteracting plaques which cannot easily cause infection, but the wires might be more effective at binding smaller aggregates. These potentially could more easily cause infection.

A further experiment along these lines was done by placing a prion-coated wire

in contact with a monolayer of cells and then removing the wire, along with adhering cells, to another culture. Only the cells that had contacted the electrode and thus were moved were PrP^{Sc} positive and infectious [1]. Thus, at least two separate lines of evidence suggest that PrP^{Sc} spread from cell to cell is contact-dependent and may possibly be due to templated conversion of PrP^{C}.

1.1.4 Function of the Prion Protein

A key question in the study of prion diseases is the function of the normal form of the protein, PrP^{C}. As mentioned above, knockout mice lacking the prion protein appear to be relatively normal, so either the prion protein's function is subtle or redundant. Some work in the mid-1990s suggested that PrP^{C} can bind copper [71]. Following this work, Brown *et al.* found that brain extracts from these knockout mice have substantially lower copper content than wild-type mice, suggesting that this copper binding is biologically relevant [72]. However, later work found that the levels are similar in knockout mice, so there is some question about these results [73], although work looking at copper levels in sCJD patients has found that they, too, have decreased copper levels [74]. There have also been reports of various other effects such as excess oxidation, possibly due to uncomplexed copper, in knockout mice. See Millhauser's work for a discussion [71]. The important point, however, is that, although the role of the prion protein's copper binding remains an open question, it does bind copper.

Apparently, the region of the prion protein that is involved in copper binding is the so-called octarepeat domain, which has repetitions of an eight-residue sequence (PHGGGWGQ). This region of the protein is normally flexible, with no stable native

fold [71, 75], and falls in the region from residues 60-91 or so (for humans) although the region prior to this is also flexible [71]. There is also another copper binding site slightly after this, not in the octarepeat region [71, 75], as will be discussed in more detail below. The affinity of these binding sites for total copper appears to be in the range 2-10 μM which is at or below brain and CSF concentrations, and the actual affinity for free copper may be much higher [75].

The specific function of this copper binding is as yet uncertain [71] and there have been a variety of suggestions, as mentioned briefly above. Significant evidence indicates that copper and zinc stimulate endocytosis of PrP^C at biologically relevant concentrations, suggesting that PrP^C may play a role in cellular uptake or efflux of copper [75]. This appears to be stimulation of a pathway that operates at a lower level even in the absence of metal ions [75]. However, it is likely that if PrP^C is involved in copper uptake or efflux, it is part of a specialized pathway that does not establish a net efflux or uptake of copper, because cells expressing different amounts of PrP^C do not show differences in net uptake of radioactive copper [75]. It has also been suggested that PrP^C may serve as a copper buffer which binds excess metal ions at the cell membrane [71] and it has been reported that a fragment of the prion protein containing the octarepeat domain protects against copper toxicity when injected into rats. Specifically, copper injected into the rat hippocampus typically impaired spatial learning and caused some cell death in a concentration-dependent manner, and co-injection of the PrP fragment protected against this damage [76]. Furthermore, cuprizone, a copper binding reagent, can induce neuropathological changes similar to those in prion diseases [49]. On the other hand, it has also been argued that prion-infected cells show a reduction in copper binding [77].

The structure of the prion protein's octarepeat copper binding sites have now been worked out using NMR and by crystallizing small peptides containing the copper binding site binding a copper (and two water molecules, which turn out to be important in binding) [71, 78, 79]. In addition, there is another copper binding site (GGGTH) between residues 91 and 96 of the prion protein [71]. All of the copper binding sites involve histidines [79]. It is worth noting that there is significant cooperativity between these binding sites. For example, the entire octarepeat region has a higher affinity for copper if the region through residues 98 is included, rather than just through the end of the octarepeat region at residue 90 [79]. It is also important to note that the octarepeat region falls outside of the region which becomes protease resistant in prion diseases (residues 90-231); protease resistant PrP^{Sc} is able to be infectious. So the octarepeat bindings sites are not necessary for infectivity, but the other binding site does end up in this protease resistant core [79]. In addition, mice expressing PrP with the N-terminus deleted up to residue 93 can be infected with prion disease (with a longer incubation time) [80]. Yet, strangely, increasing the number of octarepeats can cause familial CJD and GSS [80]. Perhaps the octarepeat region is not essential for propagation of the disease, but in some cases can facilitate it.

If the prion protein has a biologically relevant interaction with copper, why isn't there a significant phenotype associated with prion knockouts? This question probably remains to be answered conclusively. There is another protein that is homologous (about 25% identical sequence) to the prion protein and its gene is located directly downstream from the gene for the prion protein [81]. This protein is named doppel, or Dpl (for "downstream of the prion locus" or doppel, meaning

double). At first glance, one might think that this protein could fill in for PrP^C in the case of knockouts, as it, too, is a GPI-anchored membrane protein [81], and shares some structural similarities to PrP^C, and even more so to a prion protein lacking the octarepeat region and residues 106-126 [81]. Its C-terminal domain is strikingly similar structurally, despite the incomplete homology [82]. Doppel is conserved in humans, sheep and cattle. However, expression of doppel is very low in the central nervous system and is only abundant in the adult testis [81, 82]. The only phenotype in doppel knockout mice observed so far is sterility in male homozygotes [81, 81]. In prion knockouts, doppel expression varies in the CNS. In many cases, doppel is still not expressed in the CNS and mice remain healthy. However, in some cases, doppel *is* expressed in the CNS and mice develop ataxia due to neuronal degeneration [81, 82]. This occurs in every case that doppel is expressed in the CNS, and rapidity of the onset of this effect is proportional to the level of doppel expression [82], suggesting that doppel has a causative role. Since not all PrP-null mice have this increased doppel expression, it is possible it is an effect of the genetic construct used to eliminate PrP [81, 82]. It is an interesting side point to note that reintroduction of a normal PrP transgene into these doppel-expressing mice abrogates the harmful effects of doppel. In other words, somehow PrP is able to protect against toxicity induced by doppel expression in the CNS [81, 81]. It is interesting to note that doppel is quite similar to a PrP construct created by Shmerling *et al.* [83] which lacks residues 32-121. This construct, also, leads to ataxia and neuronal death in mice devoid of normal PrP (this has been called Shmerling syndrome [82]) but expression of regular PrP abolishes the effect [83]. The results of Shmerling *et al.* suggested to the author that toxicity was due to

the lack of the copper binding regions of PrP, and having normal PrP present also could provide the necessary copper binding. In knockouts, doppel expression in the brain could provide the copper binding role, since it is known that doppel also binds copper [84]. However, this view now seems improbable since doppel expression in the brain is actually harmful and does not appear to be linked to levels of PrP [81].

While the remarks above have focused on the prion protein, doppel, and copper binding, in the interest of completeness it is important to point out that there have been many other suggestions for possible biological functions of PrP^C. The interested reader is referred to the brief review by Lasmézas for more details [85]. It is worth pointing out that a wide variety of molecules have been identified which interact with the prion protein, including heat-shock proteins, membrane-bound receptors and others. There is considerable evidence that the prion protein may play a role in synaptic function. Although the protein is not required for vital synaptic functions, knockout mice have exhibited unusual sleep patterns and other effects, suggesting a synaptic role [80, 85]. Impairment of long-term potentiation has also been observed [80], also consistent with a synaptic role. Aside from the copper role, it has also been suggested that PrP may play a role in several signaling cascades involved in cell survival and differentiation. There are also several candidates for a receptor for PrP^C [85].

In summary, it is probably accurate to say that it is difficult as yet to form a consistent picture of the function of PrP, and the existence of doppel further complicates matters. The fact that these proteins are conserved suggests that they have an important function, and that they both bind copper is highly suggestive. However, the role of the proteins and their copper binding is so far uncertain and

presents a fascinating problem for future research.

1.1.5 Previous Modeling Work

The discussion above has provided a general overview of the current state of knowledge of prion diseases. A great deal is known, but mechanisms in many areas remain to be worked out. In particular, how can the prion protein be infectious? How can infectivity be encoded in conformation? Even more, how can information about strains also be encoded in conformation? And how can incubation times be so reproducible for a given strain at high doses? These questions (and others) are some of the fascinating issues remaining to be resolved. A variety of modeling work has been done at various levels with the goal of helping to address some of these questions. Some of it is the subject of this work (Chapter 2), but it is worth giving a brief overview of previous modeling work here.

There has been a fairly wide variety of modeling work done on prion diseases. In this review chapter, I will focus on kinetic aspects such as the kinetics of creation of infectious material, PrP^{Sc}, in more or less chronological order. However, I will first highlight some of the recent work that has been done on a more molecular level. A molecular-level model has been used to examine dimerization of a small region of PrP (residues 106-120) following the octarepeats, either with itself or with doppel, in the hopes of explaining how PrP^{C} interaction with doppel, or with a truncated form of PrP, can prevent ataxia onset, as discussed earlier. Results suggest that this may bind doppel and that a helix from residues 106-118 may interact with membranes. The work also suggests implications for fibril formation [86]. Molecular dynamics has been used to simulate the whole human prion protein including the

GPI anchor and N-linked oligosaccharides. Results indicate that the sugars help stabilize the structure of PrP^C, and that the GPI-anchor is highly flexible and unlikely to influence the structure or orientational freedom of PrP^C [87]. Phenomenological modeling of PrP using a six-sphere amino acid representation suggests that the middle region of the prion protein (residues 127-164) has two conformations with the same energy, hinting that this may play a role in the transition from PrP^C to PrP^{Sc} [88]. Finally, a "prionlike" object has been found in lattice-protein folding models. It is prion-like in that it has two states which both have low energies. Surprisingly, contrary to conventional protein-folding wisdom, the lattice model protein is able to switch between the two states without backtracking to any intermediate states reached earlier on the folding pathway [89]. While these detailed modeling results are interesting, it is clear that computational costs limit the usefulness of these models in addressing many questions. In particular, to address issues on larger scales, such as long time kinetics (over the many days or years of prion incubation) it is probably necessary to use more coarse-grained models, or kinetics-based models.

A variety of kinetics-based models have been used previously. One very early work was that of Come, Fraser and Lansbury [57]. This was not examined numerically, just as a suggestion for a pathway. This was later followed by the work of Eigen, who examined several ideas which had been discussed in the literature (including that of Come *et al.*, which he refers to as the Lansbury model) using kinetics-based models. For example, he looked at a scenario suggested by Prusiner, where PrP^C can occasionally spontaneously convert to a PrP^{Sc} monomer, or PrP^C can react with a PrP^{Sc} monomer to catalyze formation of PrP^{Sc}, basically a linear autocatalysis scheme. Parameters have to be too finely tuned in this model for it

to be likely biologically [90]; it is more likely that cooperativity is necessary for catalyzing formation of PrP^{Sc}. Eigen also examined an autocatalytic model where multiple PrP^{Sc} molecules are required to catalyze the PrP^{C} to PrP^{Sc} reaction by first binding to PrP^{C}. This can work over a wider range of rate constants and is probably more realistic [90]. Eigen also demonstrated that a mechanism suggested by Lansbury can work. In this mechanism, only aggregates are harmful; free PrP^{Sc} particles can exist but formation of large aggregates requires crossing a nucleation barrier. This mechanism could work as well as the cooperative version of the Prusiner mechanism. Eigen could find no means to distinguish between these two mechanisms and concluded that both are right [90]. In a brief paper, Orgel suggested that, if nucleation proves right, secondary nucleation may also be important, where an initial aggregate can fragment and generate secondary aggregates, thus explaining the occurrence of multiple large aggregates in brains of affected individuals [91].

Somewhat similar to the suggestion of Come *et al.* [57], Nowak *et al.* developed a general model of aggregation where aggregation growth rate can depend on size, and aggregates break at some size, allowing formation of multiple aggregates. There may be an initial nucleation barrier, but all aggregated material is PrP^{Sc} (they refer to it as $PrP-res$, but the distinction is unimportant to this discussion). In the simplest model, which they examine, the aggregate growth rate is uniform (i.e. one-dimensional (1D) aggregates) and thus this results in an exponential growth in the number of aggregates until saturating due to using all of the available PrP^{C} monomers. With results from this model, they model infection dynamics of "cells" on a two-dimensional array. Cells are either uninfected, infected, or infectious, able

to infect nearby cells within a certain radius. The interested reader is referred to the paper for more details [92]. Their key results are: (i) an idea for how the number of aggregates can increase following introduction of one or several initial infectious seeds (nuclei); (ii) the suggestion that the rarity of spontaneous nucleation can explain the rarity of sporadic forms of these diseases; and (iii) the fact that the incubation period is set by the slowest stage in the life cycle of a prion – which they suggest to be the lifetime of an infected cell (assuming it is only infectious when it dies) [92]. Masel *et al.* used a somewhat similar nucleated polymerization model with breaking, but worked to extract actual parameters from experimental data. For example, the exponential growth rate was extracted in three ways for a variety of different strains – from incubation times (which are reproducible given an inoculation dose, so they calculated inoculation dose from incubation time), from infectivity accumulation, and from accumulation of protease-resistant PrP [62]. To apply this method, the authors assumed that the amount of infectious material grows exponentially throughout the entire disease, which may or may not be true, as discussed above. For an opposing viewpoint, see Slepoy *et al.* [4] and Kulkarni *et al.* [6]. Masel *et al.* pointed out that their model is consistent with published kinetic data [62] and, from my viewpoint, is interesting as a legitimate attempt to extract real parameter values from experiment. This work was later extended [93].

Somewhat different work has been done by Stumpf and Krakauer [94], who assumed simple linear catalysis of PrP^C to PrP^{Sc} by PrP^{Sc}, then assembly of PrP^{Sc} into large aggregates. The big difference in their work is that they modeled the spread from cell to cell, including variable local connectivity between neurons. They also explored the effects of impaired axonal transport on spread of infection.

The interested reader is referred to the paper for more details [94]. Kellershohn and Laurent [95] examined a model similar to Eigen's cooperative autocatalysis model, where dimers of PrP^{Sc} are required to catalyze conversion of PrP^{C}. They found that their model displays bistable properties and suggested it could exhibit very long incubation times [95].

The modeling work discussed so far has mostly focused on ensuring that formation of PrP^{Sc} is sufficiently rare without initial PrP^{Sc} seeds present as to ensure the rarity of spontaneous CJD in humans, which has an incidence on the order of 1 death per million people per year worldwide [4], while at the same time ensuring that initial PrP^{Sc} causes infection. Some models go further and try to explain the entire incubation time or the progression of disease until death. A common theme of several of these models is exponential growth in the number of aggregates.

A different approach has been taken by several models which are based partly upon the observation that occasionally (as discussed above) there are lag or zero phases observed in the amount of infectious material in the brain, suggesting that it is, at least, unreasonable to assume that the entire disease progression is governed by exponential growth in the amount of infectious material. For there to be a zero-phase numbering in the days, weeks, or months requires a slow process, and these models have suggested this is growth of a large aggregate up to a certain size at which it can begin to fission. In addition, the suggestion is that these aggregates are two-dimensional, as this can provide an acceleration in aggregation at later times in the disease (for larger aggregates) [4, 6]. These models are not the subject of this introduction, as the present work is closely related to these, so they will be mentioned in Chapter 2. It is worth noting, however, in its first incarnation, the

model proposed by Slepoy *et al.* [4] suggested that two-dimensional aggregates were capable of explaining certain remarkable features about prion diseases such as those just described. However, no 2D aggregates had so far been observed experimentally. Subsequently, 2D aggregates *have* been observed experimentally [96]. One of the goals of this present work is to extend the work of Slepoy *et al.* to model aggregates like those actually observed experimentally.

Finally, it is also worth pointing out that the approach of Kulkarni *et al.* [6] can extend these sorts of models to make predictions about dose-incubation curves, and explain some features which previously had gone unexplained. This highlights the value of relatively simple models like these.

1.2 Alzheimer's Disease

1.2.1 General Introduction

Alzheimer's disease (AD) is in some ways less interesting than prion diseases, largely because it lacks an infectious form and thus is not remarkable in the same way as prion diseases. However, it is not accurate to say that AD is less important because of this, since it affects far more people. As the population of the U.S. ages, the incidence is expected to increase from around 4.5 million cases in the U.S. (2000) to 13.2 million by 2050 [97]. Annual costs in the U.S. alone are more than $141 billion (1997 dollars) [98], and is the third most common cause of death in the United States (in a tie with stroke) [98]. Clearly, AD is far more important than prion diseases in terms of public health effects.

AD does share several features with prion diseases. Both are members of the

larger group of amyloid diseases, where amyloid describes the staining properties of large plaques or abnormal protein deposits found in the brains of affected individuals [49] and means that these plaques respond to certain dyes (stain) like starch. This group of diseases includes a variety of other diseases as well, such as Parkinson's disease, Huntington's disease, cystic fibrosis, poly-glutamine diseases [99], familial ALS (Lou Gehrig's disease) [100] and others. AD is also similar to prion diseases in that it involves misfolding and aggregation of proteins or (here) peptides. In this case, at least two different proteins aggregate. One, which largely makes up the extracellular amyloid plaques in AD, is a peptide called Amyloid-β or Aβ. The Aβ peptide forms fibrils within these large aggregates [100, 101]. Incidentally, these aggregates were described by Alois Alzheimer himself shortly after he first described the disease [100]. The second protein that aggregates is called Tau and aggregates intracellularly [98]. More on these will follow below. As in prion prion disease, this appears to be a disease involving misfolding or alternative folding. That is, both Tau and Aβ appear to change fold, or adopt a wrong fold, before or during aggregation [99]. This makes AD, and other amyloid diseases where this happens, interesting from a physical point of view, like prion diseases. Again, an important question is how the proteins involved can adopt the alternative folds which allow the disease-associated forms to exist.

AD has a somewhat less interesting historical story than prion diseases, so that will not be covered in detail here. However, it is nevertheless worth giving a brief overview of the current state of knowledge on AD by way of background for the modeling work that will be done here in Chapter 2. In addition, previous modeling work by other authors on AD will be discussed briefly below.

1.2.2 Current knowledge on AD

As mentioned above, it is known that several proteins are involved with AD, as there are often large extracellular aggregates composed mostly of fibrils of the Aβ peptide observed, and intracellular aggregates of a protein called Tau. Aβ aggregates are composed of the peptide, a protealytically cleaved fragment of a protein called APP for Amyloid Precursor Protein (of unknown function), largely in 40- or 42-residue forms, differing by an isoleucine and alanine at positions 41 and 42. Much of the fibrillar Aβ found in these plaques is the 42-residue form, which is known to be particularly prone to aggregation *in vitro*, although it is colocalized with Aβ40 (presumably not in fibrils) [98, 102, 103]. APP itself is normally a transmembrane cell glycoprotein, and the Aβ fragment is likely part of the transmembrane domain, with its hydrophilic N-terminus on the extracellular side and the hydrophobic C-terminus in the membrane [99]. The Aβ peptide has no stable native fold. Tau, on the other hand, is a hydrophilic microtubule-associated protein which is known to function in microtubule stabilization [99]. What exactly does damage in the brain in AD is the subject of some debate, and it is worth giving a brief overview of some of the suggestions and research in this regard.

The research relating to AD is extensive, so by no means will this work provide an encompassing review. With more than 500 review articles published in 2002 alone (a list of reviews is available on the web [104]), this task is best left to others. Here, a brief overview of some of the current thinking on toxicity mechanisms is provided, along with a more detailed discussion of some of the recent focus on oligomers of Aβ as the toxic species.

Suggested toxicity mechanisms and therapeutic strategies

Obviously, with the huge numbers of people facing AD, it is especially important to develop therapeutic strategies. One big question in AD research, however, has been what one should target with therapeutics. Is formation of amyloid plaques harmful, or protective? Would breaking up or preventing formation of these plaques help, or cause buildup of toxic precursors? Or are the plaques themselves a downstream event? And what is the role of the tangles of Tau? One can imagine developing drugs to target just one of these items and finding that it is only a marker of the disease, not a causal agent. The dominant view is that plaques of Aβ are toxic [99, 101]; this forms the basis of the amyloid hypothesis that will be discussed more below. However, it is first worth discussing some other suggested toxicity mechanisms before giving an overview of the evidence for the amyloid hypothesis, and the problems with it.

Clark and Karlawish [98] provide a fairly general overview of some of the different suggestions for the causes of AD, as well as suggestions for treatment strategies. They argue that amyloid plaques are insufficient to account for the degree of cognitive impairment in AD and argue that neurofibrillary tangles – Tau tangles – are what is important for toxicity. A suggestion they mention is that an alteration in the processing of APP may be the first step. APP is normally protealytically cleaved by α or β secretases, followed by γ secretase. It is the β then γ cleavage pathway that produces the Aβ peptide [98] (the role of secretases in AD is reviewed by Wolfe [105]). The argument, then, is that the putative alteration increases intraneuronal accumulation of Aβ and loss of APP, leading to increased phosphorylation of tau (by an unknown mechanism), disrupting its function in stabilizing the micro-

tubule system and causing formation of neurofibrillary tangles [98]. This picture is consistent with an observation that Tau in the cerebro-spinal fluid (CSF) increases during AD [98], but some problems with this idea will be discussed below when discussing evidence for the amyloid hypothesis. Clark and Karlawish also provide an overview of some current and potential AD diagnostic tests; we refer the interested reader to their work [98]. An interesting point is that MRI is able to observe regional and whole-brain atrophy in AD, which is an invariant consequence of the extensive neuronal death in AD [98]. So far, however, it is difficult to diagnose patients in the earliest stages of the disease. In terms of treatment strategies, Clark and Karlawish present a few therapeutic strategies which have been approved for treating (in the short term) cognitive effects of the diseases, but so far only high-dose vitamin E has been shown to slow progression, and there is so far no known cure for the disease. Several new treatments are under development [98]. A vaccine based on the Aβ peptide had recently entered clinical trials and appeared to be helpful in some subjects, but trials had to be discontinued as the vaccine engendered central nervous system (CNS) inflammation in some of the study participants. Vaccination may still be a possible strategy for future therapies [106]. However, news reports have recently pointed out that drugs approved so far for treating AD are generally disappointing [107].

Another somewhat more sophisticated toxicity mechanism relating to microtubules has been suggested in the context of Parkinson's disease which could possibly apply in the AD case as well. In particular, cells use the ubiquitin-proteasome pathway to degrade proteins that do not fold properly upon production. In order for proteins to enter the proteasome where they can be degraded, however, they

must first unfold. This provides a problem when there are large intracellular aggregates which will not easily unfold, as they could be hard to degrade. Thus Kopito has done a significant amount of work relating to the common feature in some of these protein aggregation diseases, and finds that abnormal intracellular aggregates of protein appear to be transported along microtubules to a microtubule organizing center, where they are often deposited in a large inclusion body, possibly like a cellular garbage dump. It may be that this is ordinarily protective and helps keep cells from getting swamped by these aggregates, but in these cases, the aggregates win and cause problems for the cell, possibly in terms of further aggregation interfering with the proteasome mechanism. A review of these ideas is found in ref. [108]. This mechanism is probably less plausible if Aβ turns out to be the toxic species (which will be discussed below), since Aβ deposits are extracellular and less likely to cause problems than Tau.

In terms of toxicity mechanisms, it has also been suggested that oxidative stress and metals play an important role. In particular, certain metal ions are known to accelerate Aβ aggregation, and zinc appears to protect against Aβ toxicity in some circumstances, yet at the same time cause Aβ to aggregate and precipitate [109]. Cuajungco *et al.* suggest in their review article that perturbation of a delicate metal balance in the brain may lead to accumulation of excess zinc or Aβ in the brain. Either of these could cause inappropriate Aβ interaction with redox metals like copper and iron, leading to oxidative stress and cytotoxicity, possibly through H_2O_2 production [109]. It is interesting to note that this is another way in which Aβ and the prion protein are similar: they interact with metals. The group of Bush at Harvard has also provided extensive evidence and suggestions relating to the Aβ

peptide and oxidative damage, including H_2O_2, and there is evidence suggesting this may also play a role in Parkinson's disease and ALS. The interested reader is referred to the review by Barnham *et al.* [110]. This body of work suggests that metal chelators may be potential therapeutic agents for AD [110, 109]. This work on metals and oxidative stress should probably not be separated entirely from that on aggregation, as the suggestion is not that the metals play the entire role, but that Aβ interacts with metals in a way that in some circumstances can cause oxidative damage to cells. So when the amyloid hypothesis is discussed below, it is best to remember that metal interaction and/or oxidative damage *are* potential ways in which amyloid could be toxic.

An excellent review of the amyloid hypothesis is provided by Hardy and Selkoe [101] and this section will draw heavily on this. As mentioned above, the amyloid hypothesis currently the dominant view in AD research [99]. In this hypothesis, it is the deposition of plaques or aggregates of the Aβ peptide which are thought to be toxic and cause AD. The background of this hypothesis is that the plaques, as mentioned above, were one of the first markers of the disease noted by Alzheimer [102]. Aβ itself was first sequenced from blood vessels and individuals with Downs syndrome, who typically have Aβ deposition in plaques and other AD neuropathology. This was done around 20 years ago, and Aβ was shortly thereafter recognized as the primary component of AD amyloid plaques [101]. It is interesting to note that the gene for APP is on chromosome 21, of which Downs patients have three copies, partially explaining why they are prone to AD [101].

Current evidence supporting the amyloid hypothesis (and opposing the idea that Tau is the causal agent) is summarized by Hardy and Selkoe as follows: First,

mutations in the gene encoding the Tau protein cause different neurodegenerative diseases, not AD [101]. This has been pointed out by others, as well [99, 98]. The important point is that alterations in Tau that can cause Tau tangles are not sufficient to cause Aβ deposition and AD. Thus in AD, it is likely that Tau deposition is downstream of changes in Aβ metabolism. Furthermore, Tau deposition has also been observed in healthy individuals [98]. Second, transgenic mice over-expressing APP and Tau undergo increased formation of Tau tangles when compared to mice expressing Tau alone, while presence of Aβ plaques appears unaltered by expression of Tau in these mice. Thus apparently altered APP processing, facilitating plaque formation, is upstream of altered formation of tangles [101]. Third, in AD, the allele people have of a particular lipoprotein, apoE, strongly affects likelihood of getting the disease. In mice expressing APP which are deficient of apoE, Aβ deposition is reduced, suggesting that the effect of apoE on AD involves APP and Aβ [101]. Fourth, genetic variability in Aβ degradation and clearance appears to contribute to the risk of AD [101]. A final point that these authors did not add which is worth mentioning is that large fibrillar aggregates of Aβ have been shown many times to be neurotoxic in cell culture [100]. It is also interesting to note that Aβ itself is not toxic – fresh solutions containing Aβ monomer are not toxic, but stored solutions develop neurotoxicity [111]. The conventional wisdom is that this is due to fibrils of Aβ which are formed over time, seeded by Aβ42, which aggregates more rapidly than Aβ40 [99]. Alternatives to this will be discussed below, but there is more to be said on the amyloid hypothesis first.

There are also some concerns with the amyloid hypothesis. One is that the number of amyloid deposits does not correlate well with the degree of cognitive im-

pairment; in fact, some healthy individuals have many Aβ deposits [101]. However, it can be argued that there is a stronger correlation with dense plaques (some are diffuse) [101] and also, there appear to be stronger correlations with total Aβ levels. In addition, as will be discussed below, the correlation is stronger with concentrations of soluble Aβ species, especially oligomers [101, 111], and this is one reason why the focus (in a modification of the amyloid hypothesis) is now shifting to oligomers of Aβ. An additional problem is that a number of mutations in APP, or one of two presenilin proteins important in AD (PS1 and PS2) increase Aβ deposition but the degree to which they increase it does not seem strongly correlated to the age of AD onset [101]. Hardy and Selkoe argue that the biggest reason this hypothesis is still controversial, however, is simply because the specific neurotoxic species has not yet been defined, nor have its specific effects on neuronal function. They detail several other minor problems with this hypothesis and conclude that none of these provides a compelling reason to abandon the hypothesis, although these arguments point to gaps in our understanding [101]. Work on oligomers, which will be addressed below, appears to be making progress at filling in some of these gaps.

Evidence for the role of oligomers of Aβ

There has been a variety of work pointing to smaller assemblies of Aβ as the toxic species. This idea is not too surprising if one believes Aβ is causing the problems. For example, large aggregates of Aβ are extracellular and cannot interfere directly with the cell metabolism. So either they must set off some process that does (i.e. oxidative stress) or it is smaller aggregates – which can interact with the cell surface or interior of the cell – which are doing the damage [99]. This also connects to

the idea that plaques might serve as reservoirs of smaller aggregates, oligomers of some sort, with which they are in equilibrium [112]. It has even been suggested that aggregates could be protective – by storing harmful oligomers instead of allowing them to interfere with cell metabolism [99]. Here, some of the research in this area will be discussed briefly, but the reader is referred to reviews by Kirkitadze *et al.* [100] and Klein [111] for more details.

There is now substantial evidence that oligomers of Aβ are more important to toxicity than large aggregates. As hinted at above, simple measures of total amount of amyloid or number of plaques do not correlate well with severity of AD [100]. AD, however, is region specific, affecting especially the hippocampus, entorhinal cortex, and some areas of the neocortex [98]. It turns out that the area of these regions occupied by Aβ plaques correlates somewhat more strongly with severity of dementia [100]. Many plaques are also observed in healthy individuals, however [99, 111]. There are more significant correlations between soluble Aβ levels and severity of brain pathology [100]. Even more interestingly, soluble Aβ levels correlate with density of tangles [100]. Soluble Aβ levels also correlate well with synapse loss [100, 111]. And soluble Aβ levels are high in Downs syndrome patients who will later get AD, at least suggesting that soluble Aβ species may play an early role in AD pathogenesis [100]. Furthermore, a protein called ApoJ is known to block formation of large (sedimentable) Aβ aggregates but does not block Aβ toxicity, suggesting smaller aggregates are toxic [111]. In fact, ApoJ-treated solutions appear to be *more* toxic than untreated ones [111]; perhaps oligomers are more toxic and treating with ApoJ prevents formation of aggregates, thus leaving more oligomers.

In transgenic mice expressing APP, significant neuronal injury occurs even be-

fore the appearance of plaques. Mice expressing presenilin mutations which cause FAD show even more neurodegeneration while plaques are still absent [100]. And injection of oligomers of human Aβ naturally secreted by cells, when collected and injected into rats, inhibit hippocampal long-term potentiation in the absence of fibrils. This suggests that Aβ oligomers may play an early role in synaptic dysfunction [112]. Previously, oligomeric intermediates to fibrils have been discovered and called protofibrils. They are typically relatively short and flexible filaments which often appear beaded [100]. These have been found to be neurotoxic, and one mutation in APP which cases familial Alzheimer's disease (FAD) accelerates formation of protofibrils, even though it decreases total Aβ levels, suggesting that protofibril formation could be the explanation for its toxicity [100, 113, 114, 115]. Annular protofibrils have also been found, and similar protofibrils have been observed in Parkinson's disease, where the relevant protein is α-synuclein. It has been suggested that annular protofibrils in these diseases, which are also promoted by some disease-causing mutations in Parkinson's disease, may form pores or channels through cell membranes [114]. Some other proteins important in amyloid diseases, such as huntingtin (in Huntington's disease) and IAPP also appear to have channel or pore activity [114]. More on pores will follow in Chapter 3.

In AD, globular oligomers have also been observed and called ADDLs, for AD disease diffusible ligands [100, 111]. These have been suggested to cause specific aberrations in synaptic signaling [111]. These appear to be quite toxic to some cultured cell lines, and specifically inhibit long-term potentiation, similar to the work of Walsh *et al.* [112] described above. In addition, ADDLs appear to have regionally specific effects on the brain – killing hippocampal but not cerebellar neurons. This is

an important observation as AD has region-specific effects like this, but this has not been observed with fibril preparations [111]. ADDLs may exist in equilibrium with protofibrils, but can exist without protofibril formation [111]. ADDLs only form from Aβ42, not Aβ40, which would explain why Aβ42 is usually regarded as the disease-associated form [100, 111]. ADDLs form at low concentrations of Aβ that are probably biologically relevant [111]. ADDLs have also been detected at elevated levels in AD affected brains but not in normal brains [111]. An additional interesting piece of the puzzle is that a particular tyrosine kinase, Fyn, is up-regulated in AD-affected neurons, and is known to be relevant to apoptosis in development. ADDLs are not toxic to cells in hippocampal slices of Fyn-knockout mice (where they usually would be toxic) [116] suggesting that ADDL toxicity is dependent on the apoptosis pathway involving Fyn. In addition, two proteins in rat cortex and hippocampus which bind ADDLs at high (nanomolar) affinities have been identified which are absent from cerebellum (helping to explain regional specificity) [111]. Vaccination has been suggested to help prevent damage due to ADDLs [111] and, interestingly, some mouse trials of vaccination found that it was beneficial [111, 117], but not because of removal of amyloid plaques, suggesting beneficial effects were on soluble Aβ [111]. We refer the reader to the review by Klein for more on ADDLs [111].

Overall, the main point is that there has been increasing emphasis in AD recently on oligomers. There have been a variety of suggestions for oligomer toxicity mechanisms, and even toxic species, and one of these will be discussed in more detail in this work in Chapter 3. Suggestions for toxicity mechanisms range from the very specific (i.e. binding to a specific receptor and interacting with a specific signaling pathway), to intermediate (i.e. making membranes permeable to some ions which

cause cell damage due to ion leakage, a mechanism that will be discussed here), to very general (i.e. general membrane permeabilization). Nailing down the exact mechanism or mechanisms is quite important for drug discovery. This emerging role of oligomers – and the search for their toxicity mechanisms – is common not just to AD but to other amyloid diseases [100] and thus is even more important.

At this point, it is also worth mentioning that there are a number of point mutants in the Aβ peptide (as well as its precursor protein) which are known to cause AD. These will be discussed in some more detail in Chapter 3. However, although they are responsible only for a small fraction of AD cases [102], they provide a tool for assessing potential toxicity mechanisms. In other words, when the toxicity mechanism(s) in AD are understood, one should be able to explain why these mutants cause AD. Unfortunately, at this point, these mutants fit with several different pictures of the disease. For example, as will be discussed in Chapter 3, four of five FAD Aβ mutants increase propensity of Aβ42 to aggregate, and four of five increase Aβ levels – both of which have been suggested to be important for toxicity (see Chapter 3 for discussion and references). On a smaller scale, these mutations are also quite close to the α secretase cleavage site of APP (four to seven residues away), suggesting that they might cause abnormal processing of Aβ [101]. It also has been suggested that these residues (21-23 of Aβ) lie in a key turn region within the Aβ fibril [118], at least in one proposed structure, so mutations could destabilize fibril formation. These residues are also key in a turn region for a fibril structure suggestion based on NMR [119]; some modeling work suggests this structure may be reasonable [120]. It has also been pointed out that many of these mutants involved altered charge states, which may drastically affect fibrillogenesis properties [121].

And a final suggestion involving the mutants will be provided here in Chapter 3, where it is shown that most of the point mutants which cause FAD may affect the conformation of Aβ within cell membranes in a way that may cause disease. Given all these suggestions of the role of mutants, it may seem that the mutants cannot strongly constrain possible toxicity mechanisms. However, this is perhaps one place where modeling can play a very useful role in AD research: modeling can provide insight into whether the effects these mutants have really can be correlated with these suggestions. In other words, it is one thing to guess that mutants may affect a conformation in a particular way, but modeling can help to determine whether or not it really will – and thus help narrow down which of the suggested toxicity mechanisms are relevant biologically.

As mentioned above, there have been various claims that the toxicity mechanisms in amyloid diseases may not be unique to a particular disease – that is, amyloid and amyloidogenic proteins may have some common properties that mean that what is learned from studying, say, AD or prion disease can apply to the study of Parkinson's disease, and so on. In particular, toxic oligomers have been suggested to have similar toxicity mechanisms in several diseases, including Parkinson's and AD (see for example, Lashuel and collaborators [114]). The present author has been fairly skeptical of these claims, but a compelling new piece of evidence suggests that there may really be something to suggestions of links between these diseases. The new evidence comes from work developing an antibody which can recognize Aβ oligomers but not large aggregates. This work has shown that ADDLs and protofibrils are both recognized by this antibody – thus having some key structural similarity – while large fibrils are not. Furthermore, this antibody reacts with all amyloidogenic

soluble oligomers tested so far! This includes aggregates of α-synuclein, islet amyloid polypeptide, polygutamine, lysozyme, human insulin, and the prion protein [122]. Furthermore, the antibody inhibits oligomer toxicity and can recognize oligomers in diseased brain (but not in healthy brain) [122]. This is a startling and amazing result to the current author and represents a fascinating question for future modeling work: how can all of these different proteins adopt conformations so similar that their oligomers can be recognized by the same antibody, despite huge sequence differences? This means that these diseases are interesting in two different ways from a protein folding point of view: (1) as proteins that themselves have multiple stable folds which are biologically relevant; and (2) as proteins which have common features in oligomerized, disease-associated folds despite huge sequence differences.

These protein folding modeling and theory challenges are not the subject of this work, but represent a challenge for the future. Chapter 3 of this work, however, will be focused on testing a particular oligomer toxicity mechanism and the effect of FAD mutants on that mechanism to see whether it may be relevant biologically, as described above. Thus we will first provide a brief overview of previous modeling done relating to AD.

1.2.3 Modeling background

A variety of work has been done in terms of theoretical models relating to AD. Some early work was quite similar to some of the early work done on prion aggregation – modeling formation of large aggregates or fibrils of the Aβ peptide. A key point for this work was that formation of Aβ fibrils *in vitro* – and prion fibrils, which were included in the same model – can be accelerated by addition of a pre-formed

fibril. This model is nucleation-based; that is, formation of a critical nucleus for aggregation is a slow process, so aggregation can be accelerated by introduction of an initial aggregate which is already past the critical nucleus stage. Formation of the nucleus is the slow step in aggregation [123]. In this model, the concentration of monomer is thought to be low enough that nucleation only rarely happens by chance; in AD, something has to happen to increase the Aβ concentration past some critical concentration necessary to allow nucleation [123]. For this model to be reasonable, this critical concentration must mark a sharp decrease in nucleation probability as a function of concentration. Otherwise, the shift from no AD to likely AD due to nucleation would require several orders of magnitude change in concentration, which would be very unlikely to happen – a weakness of this model. A nucleation barrier like this would involve a similar model to the one which will be discussed in Chapter 2 for formation of soft hexamers. However, it will be seen there that this model does not produce a true "critical concentration" but rather a transition concentration, which one might also expect would be the case here. Therefore this mechanism seems to the present author to be unlikely to provide a satisfactory explanation for the disease simply because the change in concentration necessary to induce disease would be too large. In addition, oligomers increasingly appear to be the toxic species.

In a series of papers in the late 1990s, Stanley and collaborators analyzed the three dimensional structure of Aβ plaques from AD brains, and developed a dynamical model for the growth of these large aggregates, including competing aggregation and disaggregation and surface diffusion of Aβ deposits. This model was able to produce plaques with similar, fairly irregular structures like the aggregates really

observed [124, 125, 126]. The authors point out that earlier models like the one described above, with nucleation and growth, would result in compact aggregates [124]. Their model, in contrast, includes disaggregation, which is able to produce a porous structure [124]. They later refined the model based on observing plaques at different times taken from laboratory mice to match the observed time progression [125]. This work suggested that Aβ deposition may be reversible, and that diffuse plaques of Aβ, which have been previously thought to be precursors to the typical Aβ dense-cored plaques, may not be precursors after all [125].

Because of the propensity of Aβ to form fibrils, a variety of molecular dynamics simulations (MD) have been done to look at the ability of Aβ to form β-sheets, and at the stability of Aβ oligomers in different suggested fibril structures [120, 127, 128, 129]. In addition, the E22Q mutant is known to increase the fibrillization rate. MD simulations have suggested this is due to the charge alteration decreasing the peptide's stability in water, rather than increasing its propensity to form β-structure [121], while Monte Carlo (MC) simulations suggest that the mutation allows stronger hydrogen bonding within fibrils [130]. Carol Hall at North Carolina State University and collaborators have also begun working on a discrete molecular dynamics (DMD) model of formation of larger β sheets of Aβ on longer timescales [131], but this work is still largely at the level of model development and refinement. Baumketner and Shea have also begun applying MD to model dimerization of Aβ and comparing to a mutant, F19P, which is known to reduce dimerization [132]. Various possible fibril structures have also been explored using an MC simulation to equilibrate and compare energetics [130].

With the emergence of the more recent focus on oligomers, some workers have

turned to trying to model formation of oligomers to help gain a better understanding of the sizes and structures of the oligomers experimentalists are observing. This is difficult to do with MD because of the large number of atoms and timescales involved, so a DMD model of the process is being developed by Urbanc, Buldyrev, Stanley and collaborators at Boston University [133]. Again, the model here is still being developed, but this work is something which shows promise for the future.

Since APP is a transmembrane protein, some modeling work has also been done on the structure of Aβ, the nominal transmembrane domain, in a membrane environment. This was done in the process of developing a phenomenological model for predicting protein folds in membrane environments based on both bioinformatics structure predictions and energies of interaction between amino acids and the membrane environment. This method predicted that Aβ, after residue 16, will insert into cell membranes in a transmembrane helix and that the part prior to that will remain outside the membrane in a β-turn, consistent with earlier NMR data [134]. This is the work most closely related to what will be presented here in Chapter 3.

Some much earlier protein structure work had also predicted that the Aβ peptide might insert into cell membranes and form harmful pores or ion channels [135]. With some experimental confirmation of this [136, 137], interaction of Aβ with cell membranes has begun to look even more important. While the work mentioned just above dealt with insertion of Aβ into lipid bilayers, one thing the researchers did not examine was the effect of mutations in Aβ on its insertion behavior. As was argued above, FAD-causing mutants in Aβ provide a tool for assessing toxicity mechanisms. That is, if indeed this channel mechanism is correct, one would expect that the FAD mutants will either make the channel structure more favorable, or

make Aβ insert into cell membranes more easily or in a conformation more favorable for forming channels. The work presented here will address this insertion possibility and argue that four of the five FAD mutants affect insertion in a way that could make channel formation more common (Chapter 3). The possibility that the FAD mutants may affect formation of these channel structures is left for future work and will be discussed briefly in Chapter 5.

1.3 Magnetic Hysteresis in Thin Films

Magnetic hysteresis may seem to be a topic far disconnected from the other topics covered in this work, but as it turns out, this work is especially connected to, and motivated by, early work done in this group on prion diseases as described by Slepoy *et al.* [4] and Kulkarni *et al.* [6]. In particular, some experimental work had been done previously on magnetic thin films (Co-Pt multilayers) in this department (which will be reported in Chapter 4) which demonstrated unusual features of major hysteresis loops and first-order reversal curves (FORCs, the curves obtained by sweeping the applied field from a saturating positive field down to some negative reversal field and then back up to positive saturation). These features, as will be discussed, suggested that a nucleation barrier might dominate the magnetization reversal process in these materials. Thus a simple model of a nucleation barrier might lend great insight into the magnetization reversal process in these materials. Therefore, as a first pass at this sort of a model, the model which will be presented here is largely based on the earlier work mentioned above on prion diseases. As in the original model developed by Slepoy *et al.* [4], the model here uses rules such that the smallest stable new domain is seven spins (lattice sites representing small magnetic columns in the

Bibliography

[1] C. Weissmann, M. Enari, P-C. Klöhn, D. Rossi, and E. Flechsig. Transmission of Prions. *Journal of Infectious Diseases*, 186(Suppl. 2):S157–S165, 2002.

[2] Richard H. Kimberlin and John W. Wilesmith. Bovine Spongiform Encephalopathy: Epidemiology, Low Dose Exposure and Risks. In *Annals of the New York Academy of Sciences: Slow Infections of the Central Nervous System*, volume 74, pages 210–220. New York Academy of Sciences, 1994.

[3] Rosalind Ridley and Harry F. Baker. *Fatal Protein.* Oxford University Press, Inc., New York, 1998.

[4] A. Slepoy, R. R. P. Singh, F. Pázmándi, R. V. Kulkarni, and D. L. Cox. Statistical Mechanics of Prion Diseases. *Phys. Rev. Lett.*, 87(5):0581011–0581014, 2001.

[5] David L. Mobley, Daniel L. Cox, Rajiv R. P. Singh, Rahul V. Kulkarni, and Alexander Slepoy. Simulations of Oligomeric Intermediates in Prion Diseases. *Biophys. J.*, 85:2213–2223, 2003.

[6] R. V. Kulkarni, A. Slepoy, R. R. P. Singh, and F. Pázmándi. Theoretical Modeling of Prion Disease Incubation. *Biophys. J.*, 85:707–718, 2003.

[7] Reed B. Wickner. *Prion Diseases of Mammals and Yeast: Molecular Mechanisms and Genetic Features.* R. G. Landes Company, 1997.

[8] J. Cuille and P. L. Chelle. Pathologie animale. La maladie dite tremblant du mouton est-elle inoculable? *Compt. Rend. Acad. Sci. (Paris)*, 203:1552–1554, 1936. Cited by R. B. Wickner.

[9] J. Cuille and P. L. Chelle. Experimental transmission of trembling to the goat. *Compt. Rend. Seances Acad. Sci.*, 208:1058–1060, 1939. Cited by R. B. Wickner.

[10] W. S. Gordon. Advances in Veterinary Research–Louping ill, tick-borne fever and scrapie. *Vet. Rec.*, pages 516–520, 1946.

[11] Bruce Alberts, Alexander Johnson, Julian Lewis, Martin Raff, Keith Roberts, and Peter Walter. *Molecular Biology of the Cell.* Garland Science, fourth edition, 2002.

[12] Tikvah Alper, W. A. Cramp, D. A. Haig, and M. C. Clarke. Does the Agent of Scrapie Replicate without Nucleic Acid? *Nature*, 214:764–766, 1967.

[13] R. A. Gibbons and G. D. Hunter. Nature of the Scrapie Agent. *Nature*, 215:1041–1043, 1967.

[14] J. S. Griffith. Self replication and scrapie. *Nature*, 215:1043–1044, 1967.

[15] V. Zigas and D. C. Gajdusek. Kuru: clinical study of a new syndrome resembling paralysis agitans in natives of the Eastern Highlands of Australian New Guinea. *Med. J. Aust.*, 2:745–754, 1957. Cited by R. B. Wickner.

[16] D. C. Gajdusek and V. Zigas. Degenerative disease of the central nervous system in New Guinea: the endemic occurence of "kuru" in the native population. *New Engl. J. Med.*, 257:974–978, 1957. Cited by R. B. Wickner.

[17] W. J. Hadlow. Scrapie and Kuru. *Lancet*, 2:289–290, 1959.

[18] Stanley B. Prusiner. Novel Proteinaceous Infectious Particles Cause Scrapie. *Science*, 216:136–144, 1982.

[19] David C. Bolton, Michael P. McKinley, and Stanley B. Prusiner. Identification of a Protein that Purifies with the Scrapie Prion. *Science*, 218:1309–1311, 1982.

[20] Stanley B. Prusiner, David C. Bolton, Darlene F. Groth, Karen A. Bowman, S. Patricia Cochran, and Michael P. McKinley. Further Purification and Characterization of Scrapie Prions. *Biochemistry*, 21:6942–6950, 1982.

[21] Teun van Rheede, Marcel M. W. Smolenaars, Ole Madsen, and Wilfried W. de Jong. Molecular Evolution of the Mammalian Prion Protein. *Mol. Biol. Evol.*, 20:111–121, 2003.

[22] Stanley B. Prusiner. An Introduction to Prion Biology and Diseases. In Stanley B. Prusiner, editor, *Prion Biology and Diseases*. Cold Spring Harbor Laboratory Press, second edition, 2004.

[23] L. G. Goldfarb. Kuru: The old epidemic in a new mirror. *Microbes Infect.*, 4:875–882, 2002.

[24] C. Bernoulli, J. Siegfried, G. Baumgartner, F. Regli, T. Rabiowicz, D. C. Gajdusek, and C.J. Gibbs, Jr. Danger of Accidental Person-to-Person Transmission of Creutzfeldt-Jakob Disease by Surgery. *Lancet*, 1:478–479, 1977.

[25] C. J. Gibbs Jr., D. M. Asher, A. Kobrine, H. L. Amyx, M. P. Sulima, and D. C. Gajdusek. Transmission of Creutzfeld-Jakob disease to a chimpanzee by electrodes contaminated during neurosurgery. *J. Neurol. Neurosurg. Psychiatry*, 57:757–758, 1994.

[26] P. Brown, M. Preece, J.-P. Brandel, T. Sato, L. McShane, I. Zerr, A. Fletcher, R. G. Will, M. Pocchiari, N. R. Cashman, J. H. d'Augnaux, L. Cervenáková, and J. Fradkin. Iatrogenic Creutzfeldt-Jakob disease at the millennium. *Neurology*, 55:1075–1081, 2000.

[27] C. J. G. Lang, J. G. Heckmann, and B. Neundorfer. Creutzfeldt-Jakob disease via dural and corneal transplants. *J. Neurol. Sciences*, 160:128–139, 1998.

[28] N. Bons, N. Mestre-Frances, P. Belli, F. Cathala, D. C. Gajdusek, and P. Brown. Natural and experimental oral infection of nonhuman primates by bovine spongiform encephalopathy agents. *Proc. Nat. Acad. Sci. USA*, 96:4046–4051, 1999.

[29] Rosalind M. Ridley and Harry F. Baker. Oral transmission of BSE to primates. *Lancet*, 348:1174, 1996.

[30] R. G. Will, J. W. Ironside, M. Zeidler, S. N. Cousens, and K. Estibeiro. A new variant of Creutzfeldt-Jakob disease in the UK. *Lancet*, 347:921–925, 1996.

[31] John Collinge, Katie C. Sidle, Julie Meads, James Ironside, and Andrew F. Hill. Molecular analysis of prion strain variation and the aetiology of 'new variant' CJD. *Nature*, 383:685–690, 1996.

[32] M. Zeidler, G. Stewart, S. N. Cousens, K. Estibeiro, and R. G. Will. Codon 129 genotype and new variant CJD. *Lancet*, 350:668, 1997.

[33] The UK Creutzfeldt-Jakob Disease Surveillance Unit, March 2004. Current statistics updated monthly at www.cjd.ed.ac.uk/figures.htm.

[34] Holger Wille, 2002. Personal communication.

[35] E. E. Manuelidis and L. Manuelidis. Suggested Links between Different Types of Dementias: Creutzfeldt-Jakob Disease, Alzheimer Disease, and Retroviral CNS Infections. *Alzheimer Disease and Associated Disorders*, 3:100–109, 1989.

[36] Francois Boller, Oscar L. Lopez, and John Moossy. Diagnosis of dementia: Clinicopathologic correlations. *Neurology*, 39:76–79, 1989.

[37] Cristina Casalone, Gianluigi Zanusso, Pierluigi Acutis, Sergio Ferrari, Lorenzo Capucci, Fabrizio Tagliavini, Salvatore Monaco, and Maria Carmelli. Identification of a second bovine amyloidotic spongiform encephalopathy: Molecular similarities with sporadic Creutzfeldt-Jakob disease. *Proc. Nat. Acad. Sci. USA*, 101:3065–3070, 2004.

[38] Emmanuel A. Asante, Jacqueline M. Linehan, Melanie Desbruslais, Susan Joiner, Ian Gowland, Andrew L. Wood, Julie Welch, Andrew F. Hill, Sarah E. Lloyd, Jonathan D. F. Wadsworth, and John Collinge. BSE prions propagate as either variant CJD-like or sporadic CJD-like prion strains in transgenic mice expressing human prion protein. *EMBO*, 21(23):6358–6366, 2002.

[39] J. A. Yesavage, R. O'Hara, H. Kraemer, A. Noda, J. L. Taylor, S. Ferris, M. C. Gely-Nargeot, A. Rosen, L. Friedman, J. Sheikh, and C. Derouesne. Modeling the prevalence and incidence of Alzheimer's disease and mild cognitive impairment. *J. Psychiatr. Res.*, 36:281–286, 2002.

[40] U.S. Department of Agriculture. USDA Makes Preliminary Diagnosis of BSE. Dec. 23, 2003, news release 0432.02, http://www.usda.gov/Newsroom /0432.03.html.

[41] Elizabeth Weise. USDA to ramp up mad cow testing 3 times the cattle using faster method. USA Today online, March 9, 2004, http://www. usatoday.com/usatonline/20040309/5987760s.htm.

[42] Report on Measures Relating to Bovine Spongiform Encephalopathy (BSE) in the United States. USDA advisory committee report, http://www. aphis.usda.gov/lpa/issues/bse/US_BSE_report.pdf, Feb. 4, 2004.

[43] Mo D. Salman. Chronic Wasting Disease in Deer and Elk: Scientific Facts and Findings. *J. Vet. Med. Sci.*, 65:761–768, 2003.

[44] Michael W. Miller and Elizabeth S. Williams. Horizontal prion tramsmission in mule deer. *Nature*, 425:35–36, 2003.

[45] James Hourrigan, Albert Klingsporn, W. W. Clark, and M. de Camp. Epidemiology of Scrapie in the United States. In *Slow Transmissible Diseases of the Nervous System*, volume 1, pages 331–356. Academic Press, 1979.

[46] H. Büeler, A. Aguzzi, A. Sailer, R.-A. Greiner, P. Autenried, M. Aguet, and C. Weissmann. Mice Devoid of PrP Are Resistant to Scrapie. *Cell*, 73:1339–1347, 1993.

[47] Andreas Sailer, Hansruedi Büeler, Marek Fischer, Adriano Aguzzi, and Charles Weissmann. No Propagation of Prions in Mice Devoid of PrP. *Cell*, 77:967–968, 1994.

[48] Marek Fischer, Thomas Rülicke, Alex Raeber, Andreas Sailer, Markus Moser, Bruno Oesch, Sebastian Brandner, Adriano Aguzzi, and Charles Weissmann. Prion protein (PrP) with amino-proximal deletions restoring susceptibility of PrP knockout mice to scrapie. *EMBO*, 15:1255–1264, 1996.

[49] Stanley B. Prusiner. Prions. *Proc. Nat. Acad. Sci. USA*, 95:13363–13383, 1998.

[50] Sebastian Brandner, Alex Raeber, Andreas Sailer, Thomas Blättler, Marek Fischer, Chares Weissmann, and Adriano Aguzzi. Normal host prion protein (PrP^C) is required for scrapie spread within the central nervous system. *Proc. Nat. Acad. Sci. USA*, 93:13148–13151, 1996.

[51] Jiri Safar, Holger Wille, Vicenza Itri, Darlene Groth, Hana Serban, Marilyn Torchia, Fred E. Cohen, and Stanley B. Prusiner. Eight prion strains have PrP^{Sc} molecules with different conformations. *Nature Medicine*, 4(10):1157–1165, 1998.

[52] J. Safar, F. E. Cohen, and S. B. Prusiner. Quantitative traits of prion strains are enciphered in the conformation of the prion protein. *Arch. Virol.*, 16(Suppl.):227–235, 2000.

[53] Charles Weissmann. Molecular Genetics of Transmissible Spongiform Encephalopathies. *J. Biol. Chem.*, 274:3–6, 1999.

[54] F. Lopez-Garcia, R. Zahn, R. Riek, and K. Wuthrich. NMR Structure of the Bovine Prion Protein. *Proc. Nat. Acad. Sci. USA*, 97, 2000.

[55] R. H. Kimberlin and Carol A. Walker. Pathogenesis of Scrapie: Agent Multiplication in Brain at the First and Second Passage of Hamster Scrapie in Mice. *J. Gen. Virol.*, 42:107–117, 1979.

[56] Motohiro Horiuchi and Byron Caughey. Prion protein interconversions and the transmissible spongiform encephalopathies. *Structure*, 7:R231–R240, 1999.

[57] Jon H. Come, Paul E. Fraser, and Peter T. Lansbury Jr. A kinetic model for amyloid formation in the prion diseases: Importance of seeding. *Proc. Nat. Acad. Sci. USA*, 90:5959–5963, 1993.

[58] Stanley B. Prusiner, Michael R. Scott, and Stephen J. DeArmond. Transmission and Replication of Prions. In Stanley B. Prusiner, editor, *Prion Biology and Diseases*. Cold Spring Harbor Laboratory Press, 2 edition, 2004.

[59] Moira E. Bruce. Agent Replication Dynamics in a Long Incubation Period Model of Mouse Scrapie. *J. Gen. Virol.*, 66:2517–2522, 1985.

[60] Rahul V. Kulkarni, 2002. Personal communication.

[61] David C. Bolton. Prion distribution in hamster lung and brain following intraperitoneal innoculation. *J. Gen. Virol.*, 79:2557–2562, 1998.

[62] Joanna Masel, Vincent A. A. Jansen, and Martin A. Nowak. Quantifying the kinetic parameters of prion replication. *Biophysical Chemistry*, 77:139–152, 1999.

[63] C. M. Eklund, R. C. Kennedy, and W. J. Hadlow. Pathogenesis of scrapie virus infection in the mouse. *J. Infect. Dis.*, 117:15–22, 1967.

[64] Charles Weissmann, Alex J. Raeber, Fabio Montrasio, Ivan Hegyi, Rico Frigg, Michael A. Klein, and Adriano Aguzzi. Prions and the lymphoreticular system. *Phil. Trans. R. Soc. Lond. B*, 356:177–184, 2001.

[65] Jason C. Bartz, Anthony E. Kincaid, and Richard A. Bessen. Rapid Prion Neuroinvasion following Tongue Infection. *Journal of Virology*, 77:583–591, 2003.

[66] Thomas Blättler, Sebastian Brandner, Alex J. Raeber, Michael A. Klein, Till Voigtländer, Charles Weissmann, and Adriano Aguzzi. PrP-expressing tissue required for transfer of scrapie infectivity from spleen to brain. *Nature*, 389:69–73, 1997.

[67] Valérie Künzi, Markus Glatzel, Michel Y. Nakano, Urs F. Graeber, Fred Van Leuven, and Adriano Aguzzi. Unhampered Prion Neuroinvasion despite Impaired Fast Axonal Transport in Transgenic Mice Overexpressing Four-Repeat Tau. *J. Neurosci.*, 22(17):7471–7477, 2002.

[68] Adriano Aguzzi, Frank L. Heppner, Mathias Heikenwalder, Marco Prinz, Kirsten Metz, Harald Seeger, and Markus Glatzel. Immune system and peripheral nerves in propagation of prions to CNS. *British Medical Bulletin*, 66:141–159, 2003.

[69] Nnennaya Kanu, Yutaka Imokawa, David N. Drechsel, R. Anthony Williamson, Christopher R. Birkett, Christopher J. Bostock, and Jeremy P. Brockes. Transfer of Scrapie Prion Infectivity by Cell Contact in Culture. *Current Biology*, 12:523–530, 2002.

[70] Eckhard Flechsig, Ivan Hegyi, Masato Enari, Petra Schwarz, John Collinge, and Charles Weissmann. Transmission of Scrapie by Steel-surface-bound Prions. *Molecular Medicine*, 7(10):679–684, 2001.

[71] Glenn L. Millhauser. Copper Binding in the Prion Protein. *Accounts of Chemical Research*, 37(2):79–85, 2004.

[72] David R. Brown, Kefeng Qin, Jochen W. Herms, Axel Madlung, Jean Manson, Robert Strome, Paul E. Fraser, Theo Kruck, Alex von Bohlen, Walter Schulz-Schaeffer, Armin Giese, David Westaway, and Hans Kretzschmar. The cellular prion protein binds copper *in vivo*. *Nature*, 390:684–687, 1997.

[73] D. J. Waggoner, B. Drisaldi, T. B. Bartnikas, R. L. B. Casareno, J. R. Prohaska, J. D. Gitlin, and D. A. Harris. Brain copper content and cuproenzyme activity do not vary with prion protein expression level. *J. Biol. Chem.*, 275:7455–7458, 2000.

[74] Boon-Seng Wong, Shu G. Chen, Monica Colucci, Zhiliang Xie, Tao Pan, Tong Liu, Ruliang Li, Pierluigi Gambetti, Man-Sun Sy, and David R. Brown. Aberrant metal binding by prion protein in human prion disease. *J. Neurochem.*, 78:1400–1408, 2001.

[75] Lesley R. Brown and David A. Harris. Copper and zinc cause delivery of the prion protein from the plasma membrane to a subset of early endosomes and the golgi. *J. Neurochem.*, 87:353–363, 2003.

[76] M. A. Chacón, M. I. Barría, R. Lorca, J. P. Huidobro-Toro, and N.C. Inestrosa. A human prion protein peptide (PrP_{59-91}) protects against copper neurotoxicity. *Molecular Psychiatry*, 8:853–862, 2003.

[77] Walid Rachidi, Alain Mangé, Abderrahmene Senator, Pascale Guiraud, Jacqueline Riondel, Mustapha Benboubetra, Alain Favier, and Sylvain Lehmann. Prion Infection Impairs Copper Binding of Cultured Cells. *J. Biol. Chem.*, 278(17):14595–14598, 2003.

[78] Colin S. Burns, Eliah Aronoff-Spencer, Christine M. Dunham, Paula Lario, Nikolai I. Avdievich, William E. Antholine, Marilyn M. Olmstead, Alice Vrielink, Gary J. Gerfen, Jack Peisach, William G. Scott, and Glenn L. Millhauser. Molecular Features of the Copper Binding Sites on the Octarepeat Domain of the Prion Protein. *Biochemistry*, 41:3991–4001, 2002.

[79] Colin S. Burns, Eliah Aronoff-Spencer, Giuseppe Legname, Stanley B. Prusiner, William E. Antholine, Gary J. Gerfen, Jack Peisach, and Glenn L. Millhauser. Copper coordination in the full-length, recombinant prion protein. *Biochemistry*, 42:6794–6803, 2003.

[80] C. Weissmann and E. Flechsig. PrP knock-out and PrP transgenic mice in prion research. *British Medical Bulletin*, 66:44–60, 2003.

[81] Axel Behrens. Physiological and pathological functions of the prion protein homologue Dpl. *British Medical Bulletin*, 66:35–42, 2003.

[82] David Westaway, Leroy E. Hood, and Stanley B. Prusiner. Doppel, a New PrP-like Mammalian Protein. In Stanley B. Prusiner, editor, *Prion Biology and Diseases*. Cold Spring Harbor Laboratory Press, 2 edition, 2004.

[83] Doron Shmerling, Ivan Hegyi, Marek Fischer, Thomas Blättler, Sebastian Brandner, Jürgen Götz, Thomas Rülicke, Eckhard Flechsig, Antonio Cozzio, Christian von Mering, Christoph Hangartner, Adriano Aguzzi, and Charles Weissmann. Expression of Amino-Terminally Truncated PrP in the Mouse Leading to Ataxia and Specific Cerebellar Lesions. *Cell*, 93:203–214, 1998.

[84] Kefeng Qin, Janaky Coomaraswamy, Peter Mastrangelo, Ying Yang, Stan Lugowski, Chris Petromilli, Stanley B. Prusiner, Paul E. Fraser, Jonathan M. Goldberg, Avijit Chakrabartty, and David Westaway. The PrP-like Protein Doppel Binds Copper. *J. Biol. Chem.*, 278(11):8888–8896, 2003.

[85] Corinne Ida Lasmézas. Putative functions of PrP^C. *British Medical Bulletin*, 66:61–70, 2003.

[86] Jim Warwicker. Modeling a Prion Protein Dimer: Predictions for Fibril Formation. *Biochem. Biophys. Res. Comm.*, 278:646–652, 2000.

[87] Johannes Zuegg and Jill E. Gready. Molecular dynamics simulation of the

human prion protein including both N-linked oligosaccharides and the GPI anchor. *Glycobiology*, 10(10):959–974, 2000.

[88] Philippe Derreumaux. Evidence that the 127-164 Region of Prion Proteins Has Two Equi-Energetic Conformations with β or α Features. *Biophysical Journal*, 81:1657–1665, 2001.

[89] Andrew F. Wind, Josh P. Kemp, Aleksander V. Ermoshkin, and Jeff Z. Y. Chen. Structural and folding properties of a lattice prion model. *Phys. Rev. E*, 66:031909, 2002.

[90] Manfred Eigen. Prionics or The Kinetic Basis of Prion Diseases. *Biophys. Chem.*, 63:A1–A18, 1996.

[91] Leslie E. Orgel. Prion replication and secondary nucleation. *Chemistry and Biology*, 3(6):413–414, 1996.

[92] Martin A. Nowak, David C. Krakauer, Aron Klug, and Robert M. May. Prion Infection Dynamics. *Integr. Biol.*, 1:3–15, 1998.

[93] Joanna Masel and Vincent A. A. Jansen. Designing drugs to stop the formation of prion aggregates and other amyloids. *Biophysical Chemistry*, 88:47–59, 2000.

[94] Michael P. H. Stumpf and David C. Krakauer. Mapping the Parameters of Prion-Induced Neuropathology. *Proc. Nat. Acad. Sci. USA*, 97(19):10573–10577, 2000.

[95] Nicolas Kellershohn and Michel Laurent. Prion Diseases: Dynamics of the Infection and Properties of the Bistable Transition. *Biophys. J.*, 81:2517–2529, 2001.

[96] H. Wille, D. Michelistsch, V. Guenebaut, S. Suppatapone, A. Serban, F. E. Cohen, D. A. Agard, and S. B. Prusiner. Structural studies of the scrapie prion

protein by electron crystallography. *Proc. Nat. Acad. Sci. USA*, 99:3563–3568, 2002.

[97] Liesi E. Hebert, Paul A. Scherr, Julia L. Bienas, David A. Bennett, and Denis A. Evans. Alzheimer Disease in the US Population. *Arch. Neurol.*, 60(8):1119–1122, 2003.

[98] Christopher M. Clark and Jason H. T. Karlawish. Alzheimer Disease: Current Concepts and Emerging Diagnostic and Therapeutic Strategies. *Annals of Internal Medicine*, 138(5):400–411, 2003.

[99] Piero Andrea Temussi, Laura Masino, and Annalisa Pastore. From Alzheimer to Huntington: why is a structural understanding so difficult? *EMBO*, 22(3):355–361, 2003.

[100] Marina D. Kirkitadze, Gal Bitan, and David B. Teplow. Paradigm Shifts in Alzheimer's Disease and Other Neurodegenerative Disorders: The Emerging Role of Oligomeric Assemblies. *J. Neurosci. Res.*, 69:567–577, 2002.

[101] John Hardy and Dennis J. Selkoe. The Amyloid Hypothesis of Alzheimer's Disease: Progress and Problems on the Road to Therapeutics. *Science*, 297:353–356, 2002.

[102] Dennis J. Selkoe. Alzheimer's Disease: Genes, Proteins and Therapy. *Physiol. Rev.*, 82(2):741–766, April 2001.

[103] C. Wurth, N. K. Guimard, and Michael H. Hecht. Mutations that Reduce Aggregation of the Alzheimer's Aβ42 Peptide: an Unbiased Search for the Sequence Determinants of Aβ Amyloidogenesis. *J. Mol. Biol.*, 319:1279–1290, 2002.

[104] Peter T. Lansbury, Jr. Listing of reviews on his web site at http://lansbury.bwh.harvard.edu/alzheimer_disease.htm, April, 2004.

[105] Michael S. Wolfe. Secretase Targets for Alzheimer's Disease: Identification and Therapeutic Potential. *J. Med. Chem.*, 44(13):2039–2060, 2001.

[106] William J. Bowers and Howard J. Federoff. Amyloid immunotherapy-engendered CNS inflammation. *Neurobiol. Aging*, 23:675–676, 2002.

[107] Denise Grady. Nominal Benefits Seen in Drugs for Alzheimer's. *The New York Times.* April 7, 2004 news article at http://www.nytimes.com.

[108] Ron R. Kopito. Aggresomes, inclusion bodies and protein aggregation. *Trends in Cell Biol.*, 10:524–520, 2000.

[109] Math P. Cuajungco and Kyle Fagét. Zinc takes the center stage: its paradoxical role in Alzheimer's disease. *Brain Res. Rev.*, 41:44–56, 2003.

[110] Kevin J. Barnham, Colin L. Masters, and Ashley I. Bush. Neurodegenerative diseases and oxidative stress. *Nature Rev. Drug. Disc.*, 3(3):205–214, 2004.

[111] William L. Klein. Aβ toxicity in Alzheimer's disease: globular oligomers (ADDLs) as new vaccine and drug targets. *Neurochem. Intl.*, 41:345–352, 2002.

[112] Dominic M. Walsh, Igor Klyubin, Julia V. Fadeeva, William K. Cullen, Roger Anwyl, Michael S. Wolfe, Michael J. Rowan, and Dennis J. Selkoe. Naturally secreted oligomers of amyloid β protein potently inhibit hippocampal long-term potentiation *in vivo*. *Nature*, 416:535–539, April 2002.

[113] Camilla Nilsberth, Anita Westlind-Danielsson, Christopher B. Eckmman, Margaret M. Condron, Karin Axelman, Charlotte Forsell, Charlotte Stenh, Johan Luthman, David B. Teplow, Steven G. Younkin, Jan Näslund, and Lars Lannfelt. The 'Arctic' APP mutation (E693G) causes Alzheimer's disease by enhanced Aβ protofibril formation. *Nature Neurosci.*, 4(9):887–893, September 2001.

[114] Hilal A. Lashuel, Dean Hartley, Benjamin M. Petre, Thomas Walz, and Peter T. Lansbury, Jr. Amyloid pores from pathogenic mutations. *Nature*, 418:291, July 2002.

[115] Christian Haass and Harald Steiner. Protofibrils, the unifying toxic molecule of neurodegenerative disorders? *Nature*, 4(9):859–860, 2001.

[116] M. P. Lambert, A. K. Barlow, B. A. Chromy, C. Edwards, R. Freed, M. Liosatos, T. E. Morgan, I. Rozovsky, B. Trommer, K. L. Viola, P. Wals, C. Zhang, C. E. Finch, G. A. Krafft, and W. L. Klein. Diffusible, nonfibrillar ligands derived from $A\beta_{1-42}$ are potent central nervous system neurotoxins. *Proc. Nat. Acad. Sci. USA*, 95:6448–6453, May 1998.

[117] Dale Schenk, Robin Barbour, Whitney Dunn, Grace Gordon, Henry Grajeda, Teresa Guido, Kang Hu, Jiping Huang, Kelly Johnson-Wood, Karen Kahn, Dora Kholodenko, Mike Lee, Zhenmei Liao, Ivan Lieberburg, Ruth Motter, Linda Mutter, Ferdie Soriano, George Shopp, Nicki Vasquez, Christopher Vandevert, Shannan Walker, Mark Wogulis, Ted Yednock, Dora Games, and Peter Seubert. Immunization with amyloid-β attenuates Alzheimer-disease-like pathology in the PDAPP mouse. *Nature*, 400:173–177, 1999.

[118] Angela D. Williams, Erik Protelius, Indu Kheterpal, Jun-tao Guo, Kelsey D. Cook, Ying Xu, and Ronald Wetzel. Mapping $A\beta$ Amyloid Fibril Secondary Structure Using Scanning Proline Mutagenesis. *J. Mol. Biol.*, 335:833–842, 2004.

[119] Aneta T. Petkova, Yoshitaki Ishii, John J. Balbach, Oleg N. Antzutkin, Richard D. Leapman, Frank Delaglio, and Robert Tycko. A structural model for Alzheimer's β-amyloid fibrils based on experimental constraints from solid state NMR. *Proc. Nat. Acad. Sci. USA*, 99(26):16742–16747, 2002.

[120] Buyong Ma and Ruth Nussinov. Stabilities and conformations of Alzheimer's

β-amyloid peptide oligomers ($A\beta_{16-22}$, $A\beta_{16-35}$, and $A\beta_{10-35}$: Sequence effects. *Proc. Nat. Acad. Sci. USA*, 99(22):14126–14131, 2002.

[121] Francesca Massi, D. Klimov, D. Thirumalai, and John E. Straub. Charge states rather than propensity for β-structure determine enhanced fibrillogenesis in wild-type Alzheimer's β-amyloid peptide compared to E22Q Dutch mutant. *Protein Science*, 11:1639–1647, 2002.

[122] Rakez Kayed, Elizabeth Head, Jennifer L. Thompson, Teresa M. McIntire, Saskia C. Milton, Carl W. Cotman, and Charles G. Glabe. Common Structure of Soluble Amyloid Oligomers Implies Common Mechanism of Pathogenesis. *Science*, 300:486–489, 2003.

[123] James D. Harper and Peter T. Lansbury, Jr. Models of Amyloid Seeding in Alzheimer's Disease and Scrapie: Mechanistic Truths and Physiological Consequences of the Time-Dependent Solubility of Amyloid Proteins. *Annu. Rev. Biochem.*, 66:385–407, 1997.

[124] L. Cruz, B. Urbanc, S. V. Buldyrev, R. Christie, T. Gómez-Isla, S. Havlin, M. McNamara, H. E. Stanley, and B. T. Hyman. Aggregation and disaggregation of senile plaques in Alzheimer disease. *Proc. Nat. Acad. Sci. USA*, 94:7612–7616, 1997.

[125] B. Urbanc, L. Cruz, S. V. Buldyrev, S. Havlin, M. C. Irizarry, H. E. Stanley, and B. T. Hyman. Dynamics of Plaque Formation in Alzheimer's Disease. *Biophys. J.*, 76:1330–1334, 1999.

[126] B. Urbanc, L. Cruz, S. V. Buldyrev, S. Havlin, B. T. Hyman, and H. E. Stanley. Dynamic feedback in an aggregation-disaggregation model. *Phys. Rev. E.*, 60(2):2120–2126, 1999.

[127] Dmitri Klimov and D. Thirumalai. Dissecting the Assembly of $A\beta_{16-22}$ Amyloid Peptides into Antiparallel β Sheets. *Structure*, 11:295–307, 2003.

[128] Leping Li, Thomas A. Darden, L. Bartolotti, Dorothea Kominos, and Lee G. Pedersen. An Atomic Model for the Pleated β-Sheet Structure of Aβ Amyloid Protofilaments. *Biophys. J.*, 76:2871–2878, 1999.

[129] Lars O. Tjernberg, David J. E. Callaway, Agneta Tjernberg, Solveig Hahne, Christina Lilliehöök, Lars Terenius, Johan Thyberg, and Christer Nordstedt. A Molecular Model of Alzheimer Amyloid β-Peptide Fibril Formation. *J. Biol. Chem.*, 274(18):12619–12625, 1999.

[130] A. R. George and D. R. Howlett. Computationally Derived Structural Models of the β-Amyloid Found in Alzheimer's Disease Plaques and the Interaction with Possible Aggregation Inhibitors. *Biopolymers*, 50:733–741, 1999.

[131] Carol K. Hall, February 2004. Talk at ICAM workshop on Protein Misaggregation: From Biomolecules to Neurodegeneration, Boston, MA.

[132] A. Baumketner and J. Shea, February 2004. Talk at ICAM workshop on Protein Misaggregation: From Biomolecules to Neurodegeneration, Boston, MA.

[133] B. Urbanc, S. V. Buldyrev, and H. E. Stanley, February 2004. Talks at ICAM workshop on Protein Misaggregation: From Biomolecules to Neurodegeneration, Boston, MA, and personal communication.

[134] M. Pellegrini-Calace, A. Carotti, and D. T. Jones. Folding in Lipid Membranes (FILM): A Novel Method for the Prediction of Small Membrane Protein 3D Structures. *Proteins*, 50:537–545, 2003.

[135] S. R. Durell, H. R. Guy, N. Arispe, E. Rojas, and H. B. Pollard. Theoretical Models of the Ion Channel Structure of Amyloid β-Protein. *Biophys. J.*, 67:2137–2145, 1994.

[136] N. Arispe, E. Rojas, and H. B. Pollard. Alzhimer disease amyloid β protein

forms calcium channels in bilayer membranes: Blockade by tromethane and aluminum. *Proc. Nat. Acad. Sci. USA*, 90:567–571, 1993.

[137] Hai Lin, Rajinder Bhatia, and Ratheshwar Lal. Amyloid β protein forms ion channels: implications for Alzheimer's disease pathophysiology. *FASEB J.*, 15:2433–2444, November 2001.

[138] Giorgio Bertotti. *Hysteresis in Magnetism.* Academic Press, New York, 1998.

[139] Andreas Moser, Kentaro Takano, David T. Margulies, Manfred Albrecht, Yoshiaki Sonobe, Yoshihiro Ikeda, Shouheng Sun, and Eric E. Fullerton. Magnetic recording: advancing into the future. *J. Phys. D*, 35:R157–R167, 2002.

[140] Dieter Weller and Mary Doerner. Extremely High-Density Longitudinal Magnetic Recording Media. *Annu. Rev. Mater. Sci.*, 30:611–644, 2000.

[141] Dieter Weller. Assault on storage densities of a terabit per square inch and beyond, April 2004. Condensed Matter seminar at U.C. Davis.

[142] Masud Mansuripur. *The Physical Principles of Magneto-optical Recording.* Cambridge University Press, Cambridge, 1995.

[143] D. Weller et al. Growth, structural, and magnetic properties of high coercivity Co/Pt multilayers. *J. Appl. Phys.*, 89(11):7525–7527, June 2001.

[144] E. Miyashita et al. Effects of the exchange stiffness constant and distribution on the recording characteristics of perpendicular media. *IEEE Trans. Mag.*, 38(5):2075–2077, September 2002.

[145] G. N. Phillips, K. O'Grady, Q. Meng, and J. C. Lodder. Domain Structure and Magnetization Process in Magneto-Optic Co/Pt Thin Films. *IEEE Trans. Mag.*, 32(5):4070–4072, 1996.

[146] Jian-Gang Zhu and H. Neal Bertram. Self-organized behavior in thin-film recording media. *J. Appl. Phys.*, 69(8):4709–4711, April 1991.